ENGINEERING RESEARCH INSTITUTE
UNIVERSITY OF MICHIGAN
ANN ARBOR

Final Report

INVESTIGATION OF EXHAUST-GAS EJECTORS FOR THE AOS-895-3 ENGINE

FRANK L. SCHWARTZ
ROBERT H. EATON

Project 2109

DETROIT ARSENAL, DEPARTMENT OF THE ARMY
CONTRACT NO. DA-20-089-ORD-36259

May 1955

FOREWORD

The results of the investigation reported in this report were obtained in fulfillment of Contract DA-20-089-ORD-36259 between the Detroit Arsenal and the Regents of The University of Michigan.

The scope of the contract is:

The University of Michigan, under the technical supervision of the Detroit Arsenal, shall furnish, except as herein otherwise provided, the labor, materials, equipment, and facilities necessary to effect and perform the investigation study required to accomplish the following objectives:

(a) determination of design criteria, optimum size, and configuration of these ejectors;

(b) a study of the magnitude of the cooling-air pressure drop with variations in the basic ejector dimensions;

(c) determination of the magnitude of the cooling-air pressure drop with variations in the basic ejector dimensions; and

(d) determination of cylinder power with and without ejectors installed.

TABLE OF CONTENTS

OBJECT

The object of this investigation was to conduct a preliminary investigation to determine the suitability of ejectors actuated by exhaust gases of an AOS-895-3 air-cooled engine for providing additional cooling for the engine and transmission.

ABSTRACT

This report includes some preliminary work performed on a round, single-cylinder exhaust-gas ejector mounted on the AOS-895-3 engine.

Most of the results recorded herein were obtained from a rectangular exhaust-gas ejector mounted on a modified manifold leading from the three cylinders of one bank of the AOS-895-3 engine. The effects of ejector length, ratio of ejector area to nozzle area, pressure rise through the ejector, and engine rpm are explored for a wide range of conditions.

CONCLUSIONS

1. A pair of exhaust-gas ejectors, each connected to a bank of three cylinders on the AOS-895-3 engine, is capable of pumping 3600 cfm of standard air at a static pressure of 8 to 9 inches of water at full throttle, 2400 rpm. This represents a cooling air to exhaust-gas ratio (M_a/M_e) of 5 to 1.

   If the static pressure is reduced to 5 to 6 inches of water as found on some other air-cooled engines (see reference 9) the quantity pumped would increase to 5280 cfm of standard air at 2400 rpm, full throttle. This represents a cooling air to exhaust-gas ratio (M_a/M_e) of 8 to 1.

2. A pair of exhaust-gas ejectors would adequately cool the present engine oil and transmission oil coolers. This conclusion is based on the design value of 5000 cfm at 4 inches of water static pressure given in CAE Report No. 419.

3. For a M_a/M_e ratio of 5, the minimum duct area for maximum induced air flow is 27 square inches. In this test, a 3- by 9-inch duct was used.

   From Fig. 32, it is estimated that an area of about 40 square inches will be needed at a M_a/M_e ratio of 8.

4. The length of straight duct has little effect on the performance. It was determined, however, that excessive length will reduce the performance some, due to wall friction and too short a length will result in incomplete mixing.

5. A diffusing section on the ejector duct improved performance. A ratio of duct area to diffuser area (A_2/A_3) in the range of 0.4 to 0.5 is theoretically best but test results give some indication that a larger diffuser area with resulting lower ratio may improve performance at M_a/M_e ratios above 7.

6. The power output of the engine decreased less than 2 percent with the nozzle design used during the tests. A smaller area nozzle would probably improve ejector performance because of higher exit velocity but this gain would be more than offset by the resulting higher power loss.

7. The exhaust temperature was reduced from 1600°F to below 350°F with a M_a/M_e ratio of 6 to 1. Higher M_a/M_e ratios would decrease this temperature still further. This lower temperature would make detection by infrared devices more difficult.

8. The noise level of the unmuffled ejector is high.

RECOMMENDATIONS

1. If the finning on this engine could be redesigned to cool at a pressure drop of the air through the fins of 5 to 6 inches of water, the ejectors alone could cool the engine at full throttle.

2. The exhaust-gas ejector can be used to cool the transmission and engine oil.

3. Further studies should be made to determine the effect of armor protection on ejector performance.

4. Further studies should be made to determine means of reducing the sound level. A resonant type of muffler could be built around the ejector requiring little additional space and should materially reduce the sound level.

INTRODUCTION

An ejector is a kinetic machine having no moving parts, capable of pumping a fluid against a hydraulic head. An ejector consists of three parts, each part having a definite thermodynamic function. An ejector consists of a nozzle, a mixing chamber, and a diffuser. The nozzle converts enthalpy energy into kinetic energy, or in the case of the ejector used in the present investigation, the nozzle consists of a shaped tube designed to conserve the kinetic energy leaving the exhaust valve and properly direct it into the mixing chamber. In the mixing chamber, a transfer of momentum takes place. The high-velocity fluid of the engine exhaust mixes with and transfers momentum and energy to the slower moving fluid being pumped, in this case the cooling air. The mixture of cooling air and exhaust gas, moving at high velocity, are diffused in a diffuser which can be a straight tube, a diverging tube, or a combination of a straight length followed by a diverging section.

As a pump, an ejector is an inefficient device having an efficiency of something less than 20 percent. It is useful, however, in applications where small size and low maintenance are required and where the available energy used by the ejector would otherwise be wasted.

The following simple problem will illustrate the inefficiency of the ejector. The nozzle is efficient, 95 percent, and a well-designed diffuser will have an efficiency of 85 percent but the mixing process involves considerable loss.

Assume an ejector is operating under the following conditions:

M_a = weight of cooling air pumped per second = 7 lb/sec
M_e = weight of engine exhaust gas pumped per second = 1 lb/sec
V_a = velocity of cooling air being pumped = 100 ft/sec
V_e = velocity of engine exhaust gas leaving nozzle = 2000 ft/sec
V_m = velocity of mixture after mixing.

Then from the law of conservation of momentum,

$$M_a V_a + M_e V_e = (M_a + M_e) V_m$$

$$7 \times 100 + 1 \times 2000 = 8 V_m$$

$$V_m = 337 \text{ ft/sec.}$$

Before mixing, the total kinetic energy is

$$\text{kinetic energy of cooling air} = \frac{M_a}{2g} V_a^2 = \frac{7 \times 100^2}{2g} = \frac{70000}{2g} ;$$

$$\text{kinetic energy of engine exhaust gas} = \frac{M_e}{2g} V_e^2 = \frac{1 \times \overline{2000}^2}{2g} = \frac{4,000,000}{2g} .$$

$$\text{Total} = \frac{4,070,000}{2g} .$$

After mixing, the total kinetic energy is

$$\text{kinetic energy of mixture} = \frac{(M_a + M_e)}{2g} V_m^2 = \frac{8 \times \overline{337}^2}{2g} = \frac{910,000}{2g} .$$

Or after mixing, the kinetic energy is $\frac{910,000}{4,070,000} = 22.4$ percent of the kinetic energy before mixing. If all this energy were reversibly used to create pressure in a diffuser, only 22.4 percent would be available. The mixing process accounts for the low efficiency of an ejector. Similar calculations for various ratios of M_a/M_e give values of V_m and efficiencies as shown in Fig. 5. It should be noted that V_m is a measure of the pressure to be developed in the diffuser. A perfect diffuser would convert all the velocity head of V_m into static pressure head.

A number of design parameters become important in the design of an ejector. These are exhaust-gas jet velocity, ratio of cooling air to exhaust gas, ratio of mixing-chamber duct cross-sectional area to exhaust-gas nozzle cross-sectional area, length of straight section in mixing chamber, length of diffuser, angle of diffuser, and position and shape of exhaust-gas nozzle in the mixing section. The size of nozzle used was determined by the back pressure on the engine. Preliminary studies of back pressure, horsepower, and nozzle area were made to determine the power loss with decreasing nozzle size. These data are shown in Fig. 6 for the manifold of a design developed on this project. Every effort was made to conserve the kinetic energy of the exhaust in the exhaust manifold. Fortunately the firing order in the AOS-895-3 engine is such that the opening

of the valves to a manifold in one bank are 240 degrees apart and have a small overlap resulting in nearly steady flow of exhaust gas from the single nozzle fed from one bank of cylinders. The loss in power from back pressure seems to be small. To verify the excellent power-loss—back-pressure relationship, check runs were made with identical manifolds and nozzles on both banks to check the data of Fig. 6 at the nozzle area used in this investigation.

Mixing in the mixing chamber may take place at constant pressure or at constant area. Flugel[1] concluded that mixing at constant area was preferred to mixing at constant pressure. With constant area mixing, some pressure rise as well as velocity increase of the induced air can be achieved in the mixing chamber. The velocity head may then be converted into pressure head by a diffuser following the mixing chamber. Constant area mixing gives higher induced air flow than constant pressure mixing or a combination of constant area and constant pressure mixing.[2] Also, it is easier to design an ejector to have constant area mixing.

A rectangular nozzle in a rectangular duct offers more surface area for transfer of momentum than a round nozzle, and consequently produces more efficient and effective mixing.[3] Also, an ejector for use in the T41 tank fits into the available space more readily when rectangular than would a round duct.

Analysis[2] shows that the best position for the nozzle exit is in the throat of the secondary duct, especially when the area ratio (see below) is greater than 5. Experiment verifies this analysis and further demonstrates that placing the nozzle ahead of the duct throat (i.e., in the rounded entrance) is better than advancing it into the straight portion of the duct (Fig. 7). The best position of the nozzle in the duct is independent of the area ratio (duct area / nozzle area) and velocity of gas leaving the nozzle.

The theory on which the present design was based is shown in the Appendix. The derivation of Equations (19) and (20), the Appendix, is extracted from reference 3.

An examination of Equation (20)

$$\Delta p = \frac{M_e \bar{V}_e}{A_2} + \left(\frac{M_e}{A_2}\right)^2 \frac{1}{\rho_a} \frac{M_a}{M_e} \left[\frac{1}{2} \frac{M_a}{M_e} + \left(\frac{M_a}{M_e} + 1\right) \left(1 + \frac{M_e}{M_a} \frac{T_e}{T_a}\right) \left(\frac{\beta}{2} - 1\right)\right] \qquad (20)$$

shows that the pressure rise through the ejector depends on the jet velocity from the nozzle $\bar{V}_e$, the flow ratio M_a/M_e, the density of the gas ρ,

the area of the duct A_2, the temperature ratio T_e/T_a, and the diffuser design as it affects β. For a given engine rpm and throttle setting $\overline{V}_e$, T_e/T_a, and ρ are constant so that

$$\Delta p = f\left(\frac{M_a}{M_e},\ A_2 \text{ and } \beta\right).$$

For a given ejector design

$$\Delta p = f\left(\frac{M_a}{M_e}\right).$$

A typical curve Δp vs M_a/M_e is shown in Fig. 14. The magnitude of the pressure rise decreases as the mass flow increases, i.e., Δp decreases as the ejector pumps more cooling air.

Equation (20) gives an optimum value of A_2, the duct area. Three sizes of ducts were used to bracket the optimum area. Figure 38 shows the theoretical curve for Δp vs ejector duct area at a mass ratio of M_a/M_e = 3, 5, and 8. On the same sheet are shown the experimental results using three duct sizes.

For a given nozzle velocity, the mass ratio M_a/M_e increases as the area ratio A_2/A_n increases up to the optimum. Thus it might seem desirable to keep A_n small. However, A_n determines the back pressure on the engine. Various nozzles were inserted in the exhaust manifolds and engine power measured as a function of nozzle area and back pressure. These results are shown in Fig. 6. A nozzle area of 2.44 square inches was selected for all ejector designs since a smaller nozzle would have entailed an excessive loss of engine power. Fixing the nozzle area in turn determined the optimum duct area A_2. The variable which affects ejector design but does not appear in Equation (20) is the ejector length. The optimum length of straight section depends on the degree of mixing in the straight length. The optimum length was determined experimentally. Various lengths of straight section were used and then several lengths of diffuser were added at each straight length. A total included angle of 12 degrees was used on the diffuser because a larger angle is prone to cause separation of flow along the diffuser wall and inefficiency. Also, installation in a tank would not be conducive to wide-angle diffusers.

ENGINE DESCRIPTION

The AOS-895-3 engine was mounted on shock-absorbing mounts and direct-connected to a 600-horsepower, Midwest, eddy-current dynamometer. A bulkhead, similar to the wall of the crew compartment in the light tank, was constructed. The standard air cleaners were mounted on this bulkhead in the same manner as in the light tank. The inlet pipes to the air cleaners were connected to a steel drum on which a standard ASME air nozzle was mounted. The air flow to the engine was calculated from the pressure difference across this nozzle indicated on a Meriam inclined manometer. Temperature of the incoming air was determined by thermocouples mounted in the nozzle drum. The cooling air from the fan was conducted through the roof by a large steel pipe. The exhaust from both banks of cylinders was connected to an exhaust header; this exhaust header was in turn connected to the exhaust pipe to the outside. A valve was installed in the exhaust pipe to control the back pressure on the engine. This initial setup was made to determine the effect of exhaust back pressure on engine power. The engine installation is shown in Fig. 40.

For the single-cylinder ejector tests, the exhaust pipe for the number four cylinder was removed from the exhaust manifold and the ensuing hole closed with a welded patch. A new exhaust pipe was fabricated for this cylinder which conducted the exhaust gas directly to an ejector. This made possible the installation of an ejector nozzle within 10 inches of the exhaust valve, thus preserving most of the kinetic energy. An adjustable exhaust-gas ejector was fabricated as shown in Fig. 1. The curved entrance and diffuser could be moved as a unit in the outside case, thus allowing the determination of the optimum position of the nozzle in the ejector.

A new manifold was designed and fabricated for the multicylinder ejector tests. This manifold has long sweeping bends and a constant area cross section. This design helped preserve the kinetic energy present in the exhaust gas at the exhaust valve. The three cylinders on each side of the engine were manifolded together. The firing order of the engine causes exhaust gas to enter the manifold at 240-degree intervals. The exhaust valve opens at 68 degrees before bottom center and closes at 32 degrees after top center, thus having an open interval of 280 degrees. This combination of firing order and valve timing gives fairly steady exhaust pressure at the ejector nozzle on each bank. A flange was welded to the end of the multicylinder manifold so that different nozzles could be attached. The multicylinder ejector was bolted to the flange of the special exhaust manifold. This manifold is shown in Fig. 2.

In both the single-cylinder and multicylinder ejector tests, the inlet pipe carrying cooling air to the ejector was connected to a drum on which a standard ASME air-flow nozzle was mounted. A valve was installed in the drum to adjust the inlet pressure to the ejector.

The following variables were measured:

Cylinder temperature

The cylinder temperature was measured by a thermocouple imbedded in and welded to the copper spark-plug gasket.

Engine oil in and out temperatures

The engine oil temperatures were measured by thermocouples in the inlet and outlet lines of the oil cooler.

Exhaust temperature

The exhaust temperature was measured in each manifold by special radiation-shielded chromel-alumel thermocouples.

Fan-cooling air temperature

The fan-cooling air exit temperature was measured about 6 inches downstream from the exit vanes of the fan on top of the engine. The inlet temperature was the same as the room ambient temperature, which was measured by a thermocouple.

Ejector-induced air temperature

The temperature of the air induced by the ejector was measured by a thermocouple placed in the drum on which the air nozzle was mounted.

Ejector exit temperature

The exit temperature of the ejector was measured by several thermocouples placed at different locations. A long movable thermocouple probe was used to make a temperature traverse. (All the above temperatures were taken on a Brown indicating-type 48-point chromel-alumel potentiometer.)

Pressure difference across the cooling air fan

The pressure difference across the cooling air fan was determined by placing a static pressure tube on the engine side of the fan near cylinder number four and reading the pressure difference on a U-tube manometer filled with water.

Exhaust pressure

A mercury U-tube manometer was connected to the manifold on each side of the engine to obtain the average exhaust back pressure. The location of these connections is shown in Fig. 4.

Pressure difference across the ejector

A Meriam inclined water manometer was connected to the inlet of the ejector to measure the static pressure ahead of the ejector.

Cooling air flow; engine air flow

The cooling air and engine air flow were determined by standard ASME nozzles. The pressure drop across these nozzles was indicated on a Meriam inclined water manometer.

Ejector duct pressure

The pressure in the ejector duct was indicated on water-filled U tubes.

Ejector static and velocity pressure

The ejector static and velocity pressures were determined by a pitot tube traverse at several sections.

Barometer pressure

The barometer pressure was determined by a sensitive, surveying-type, aneroid barometer.

Engine power measurement

The engine power was absorbed by a Midwest eddy-current dynamometer. The speed was indicated by a Hewlett-Packard Model 521-A, electronic counter. The time was indicated on a Standard Electric Time Company stop clock.

Torque was determined by the use of a Link Unibeam torque-measuring system with a Wallace and Tiernan pressure gage. All instruments were checked and calibrated before use. A sketch of the setup showing the locations of the test points is shown in Fig. 4.

ENGINE TEST PROCEDURE

The engine was first run through a standard engine test using standard manifolds in order to determine the performance of this particular engine at full, three quarters, half, and quarter throttle. The exhaust back pressure was varied by adjusting a valve in the exhaust pipe. From these data the plot shown in Fig. 6 was made of horsepower output vs back pressure on the engine.

TEST PROCEDURE ON THE SINGLE-CYLINDER EXHAUST-GAS EJECTOR

The engine was run at full throttle and the load adjusted until the speed was 2400 rpm. The back pressure on the engine was adjusted by means of a valve in the exhaust line until the pressure was equal to the exhaust pressure on cylinder number four, which was connected to the exhaust ejector. In order to determine the best position of the ejector nozzle in the ejector throat, the movable insert was moved to several different locations, and readings of air flow and pressure difference across the ejector were taken. This procedure was followed for nozzles of the following diameters: 1.00, 1.25, 1.50, and 2.06 inches. These data are plotted in Fig. 7.

It was evident from the results of the single-cylinder ejector tests that the single-cylinder ejector would not give the pressure difference across the ejector which was desired. It was decided to manifold three cylinders on one side of the engine together, thus giving a steadier flow.

TEST PROCEDURE, MULTICYLINDER EJECTOR

It was necessary first to find the relationship between engine power output and exhaust back pressure. A series of round nozzles was made up which could be bolted to the end of the special manifold on the right bank of the engine. The exhaust back pressure on the left bank was maintained equal to the pressure on the right bank by adjusting the valve in the exhaust pipe. An engine test was run with each of the nozzles in place

and the resulting data were used to establish the curve of corrected brake horsepower versus exhaust back pressure and nozzle area versus exhaust back pressure. These curves are shown in Fig. 6.

From the above results it was decided to use an area of 2.44 square inches which would give an exhaust back pressure of 6.5 inch Hg at full throttle and 2400 rpm. This horsepower loss of 0.6 percent due to the 6.5-inch-Hg back pressure seemed low. Therefore, at the end of the tests, modified manifolds were installed on both banks of cylinders, and nozzles with the same area were installed on each side. The points taken during the tests coincide with the data taken with the special manifold installed on one side and the exhaust pressure on the other side maintained at the same value. These data are shown in Fig. 6. The nozzle-area versus back-pressure curve plotted in Fig. 6 was made from data obtained with round nozzles. It was found that rectangular nozzles of the same area gave slightly higher back pressure. The rectangular nozzle was built with an aspect ratio of 12 (length/width = 12).

The theoretical analysis indicated that an ejector duct of 27 square inches would be about the optimum size. An ejector duct with an aspect ratio of 3 and an area of 27 square inches was fabricated. A length of 45 inches was used because of space limitations in the vehicle. This ejector was bolted to the special manifold on the right side of the engine. The engine was run with full throttle at 2400 rpm. Air-flow and power measurements were recorded. Next, the air valve and nozzle drop was adjusted to give several different ejector back pressures and the power and air-flow measurements were repeated. These data of air flow versus pressure difference and ratio of cooling air to engine air at constant speed are plotted in Figs. 8 through 22.

It was desirable to determine the performance of the ejector at various speeds keeping the restriction to induced air flow constant. This was done by leaving the air valve in the nozzle drum open and adjusting the load to give speeds of 1600, 1800, 2000, 2200, 2400, and 2600 rpm. These data of air flow versus rpm and pressure difference versus rpm are shown in Figs. 23 through 26.

The above basic runs were completed on three sizes of ejectors (2-3/4" x 8-1/8", 3" x 9", and 3-5/8" x 10-3/4") in the following length combinations where S represents constant area straight section and D represents diffuser.

2-3/4" x 8-1/8"	3" x 9"	3-5/8" x 10-3/4"
45S	45S	45S
45S + 12D	45S + 12D	45S + 12D
45S + 24D		45S + 24D
33S	33S	33S
33S + 12D	33S + 12D	33S + 12D
33S + 24D		33S + 24D
21S	21S	21S
21S + 12D	21S + 12D	21S + 12D
21S + 24D		21S + 24D
15S	15S	15S
15S + 12D	15S + 12D	15S + 12D
15S + 24D	15S + 24D	15S + 24D

The curves for cooling air flow versus ejector length are shown in Figs. 27, 28, and 29.

It was desirable to make a temperature and velocity traverse of the ejector tube in several locations to check on the temperature and the degree of mixing. Holes were drilled in the side of the ejector tube and a movable pitot tube and thermocouple were inserted to take these readings. Plots of the velocity and temperature are shown in Figs. 34, 35, 36, and 37.

DISCUSSION OF SINGLE-CLYINDER EJECTOR PERFORMANCE CURVES

The curves plotted in Fig. 7 indicate that the best position for the ejector nozzle is at the ejector throat or a short distance upstream. In no case was the performance better with the nozzle placed downstream from the throat.

The maximum pressure rise of 1.45 inches water at 2400 rpm through the single-cylinder ejector was too small for the present application. It is probable that the performance could be greatly improved by additional tests and modifications. It was decided, however, that the three-cylinder ejector offered greater possibilities. The work of Manganiello and Bogatsky[3] indicated that the single-cylinder ejector would not pump successfully in the range above six inches of water.

DISCUSSION OF MULTICYLINDER EJECTOR PERFORMANCE CURVES

Figures 8, 9, and 10 show the effect of straight length in a diffuser-induced cooling air flow. Figure 8 shows that as the straight length varies from 15 inches to 45 inches without a diffuser, there is little variation in the amount of air induced. In fact, the 15-inch length induces more air than the longer lengths. It appears that the diffusion is complete in the short length and the longer length only adds friction to retard the flow.

Figure 9 shows the same kind of data as Fig. 8, but with a 12-inch diffuser added. Figure 10 shows the same sort of data but with a 24-inch diffuser added. As the length of diffuser increases, more air flow is induced. Therefore, it appears that adding diffuser length is more beneficial than adding more straight duct length.

Figures 11, 12, and 13 show the same kind of data as Figs. 8, 9, and 10 but for a 3" x 9" duct. Likewise, Figs. 14, 15, and 16 show similar data for the 3-5/8" x 10-3/4" duct. The significant difference produced by duct size is the fact that the slope of the curves increases as the duct size increases. This means the large duct is especially advantageous at smaller static pressure. To show the effect of diffuser, the data were replotted in Figs. 17, 18, and 19 for the three duct sizes. In each case the total length of the ejector was kept constant but as a longer length diffuser was added, the straight section was shortened. These figures definitely show the advantage of having a diffuser on the straight section. It should be noted in these curves that adding a 12-inch diffuser increases air flow considerably but a 24-inch diffuser, although increasing the air flow, gives only a slight increase over that of the 12-inch diffuser.

Comparing Fig. 20 with Fig. 18, each of which is for the 3" x 9" duct size, it is noted that the shorter total length of 33 inches is comparable to that of the longer total length of 45 inches. Only at low static pressures is there an appreciable difference and the shorter duct with a 12-inch diffuser is better than the longer duct with a 12-inch diffuser.

Figure 21 shows the cross plot of three duct sizes, all for a 21-inch straight length, no diffuser. A comparison of duct size shows the larger duct to have the steeper curve. At high Δp's and correspondingly low air flows, afterburning took place in the ejector duct. When afterburning took place, there was an abrupt change in performance. The temperature rose to a high value, somewhere around 1800°F, with a definite drop

in air flow. When afterburning took place in the duct, the burning occurred at two nodes along the length of the duct. This was observed by deposits placed on the sides of the duct and in the early stages of development, when a light sheet metal duct was used, the seams burst. Bursting took place at points where the nodes in the afterburning occurred.

Figure 22 shows data similar to that for Fig. 21 except that it shows a 12-inch diffuser added to the 21-inch straight length.

Figures 23, 24, 25, and 26 show changes of air flow and Δp with varying rpm at constant throttle settings and constant flow restriction. This would be the situation similar to that of air flowing over the fins of a given engine. The pressure developed drops at a faster rate than the mass air flow as engine speed is reduced. As the speed drops by 40 percent, the mass flow decreases only 20 percent to 25 percent. This indicates that at low engine speeds and full throttle, there should be adequate cooling air to cool the engine. These curves indicate that if the cooling air induced is enough to cool the air at maximum speed at full throttle, there is sufficient air induced at low speeds to adequately cool the engine.

Figures 27, 28, and 29 show the effect of straight section length for three duct sizes, without diffuser, with a 12- and a 24-inch diffuser. The flatness of the curves indicates that the performance of the ejector is practically independent of the straight section length. As observed in Fig. 29 for the largest duct size, there was some variation of performance with duct length. The 3" x 9" duct shows the least variation of performance with straight length section. This is largely because the 3" x 9" duct is closest to the optimum duct size for this engine (see Fig. 28).

Figures 30, 31, and 32 show a comparison of performance at full throttle and half throttle for an engine speed of 2400 rpm. The end points of the curves joined by dash lines are at fixed resistance to cooling air flow. As the power dropped to one half, the air flow dropped between 23 and 30 percent. Although the three curves are for the same duct size, it should be noted that as the diffuser is added, the slopes of the curves increase, again showing the advantage of having a diffuser.

Figure 33 shows horsepower and back pressure versus engine rpm for the standard manifold and the experimental or modified manifold. At low engine rpm there is little difference between the two manifolds. At engine speeds between 2200 and 2600 rpm, the modified manifold shows some improvement over the standard manifold. It was not possible to operate the engine up to 2800 rpm because of excessive vibration in the setup. It appears that the two manifolds would be of nearly equal performance at around 2800 rpm, if these curves were extrapolated. However, at somewhat

lower speeds there seems to be a distinct improvement with the modified manifold. This is to be expected since the modified manifold has long radius bends and constant cross section enabling the kinetic energy to be conserved. The corrected brake horsepower obtained from this engine on test agrees closely with the published horsepower curves of Continental Aviation and Engineering Corporation, Report AOS-895-3. For example, at 2400 rpm, the net corrected horsepower is 360 bhp with the modified manifolds whereas the CAE curve minus the fan horsepower, air cleaner, generator, and back pressure losses indicated 375 hp.

The theoretical curves plotted in Fig. 38 were calculated, using Equation (20) of the Appendix, under average conditions found in a majority of test runs and gave an indication of theoretical results which might be expected with the type ejector used in these tests.

Exhaust gas velocity was calculated from the force it exerted on a pivoted thrust plate, connected through a lever arm to a spring scale. At 2400 rpm, full throttle, a velocity of 1855 ft/sec was attained with the modified manifold and flow nozzle in operation. This is the mean effective velocity which is an indication of useful energy; the actual maximum pulsing velocity is probably approaching the sonic range. Calculations from temperature and pressure readings show this to be between 2062 and 2100 ft/sec.

For comparison, the test results of the 15S + 12D ejectors are shown to indicate losses which can be expected, due to friction and incomplete mixing. Optimum duct size for a maximum static pressure, with a ratio of cooling air to exhaust gas (M_a/M_e) of from approximately 5 to 10, falls within duct sizes used in the test and would be near the maximum cooling air obtainable unless a static pressure (Δp) could be used below 6 inches which would show sizeable gains in cooling-air pumping capacity. In this case duct sizes larger than those used in the test would be advantageous.

Figure 38a indicates the theoretical relationship between the ratio of diffuser area to duct area (A_2/A_3) on Beta. Increasing Beta increases Δp for a given set of conditions. The 12-inch diffuser for the three ducts tested is near the maximum.

BIBLIOGRAPHY

1. Flugel, G., "The Design of Jet Pumps," NACA TM 982, 1941.

2. Keenan and Neumann, "A Simple Air Ejector," Trans. ASME, 9, No. 2, A-75 (1942).

3. Manganiello and Bogatsky, "An Experimental Investigation of Rectangular Exhaust-Gas Ejectors Applicable for Engine Cooling," NACA ARR No. E4E31, 1944.

4. Elrod, "The Theory of Ejectors," Trans. ASME, 12, No. 3, A-170 (1945).

5. Keenan, Neumann, and Lustwerk, "An Investigation of Ejector Design by Analysis and Experiment," Trans. ASME, 17, No. 3, 299 (1950).

6. Marquardt, "A Theoretical and Experimental Investigation of Exhaust Ejectors for Cooling at Low Speeds," NACA ACR 3G05, 1943.

7. McElroy, "Design of Injectors for Low-Pressure Air Flow," U.S. Department of the Interior, Bureau of Mines, Technical Paper 678, 1945.

8. Pinkel, Turner, Voss, and Humble, "Exhaust-Stack Nozzle Area and Shape for Individual Cylinder Exhaust-Gas Jet-Propulsion System," NACA Report No. 765, 1943.

9. Marquardt, "Tests of an Annular Ejector System for Cooling Aircraft Engines," NACA ACR No. 3J27, 1943.

10. London and Pucci, "Exhaust Stack Ejector for Mine Sweeper Boat Gas Turbine Installations," Stanford University, Prepared for Code 541 Bureau of Ships, U.S. Department of the Navy, 1942.

11. "Power Plant Installation, T-92 Light Tank," Aircraft Armaments, Inc., Report No. ER-361.

12. Maskey, "AOS-895 Engine Cooling-Air Fan Evaluation and Improvement," CAE Report No. 419, 1951.

13. "Air Flow of Engine Cooling Fan Assembly No. 518091 on the Light Tank, T-41," Detroit Arsenal Report No. 504, 1950.

14. Flow Measurement, ASME, PTC 19.5, 4-1949.

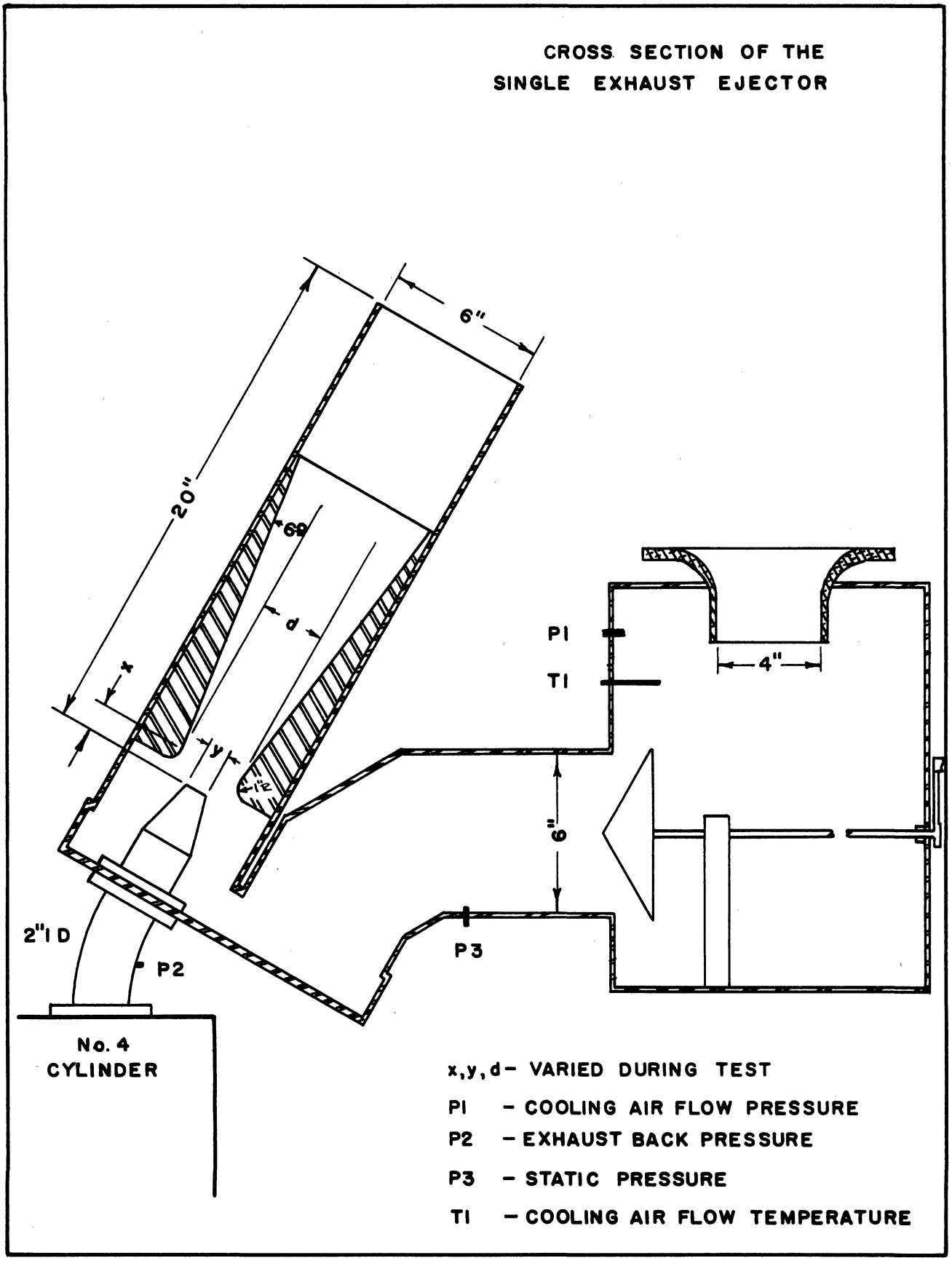
CROSS SECTION OF THE
SINGLE EXHAUST EJECTOR
6"
20"
69
d
x
y
1"-12
P1
T1
4"
6"
2"I D
P2
P3
No. 4
CYLINDER
x,y,d- VARIED DURING TEST
P1 - COOLING AIR FLOW PRESSURE
P2 - EXHAUST BACK PRESSURE
P3 - STATIC PRESSURE
T1 - COOLING AIR FLOW TEMPERATURE

Fig. 1

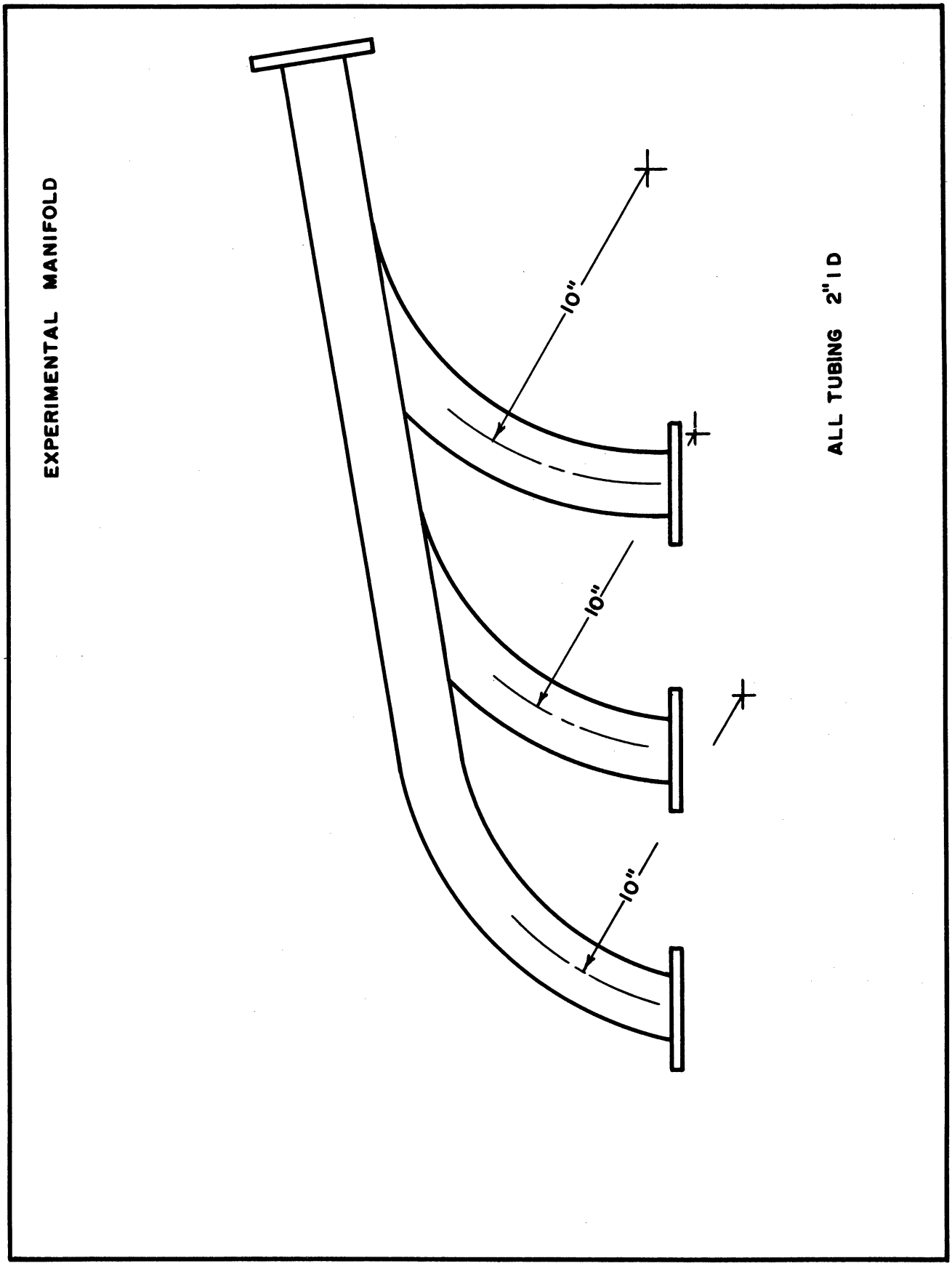

Fig. 2

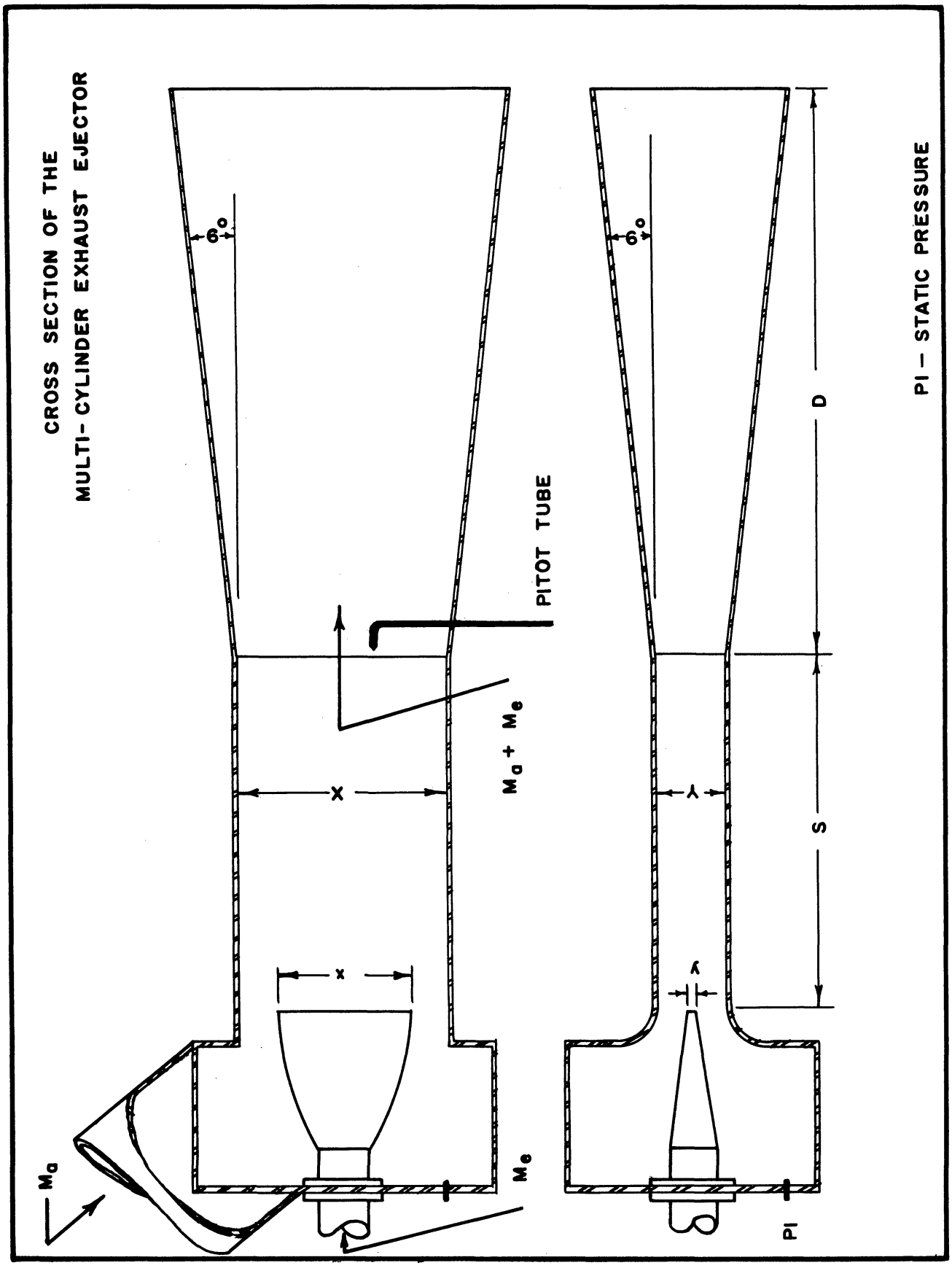
CROSS SECTION OF THE
MULTI-CYLINDER EXHAUST EJECTOR
PI – STATIC PRESSURE
6°
6°
PITOT TUBE
$M_a + M_e$
X
x
D
S
Y
y
M_a
M_e
PI

Fig. 3

Temperatures	Pressures
T1 Ejector-induced air temperature	P1 Pressure difference across cooling air nozzle
T2 Engine air inlet temperature	P2 Pressure difference across engine air nozzle
T3 Exhaust-gas temperature, right manifold	P3 Exhaust back pressure, right manifold
T4 Exhaust-gas temperature, left manifold	P4 Exhaust back pressure, left manifold
T5 Ejector duct temperature	P5 Ejector duct static pressure
T6 Cylinder head temperature	P6 Static pressure across cooling air fan
T7 Cooling fan exit temperature	P7 Static pressure across ejector

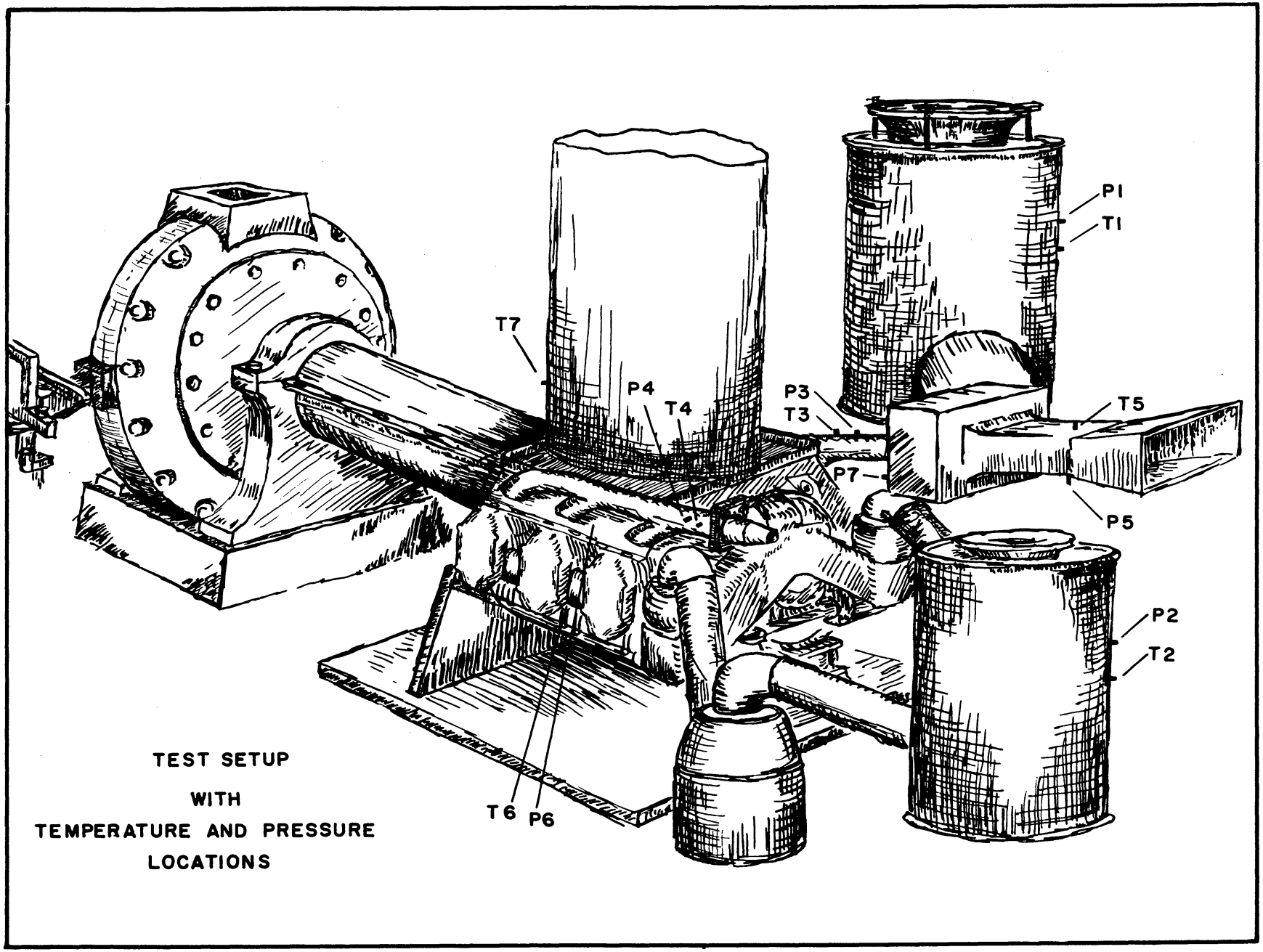
P1
T1
T7
P4
T4
P3
T3
T5
P7
P5
P2
T2
T6
P6
TEST SETUP
WITH
TEMPERATURE AND PRESSURE
LOCATIONS

Fig. 4

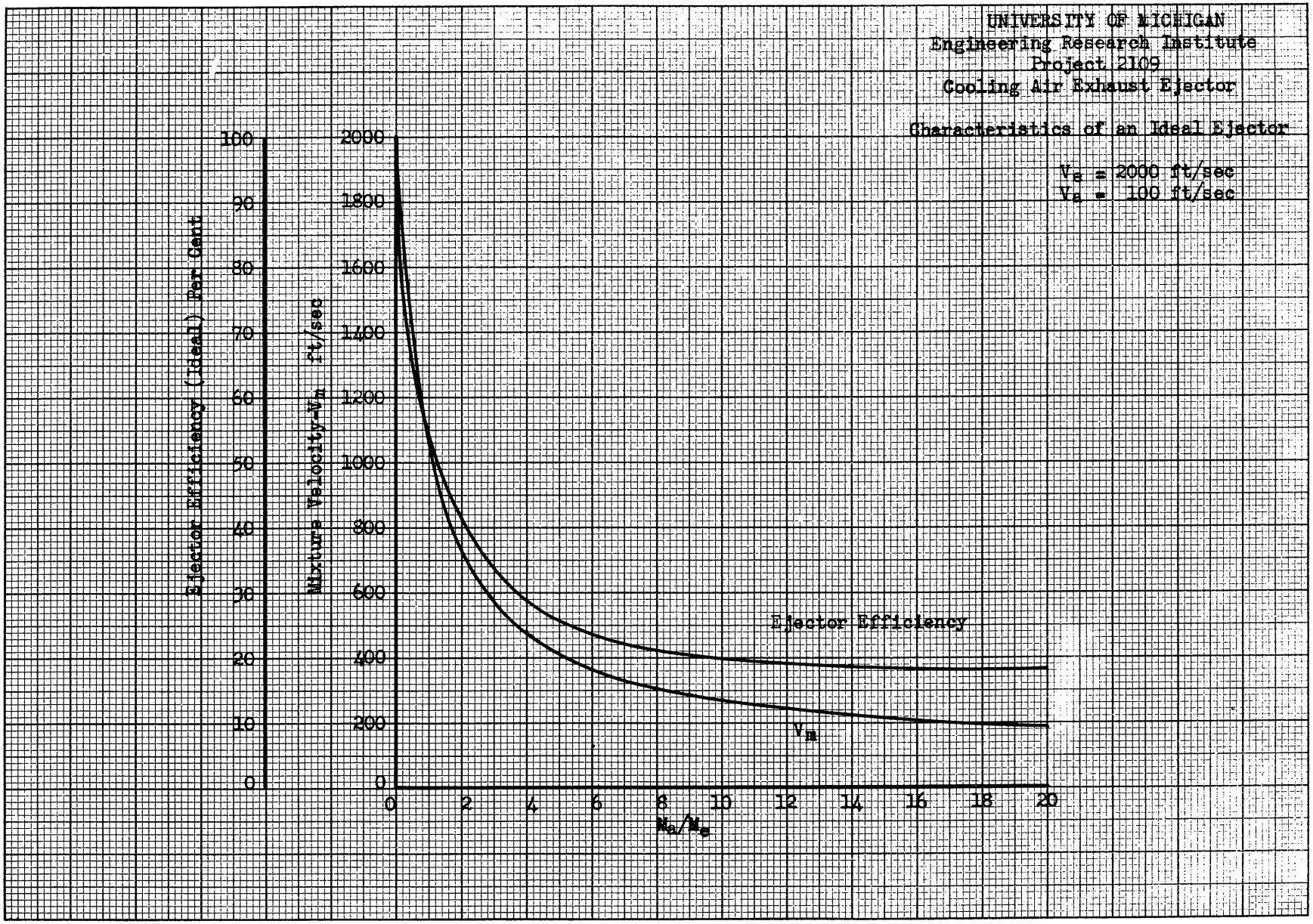
UNIVERSITY OF MICHIGAN
Engineering Research Institute
Project 2109
Cooling Air Exhaust Ejector
Characteristics of an Ideal Ejector
V_a = 2000 ft/sec
V_e = 100 ft/sec
Ejector Efficiency (Ideal) Per Cent
Mixture Velocity-V_m ft/sec
Ejector Efficiency
V_m
M_a/M_e
0
2
4
6
8
10
12
14
16
18
20
0
200
400
600
800
1000
1200
1400
1600
1800
2000
0
10
20
30
40
50
60
70
80
90
100

Fig. 5

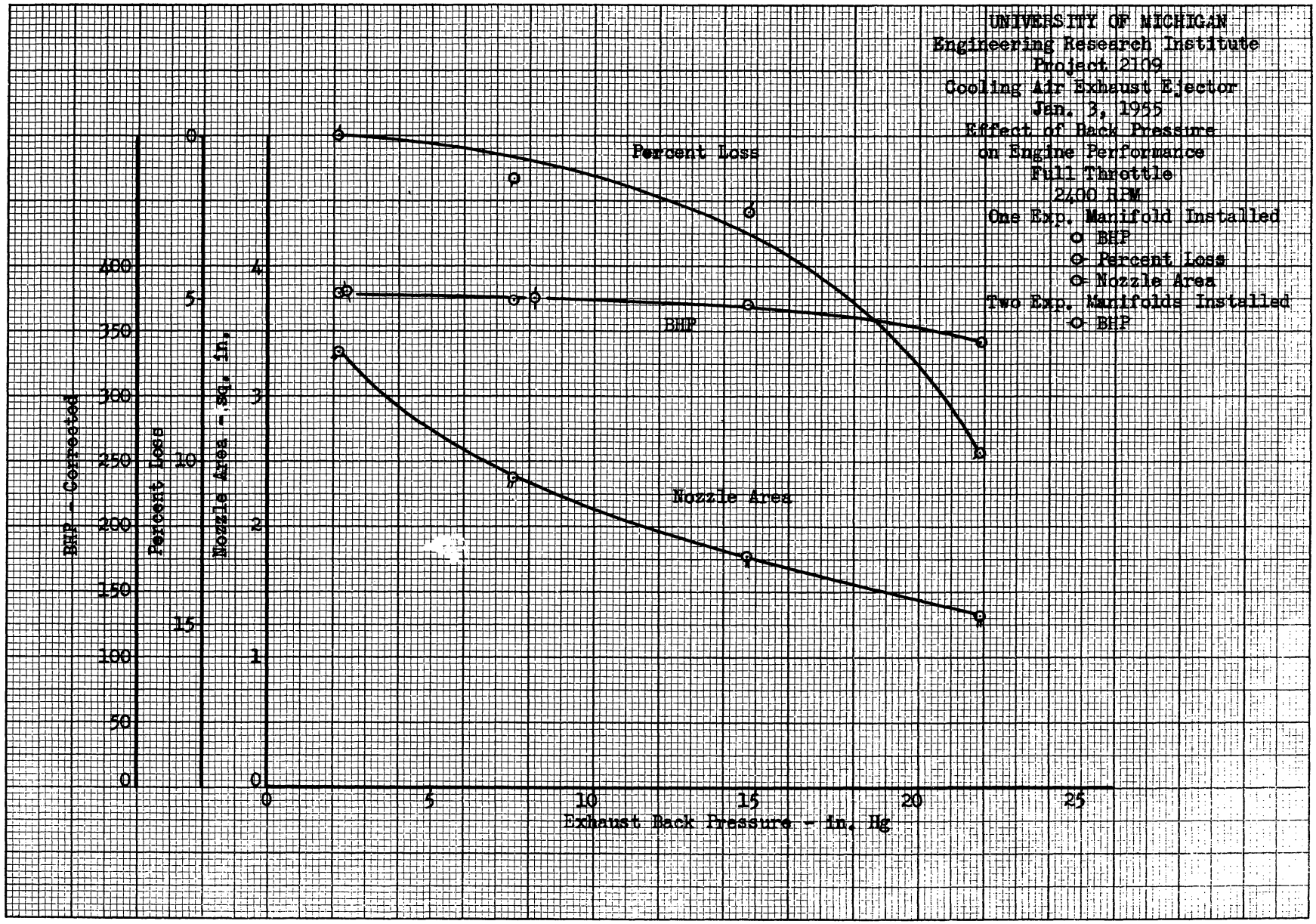
UNIVERSITY OF MICHIGAN
Engineering Research Institute
Project 2109
Cooling Air Exhaust Ejector
Jan. 3, 1955
Effect of Back Pressure
on Engine Performance
Full Throttle
2400 RPM
One Exp. Manifold Installed
o BHP
o Percent Loss
o Nozzle Area
Two Exp. Manifolds Installed
o BHP
Percent Loss
BHP
Nozzle Area
BHP - Corrected
Fuel Flow - lbs./hr.
Nozzle Area - sq. in.
Exhaust Back Pressure - In. Hg
0
50
100
150
200
250
300
350
400
0
5
10
15
20
25
0
1
2
3
4
5
0
5
10
15

Fig. 6

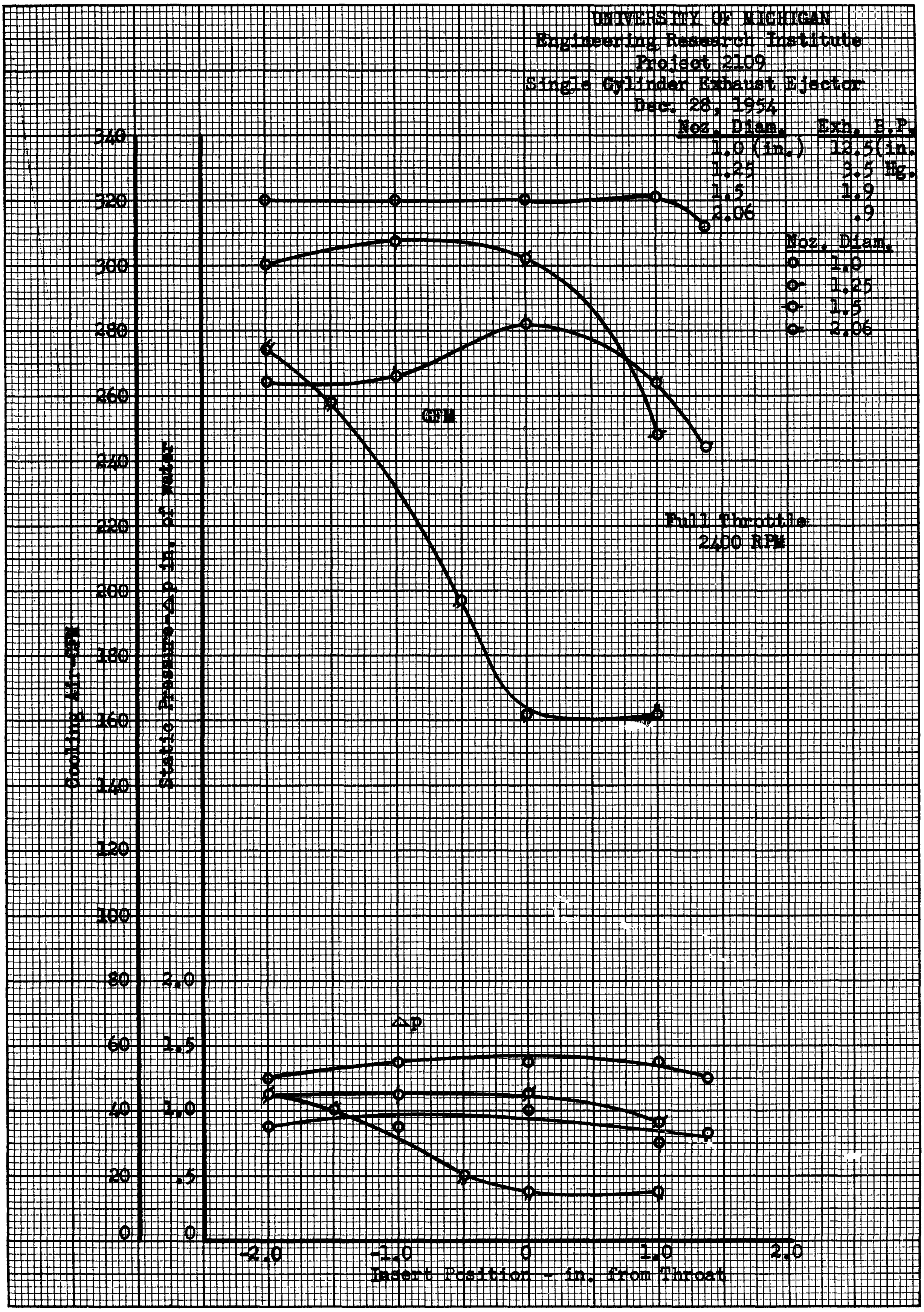

UNIVERSITY OF MICHIGAN
Engineering Research Institute
Project 2109
Single Cylinder Exhaust Ejector
Dec. 28, 1954
Noz. Diam. Exh. B.P.
1.0 (in.) 12.5(in.
1.25 3.5 Hg.
1.5 1.9
2.06 .9
Noz. Diam.
1.0
1.25
1.5
2.06
CFM
Full Throttle
2400 RPM
Δp
Cooling Air-CFM
Static Pressure-Δp in. of Water
Insert Position - in. from Throat

Fig. 7

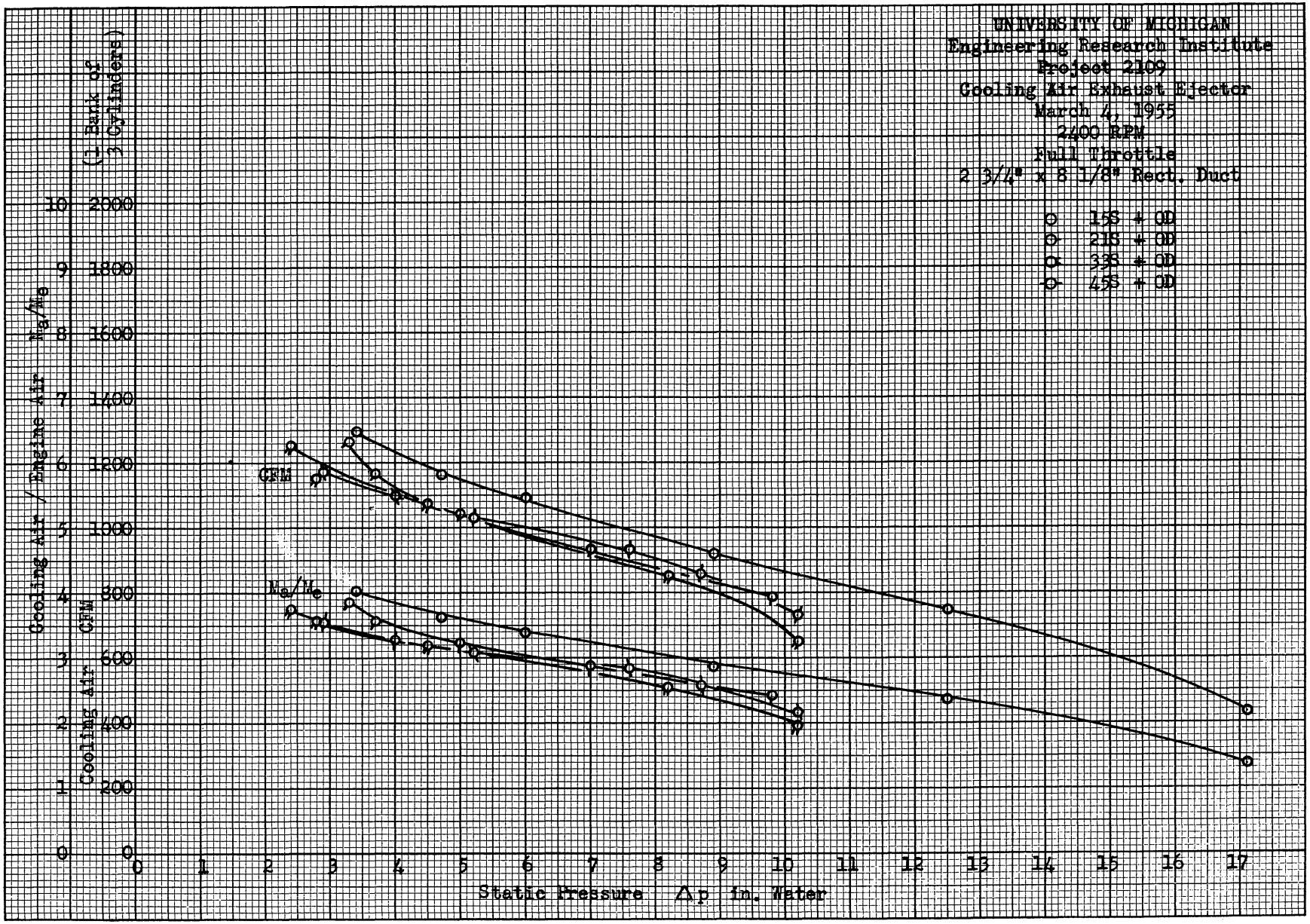
UNIVERSITY OF MICHIGAN
Engineering Research Institute
Project 2109
Cooling Air Exhaust Ejector
March 4, 1955
2400 RPM
Full Throttle
2 3/4" x 8 1/8" Rect. Duct
15S + OD
21S + OD
33S + OD
45S + OD
Cooling Air / Engine Air
Kg/Kg
Cooling Air CFM
(1 Bank of 8 Cylinders)
CFM
Me/Me
Static Pressure Δp in. Water
0
1
2
3
4
5
6
7
8
9
10
11
12
13
14
15
16
17
200
400
600
800
1000
1200
1400
1600
1800
2000

Fig. 8

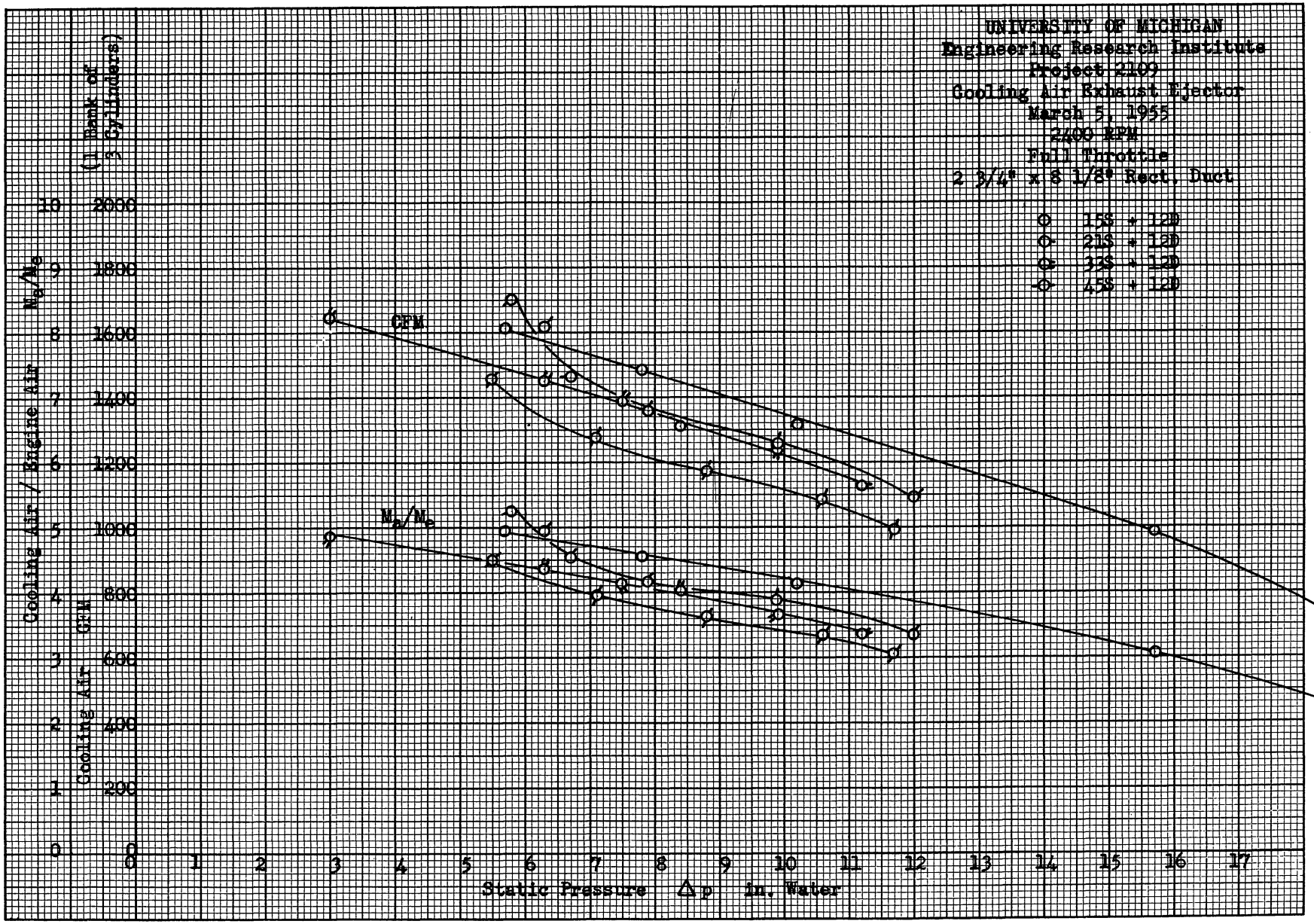
UNIVERSITY OF MICHIGAN
Engineering Research Institute
Project 2109
Cooling Air Exhaust Ejector
March 5, 1955
2400 RPM
Full Throttle
2 3/4" x 8 1/8" Rect. Duct
15S + 12D
21S + 12D
33S + 12D
45S + 12D
CFM
M_a/M_e
M_a/M_e
Cooling Air / Engine Air
Cooling Air CFM
(1 Bank 8 Cylinders)
Static Pressure Δp In. Water
0
1
2
3
4
5
6
7
8
9
10
11
12
13
14
15
16
17
200
400
600
800
1000
1200
1400
1600
1800
2000

Fig. 9

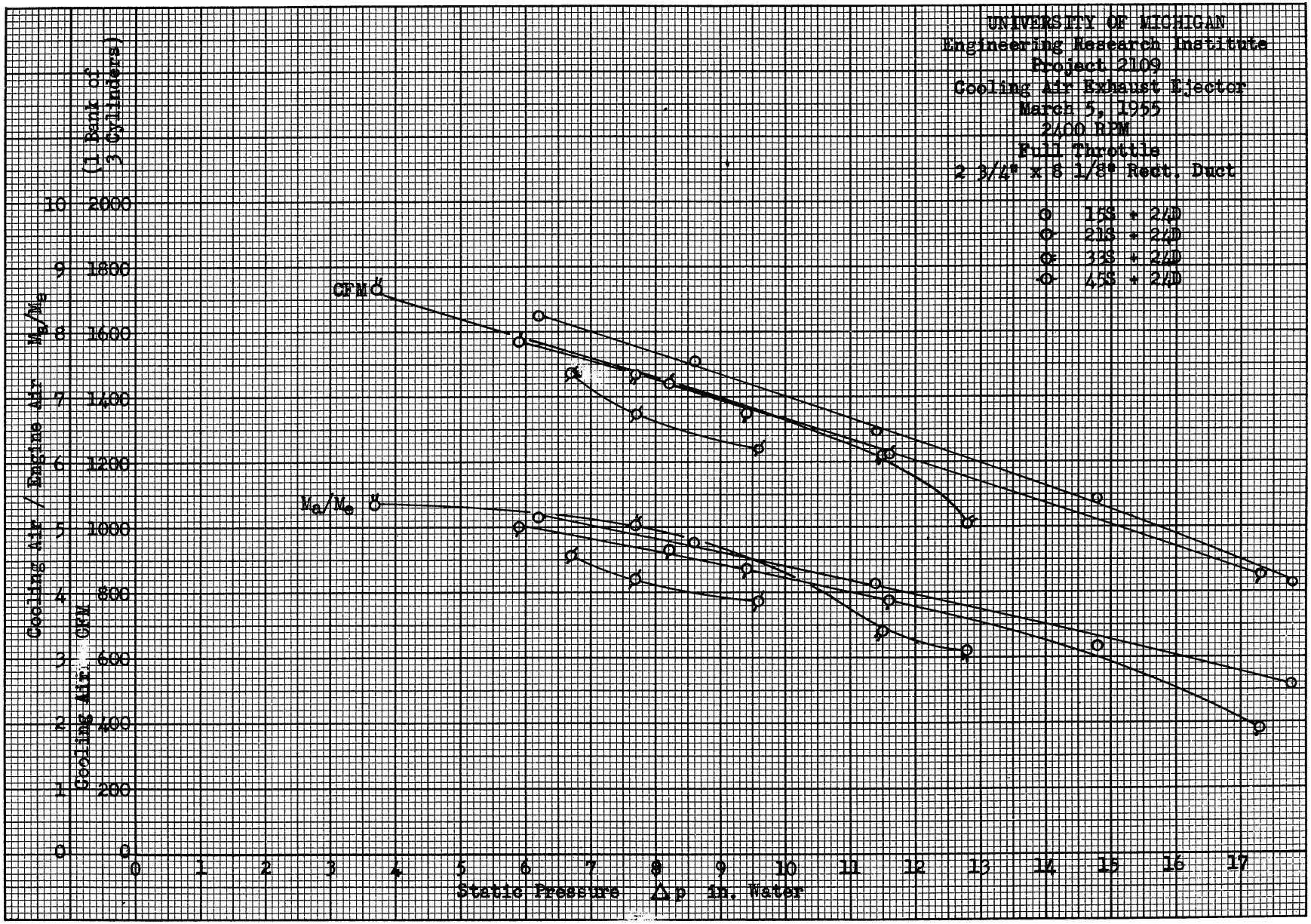
UNIVERSITY OF MICHIGAN
Engineering Research Institute
Project 2109
Cooling Air Exhaust Ejector
March 5, 1955
2400 RPM
Full Throttle
2 3/4" x 8 1/8" Rect. Duct
15S + 2Ø
21S + 2Ø
32S + 2Ø
45S + 2Ø
CFMC
Me/Me δ
Cooling Air / Engine Air Me/Me
Cooling Air CFM (1 Bank of 3 Cylinders)
Static Pressure Δp in. Water
0 1 2 3 4 5 6 7 8 9 10 11 12 13 14 15 16 17
0 200 400 600 800 1000 1200 1400 1600 1800 2000

Fig. 10

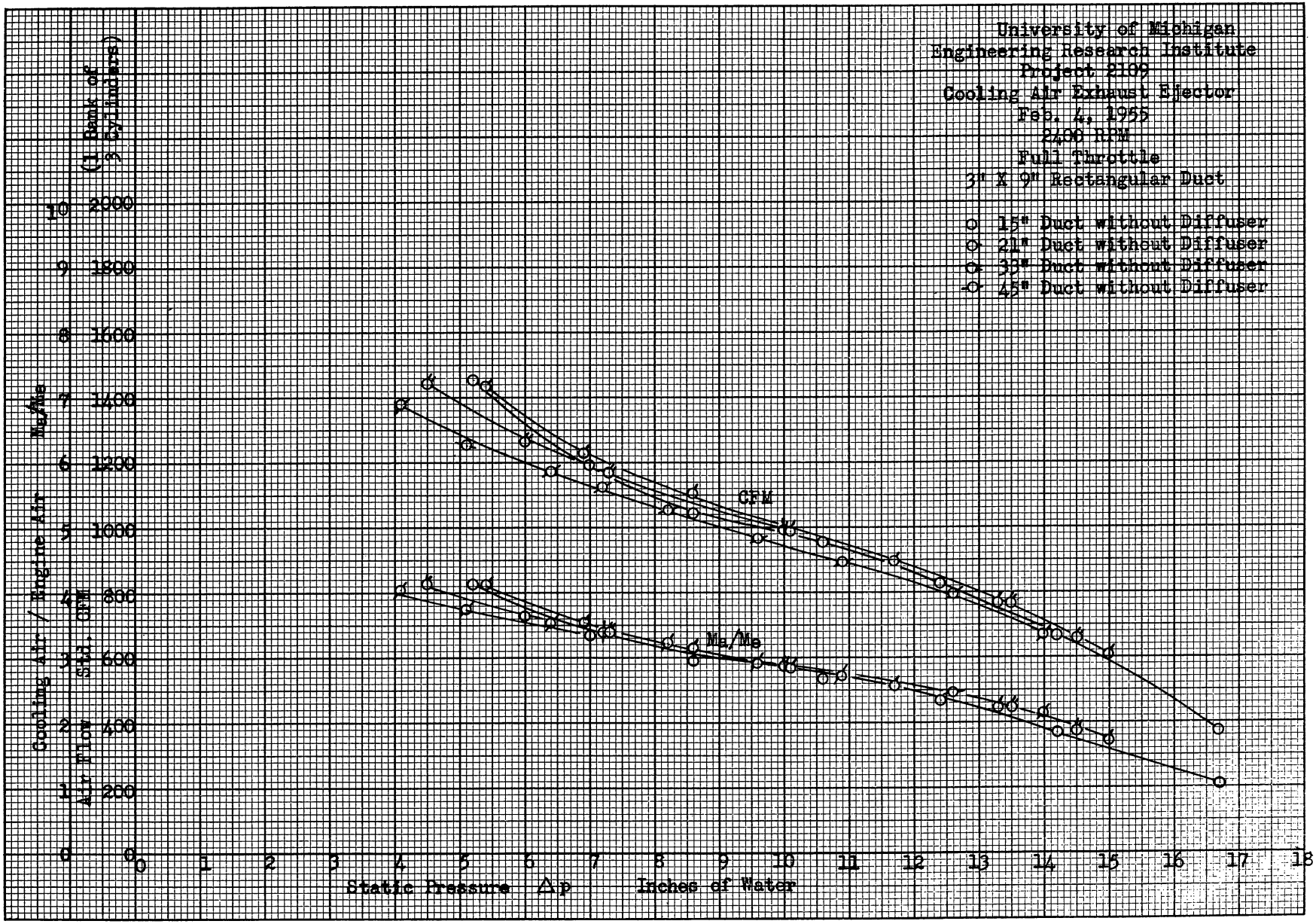
University of Michigan
Engineering Research Institute
Project 2109
Cooling Air Exhaust Ejector
Feb. 4, 1955
2400 RPM
Full Throttle
3" X 9" Rectangular Duct
15° Duct without Diffuser
21° Duct without Diffuser
33° Duct without Diffuser
45° Duct without Diffuser
CFM
Ms/Me
Cooling Air / Engine Air
Air Flow
Static Pressure Δp Inches of Water

Fig. 11

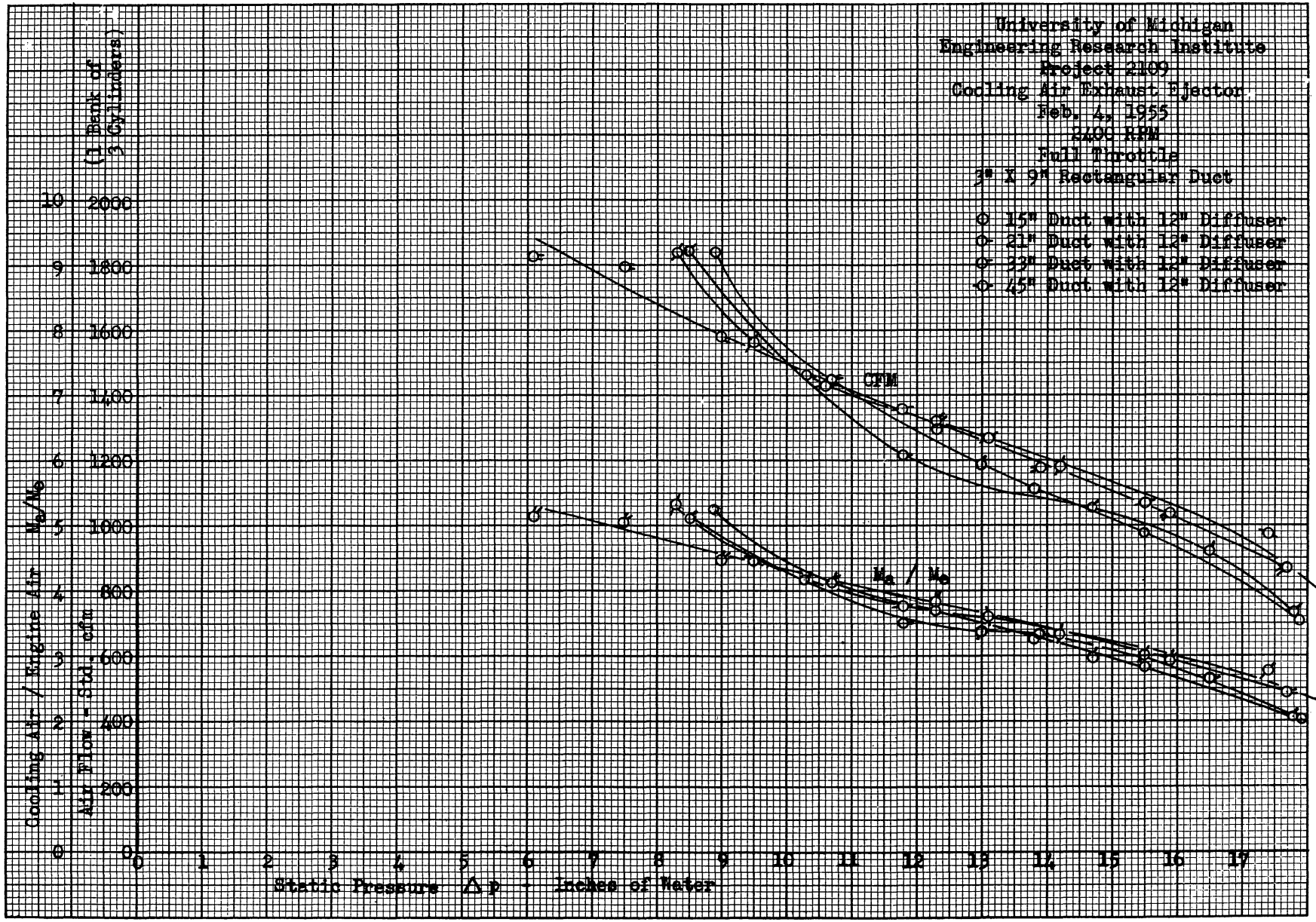
University of Michigan
Engineering Research Institute
Project 2109
Cooling Air Exhaust Ejector
Feb. 4, 1955
2400 RPM
Full Throttle
3" X 9" Rectangular Duct
15" Duct with 12" Diffuser
21" Duct with 12" Diffuser
33" Duct with 12" Diffuser
45" Duct with 12" Diffuser
CFM
W_a / W_e
Cooling Air / Engine Air
W_a / W_e
Air Flow - Std. cfm
(1 Bank of 9 Cylinders)
Static Pressure Δp - Inches of Water
0
1
2
3
4
5
6
7
8
9
10
200
400
600
800
1000
1200
1400
1600
1800
2000
0
1
2
3
4
5
6
7
8
9
10
11
12
13
14
15
16
17

Fig. 12

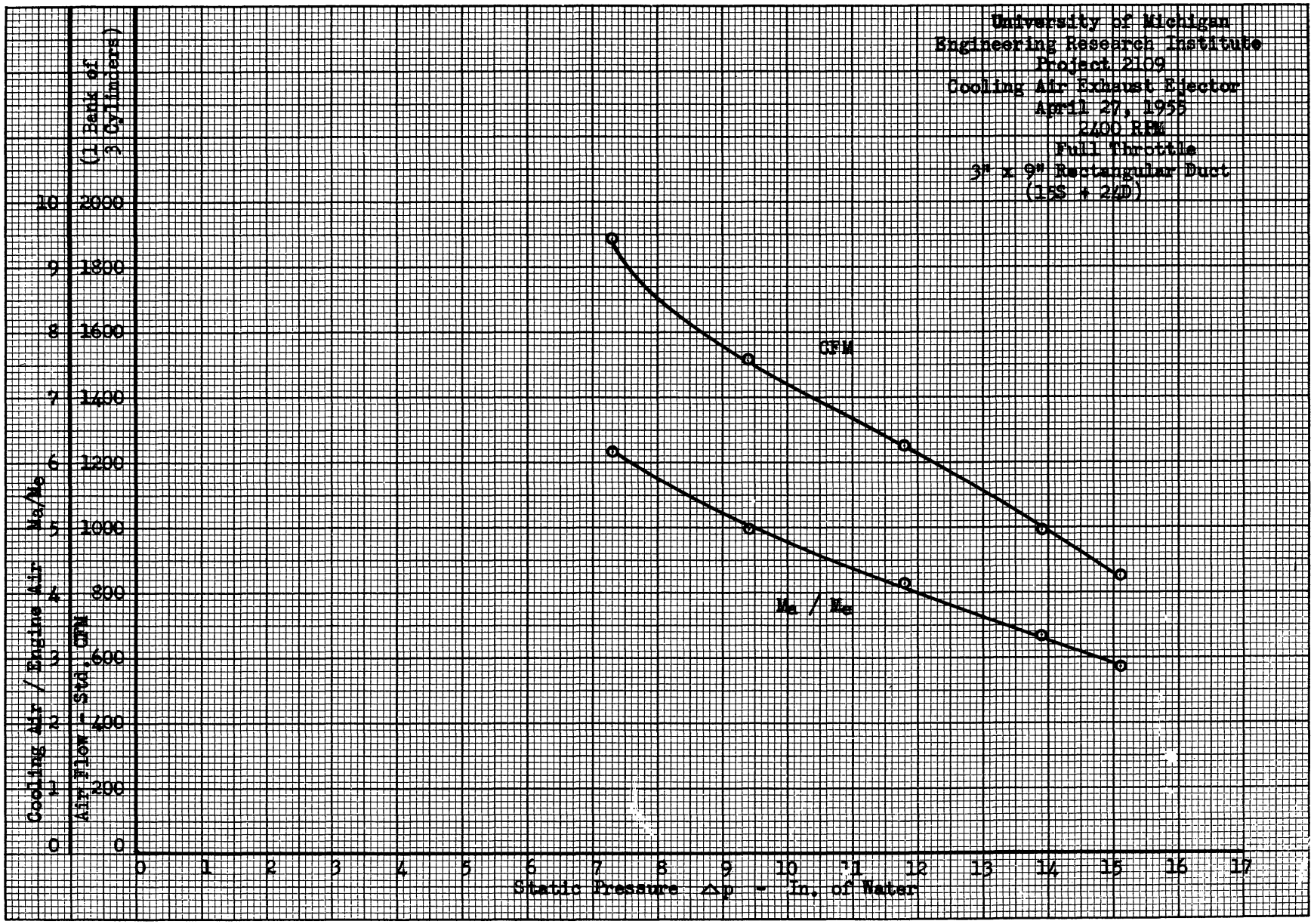
University of Michigan
Engineering Research Institute
Project 2109
Cooling Air Exhaust Ejector
April 27, 1955
2400 RPM
Full Throttle
3" x 9" Rectangular Duct
(1S + 2D)
CFM
Ma / Me
Cooling Air / Engine Air Ma/Me
Air Flow Std. CFM (1 Bank of 3 Cylinders)
Static Pressure Δp - In. of Water
0
1
2
3
4
5
6
7
8
9
10
11
12
13
14
15
16
17
200
400
600
800
1000
1200
1400
1600
1800
2000

Fig. 13

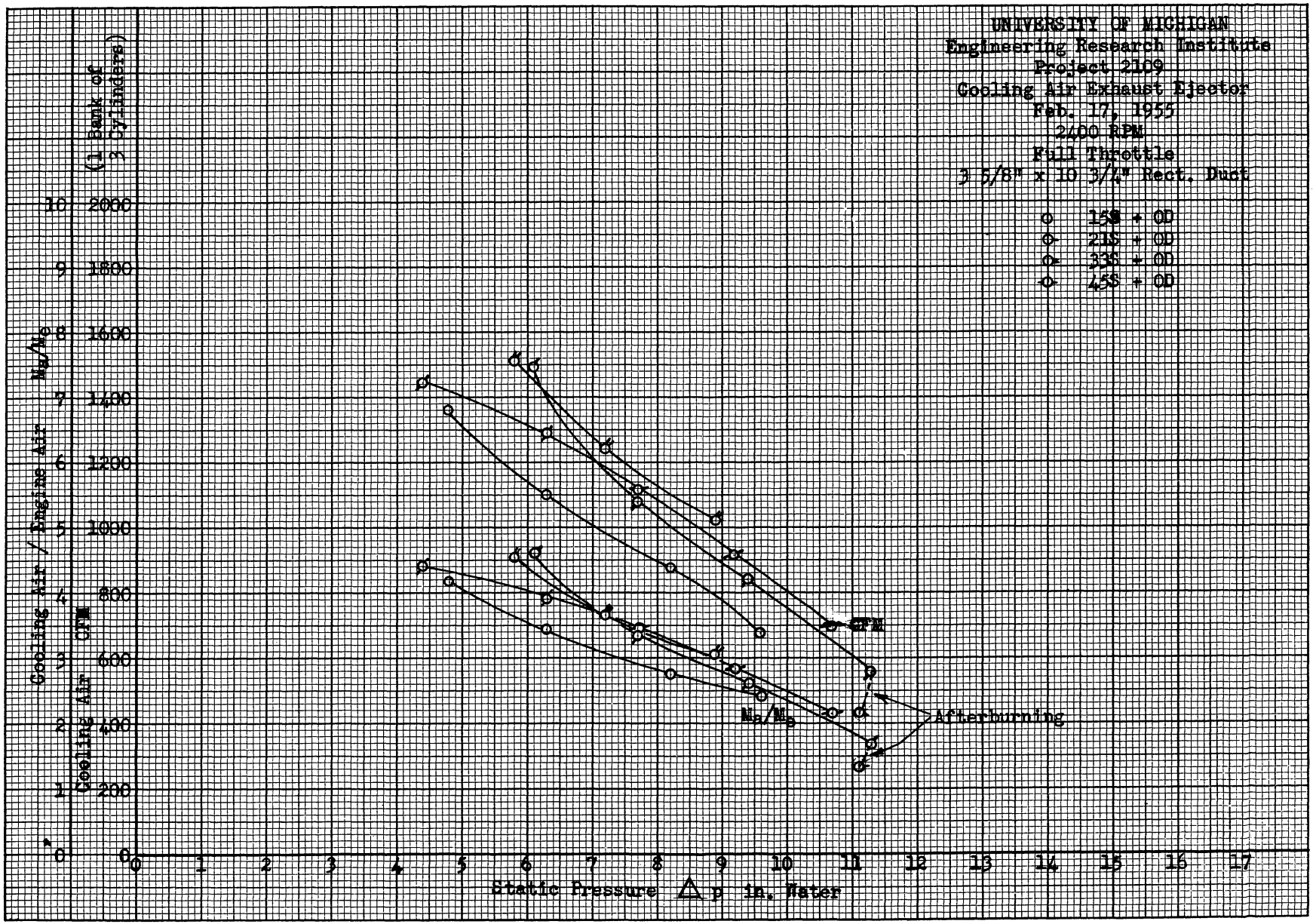
UNIVERSITY OF MICHIGAN
Engineering Research Institute
Project 2109
Cooling Air Exhaust Ejector
Feb. 17, 1955
2400 RPM
Full Throttle
3 5/8" x 10 3/4" Rect. Duct
15S + OD
21S + OD
33S + OD
45S + OD
Cooling Air / Engine Air
Mc/Me
Cooling Air lbs/min
(1 bank 6 cylinders)
Static Pressure Δp in. Water
Me/Mb
Afterburning

Fig. 14

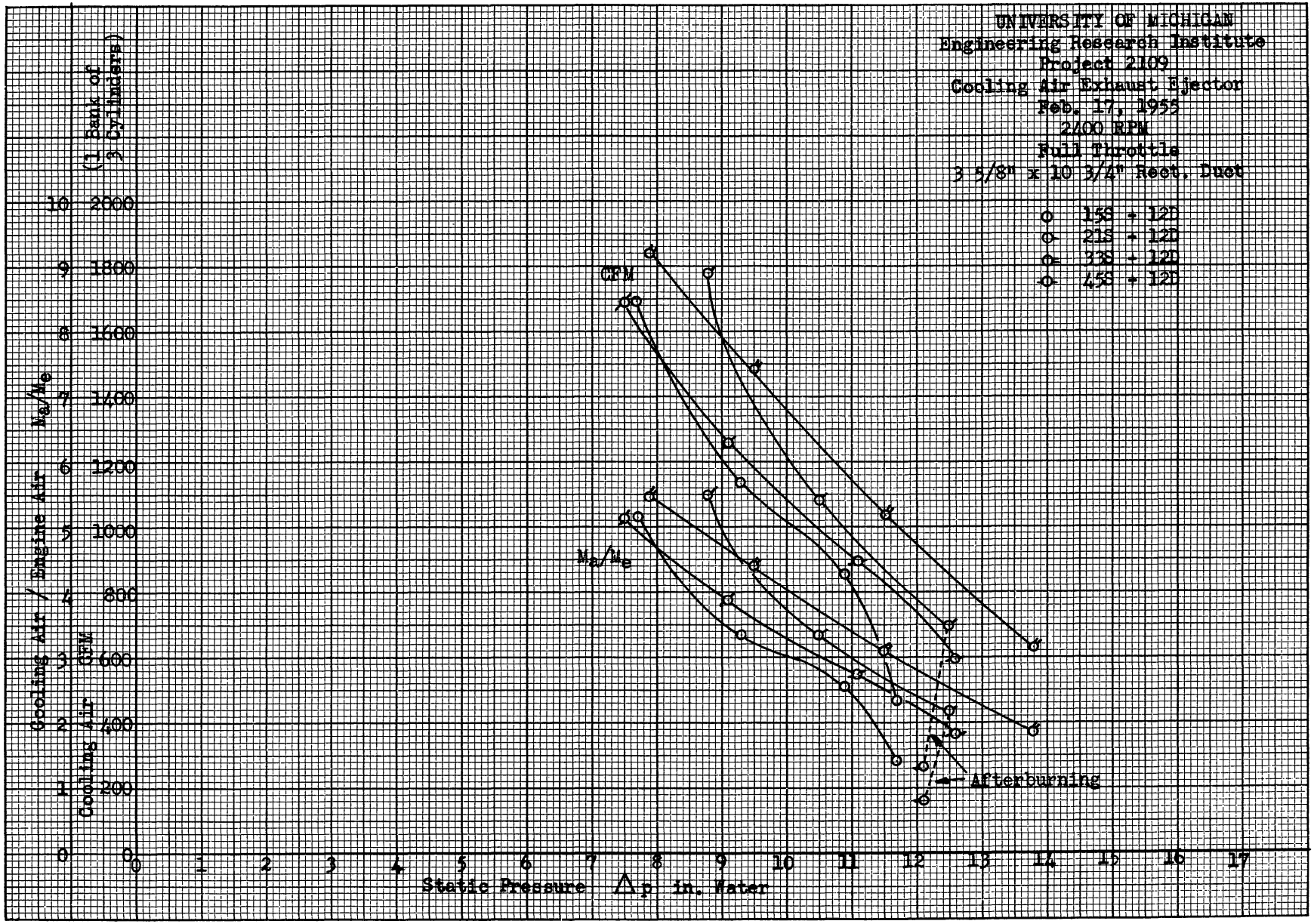
UNIVERSITY OF MICHIGAN
Engineering Research Institute
Project 2109
Cooling Air Exhaust Ejector
Feb. 17, 1955
2400 RPM
Full Throttle
3 5/8" x 10 3/4" Rect. Duct
158 + 12D
218 + 12D
338 + 12D
458 + 12D
CFM
M_a/M_e
Afterburning
Cooling Air (1 Bank of 3 Cylinders)
Cooling Air / Exhaust Air M_a/M_e
Cooling Air CFM
Static Pressure Δp in. Water

Fig. 15

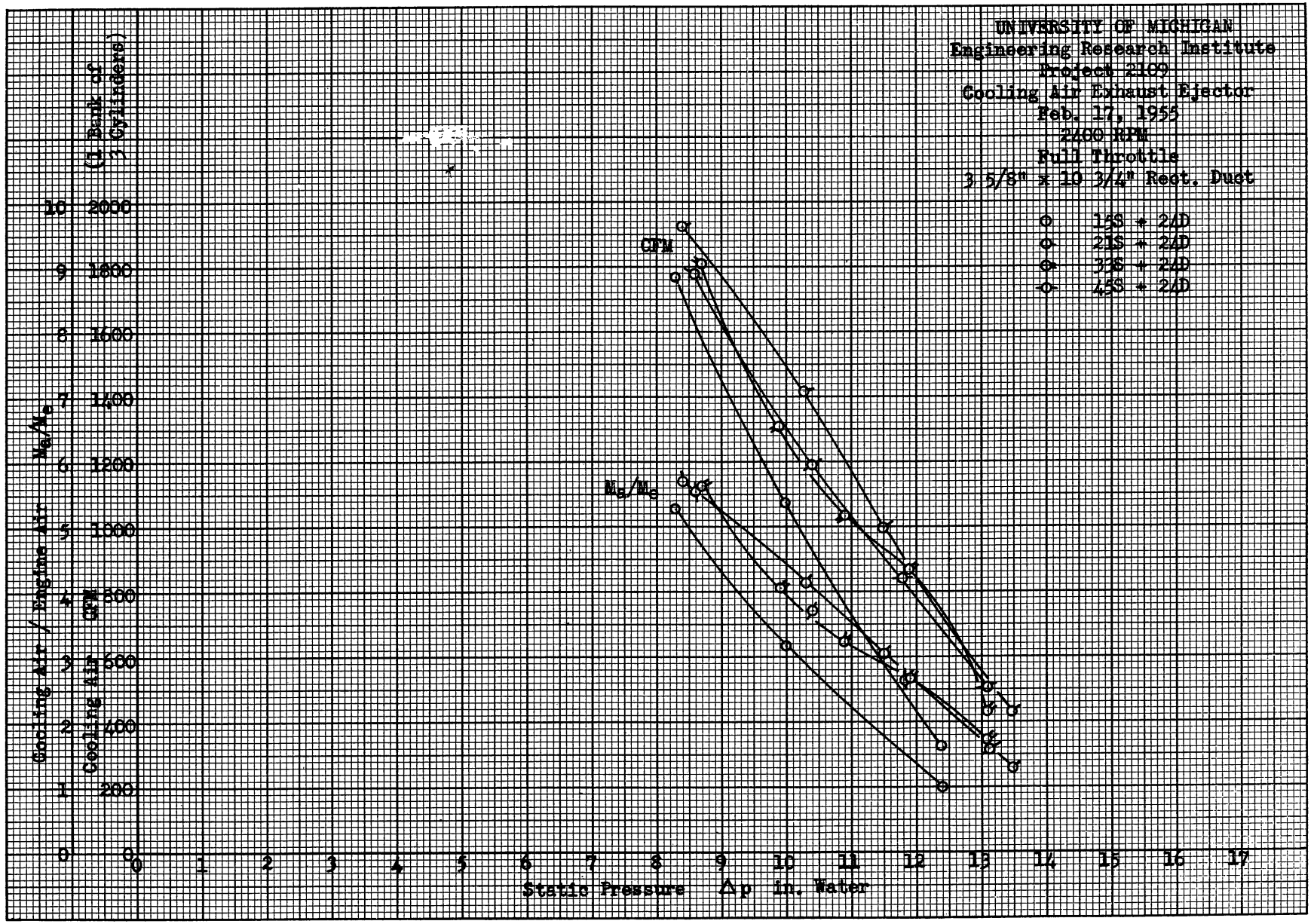
UNIVERSITY OF MICHIGAN
Engineering Research Institute
Project 2109
Cooling Air Exhaust Ejector
Feb. 17, 1955
2400 RPM
Full Throttle
3 5/8" x 10 3/4" Root. Duct
1S + 2D
2S + 2D
3S + 2D
4S + 2D
CFM
Me/Mc
Static Pressure Δp in. Water

Fig. 16

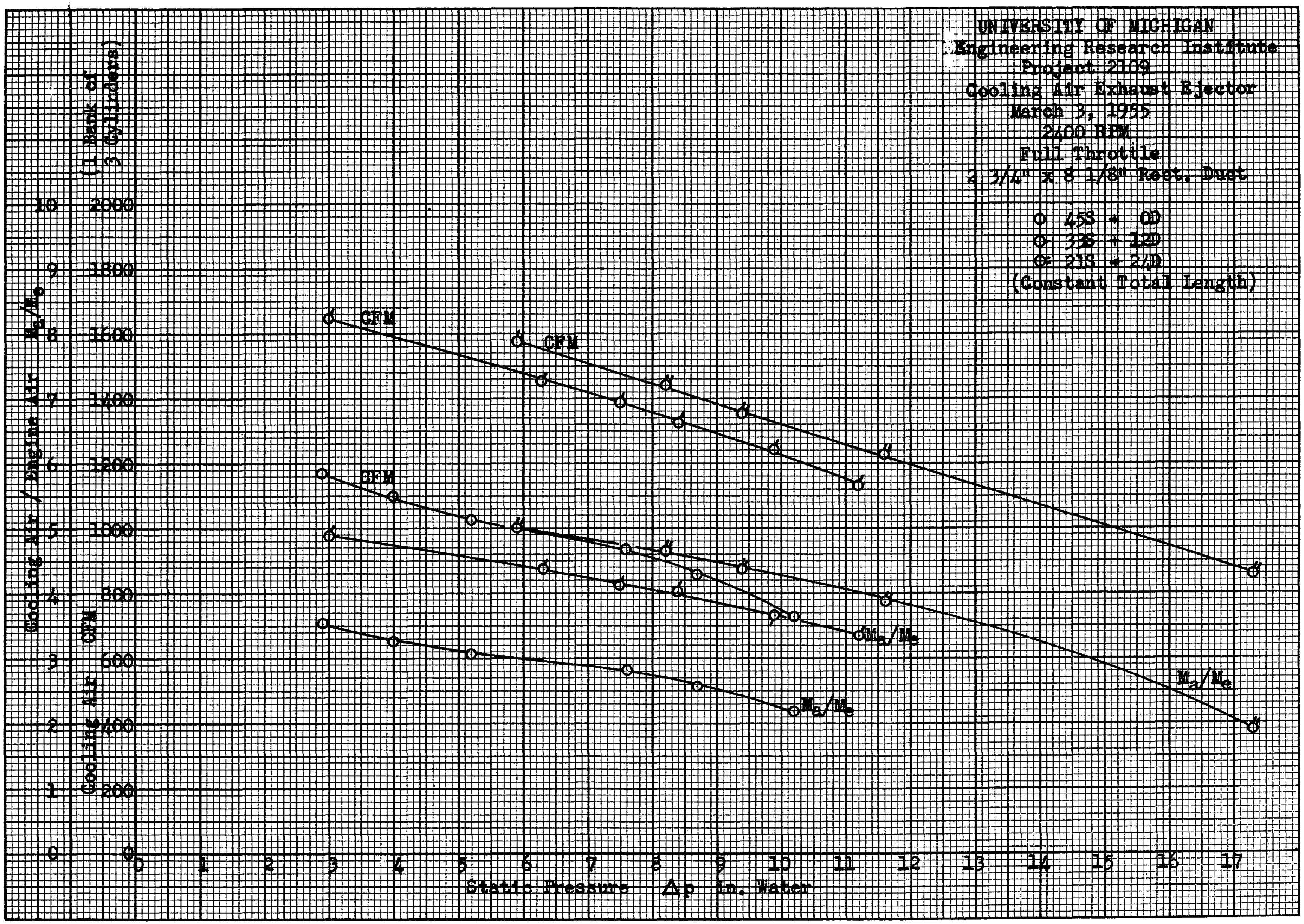
UNIVERSITY OF MICHIGAN
Engineering Research Institute
Project 2109
Cooling Air Exhaust Ejector
March 3, 1955
2400 RPM
Full Throttle
2 3/4" x 8 1/8" Rect. Duct
45S + 0D
33S + 12D
21S + 24D
(Constant Total Length)
CFM
CFM
CFM
M_a/M_e
M_a/M_e
M_a/M_e
Cooling Air / Engine Air M_a/M_e
Cooling Air CFM
(1 Bank of 3 Cylinders)
Static Pressure Δp in. Water

Fig. 17

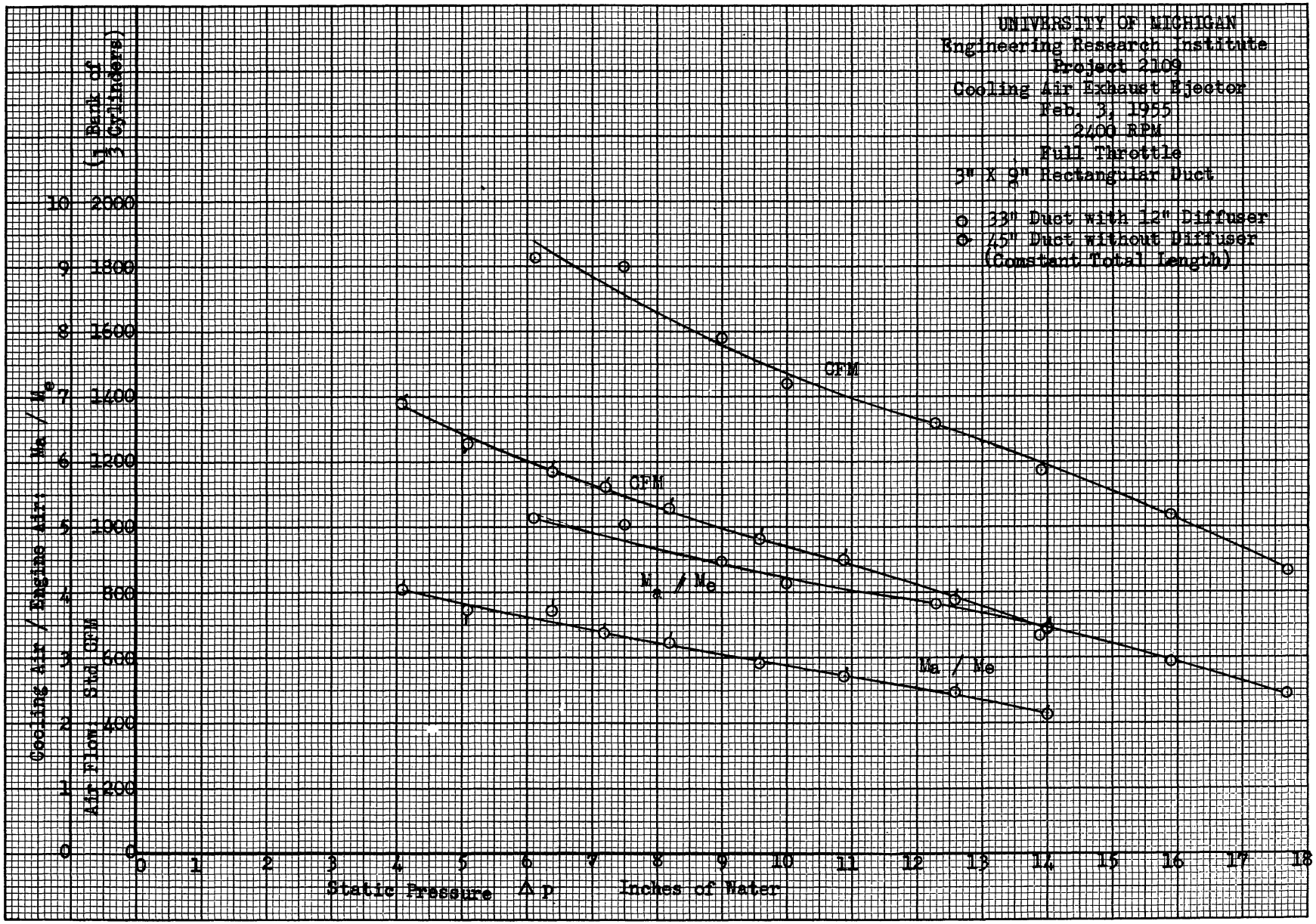
UNIVERSITY OF MICHIGAN
Engineering Research Institute
Project 2109
Cooling Air Exhaust Ejector
Feb. 3, 1955
2400 RPM
Full Throttle
3" X 9" Rectangular Duct
33" Duct with 12" Diffuser
45" Duct without Diffuser
(Constant Total Length)
CFM
CFM
Ma / Me
Ma / Me
Cooling air / Engine air: Ma / Me
Air Flow, Std CFM
Back of Cylinders (°F)
Static Pressure Δ p Inches of Water
0
1
2
3
4
5
6
7
8
9
10
11
12
13
14
15
16
17
18
200
400
600
800
1000
1200
1400
1600
1800
2000

Fig. 18

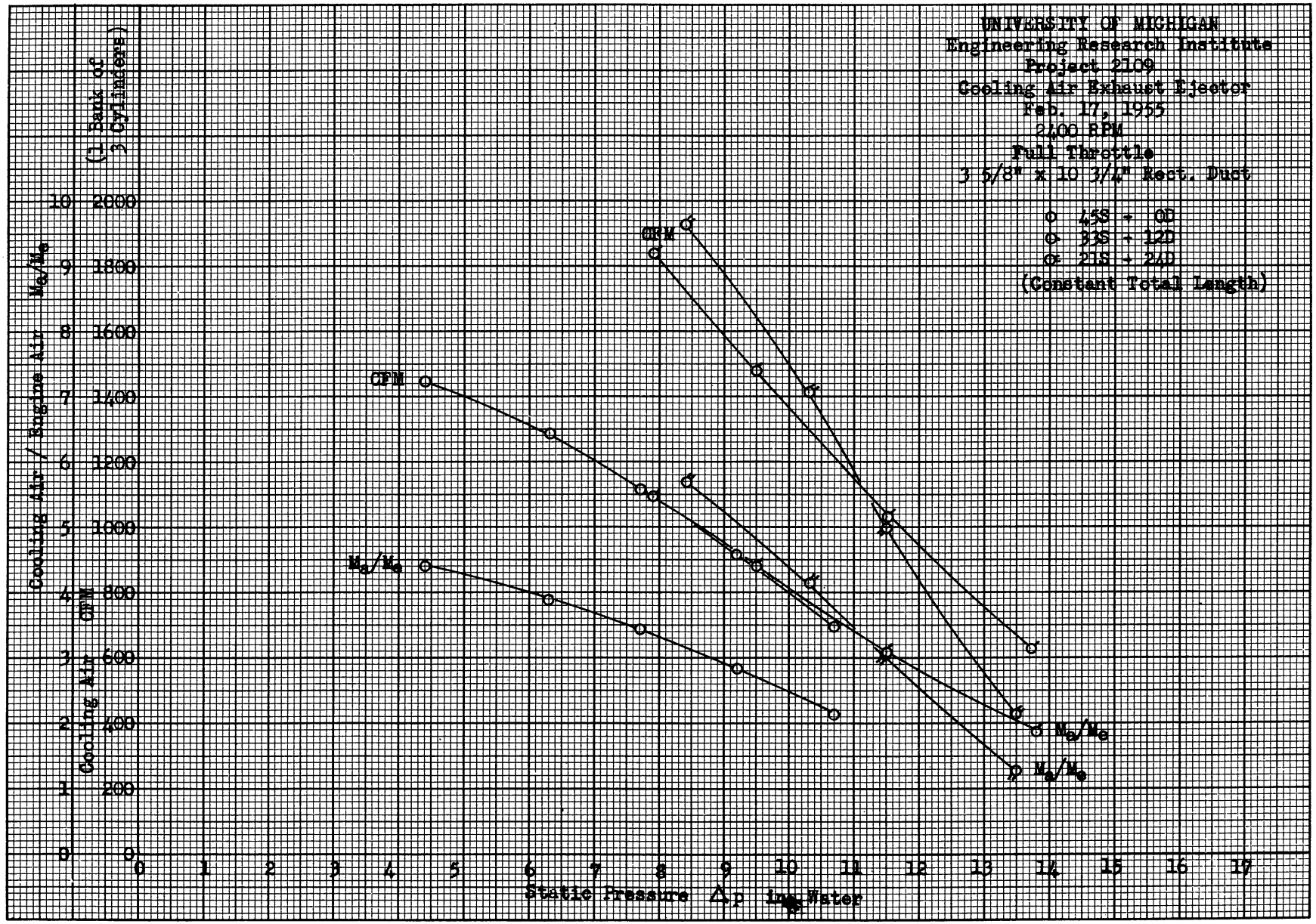
UNIVERSITY OF MICHIGAN
Engineering Research Institute
Project 2109
Cooling Air Exhaust Ejector
Feb. 17, 1955
2400 RPM
Full Throttle
3 5/8" x 10 3/4" Rect. Duct
o 45S + 0D
o 33S + 12D
o 21S + 24D
(Constant Total Length)
CFM
M_a/M_e
Cooling Air / Engine Air M_a/M_e
Cooling Air CFM (2 Banks of 3 Cylinders)
Static Pressure Δp Inches Water

Fig. 19

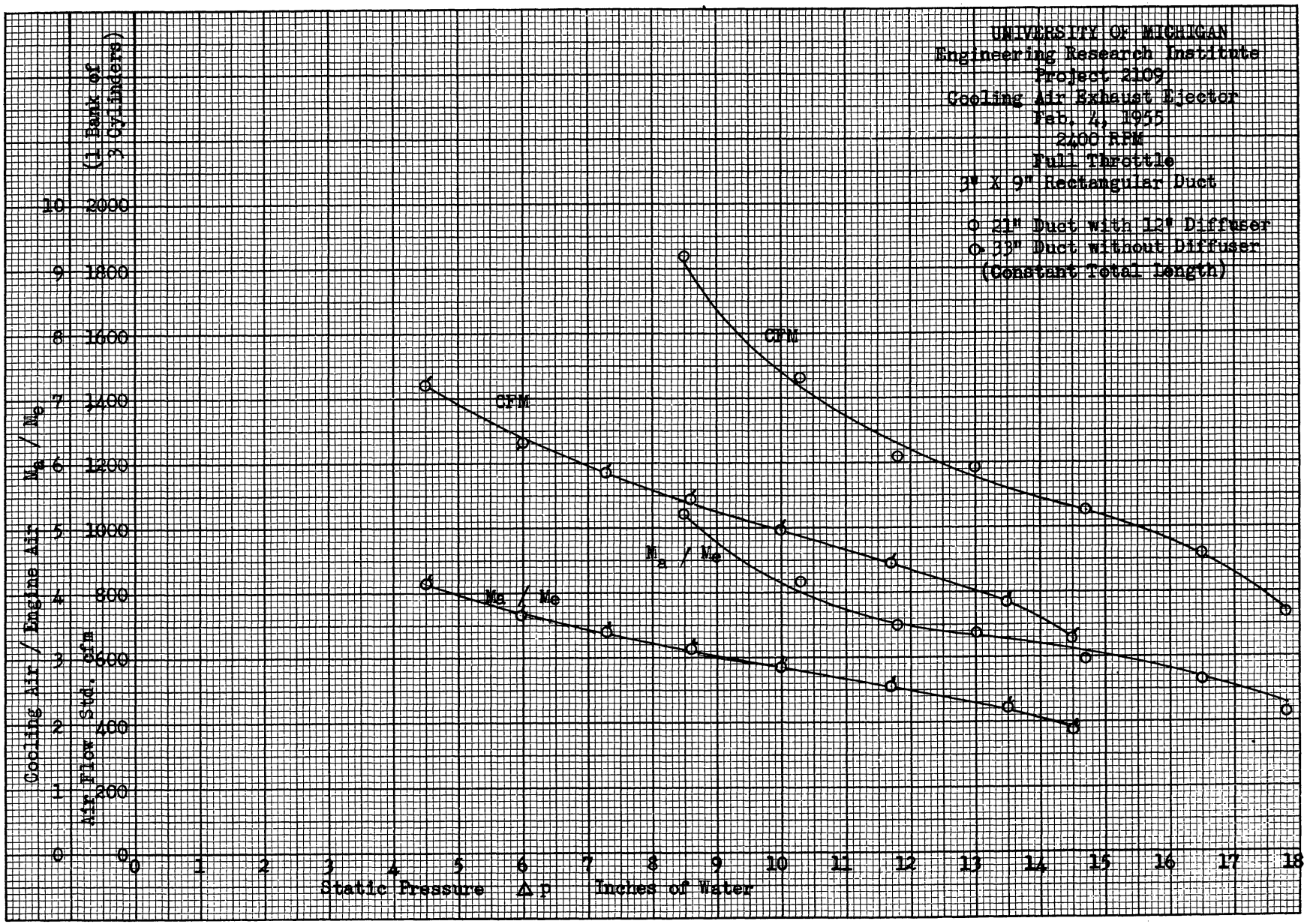
UNIVERSITY OF MICHIGAN
Engineering Research Institute
Project 2109
Cooling Air Exhaust Ejector
Feb. 4, 1955
2400 RPM
Full Throttle
3" X 9" Rectangular Duct
21" Duct with 12° Diffuser
33" Duct without Diffuser
(Constant Total Length)
CFM
CFM
M_a / M_e
M_a / M_e
Cooling Air / Engine Air M_a / M_e
Air Flow Std. cfm (1 Bank of 8 Cylinders)
Static Pressure Δp Inches of Water
0 1 2 3 4 5 6 7 8 9 10 11 12 13 14 15 16 17 18
0 200 400 600 800 1000 1200 1400 1600 1800 2000
0 1 2 3 4 5 6 7 8 9 10

Fig. 20

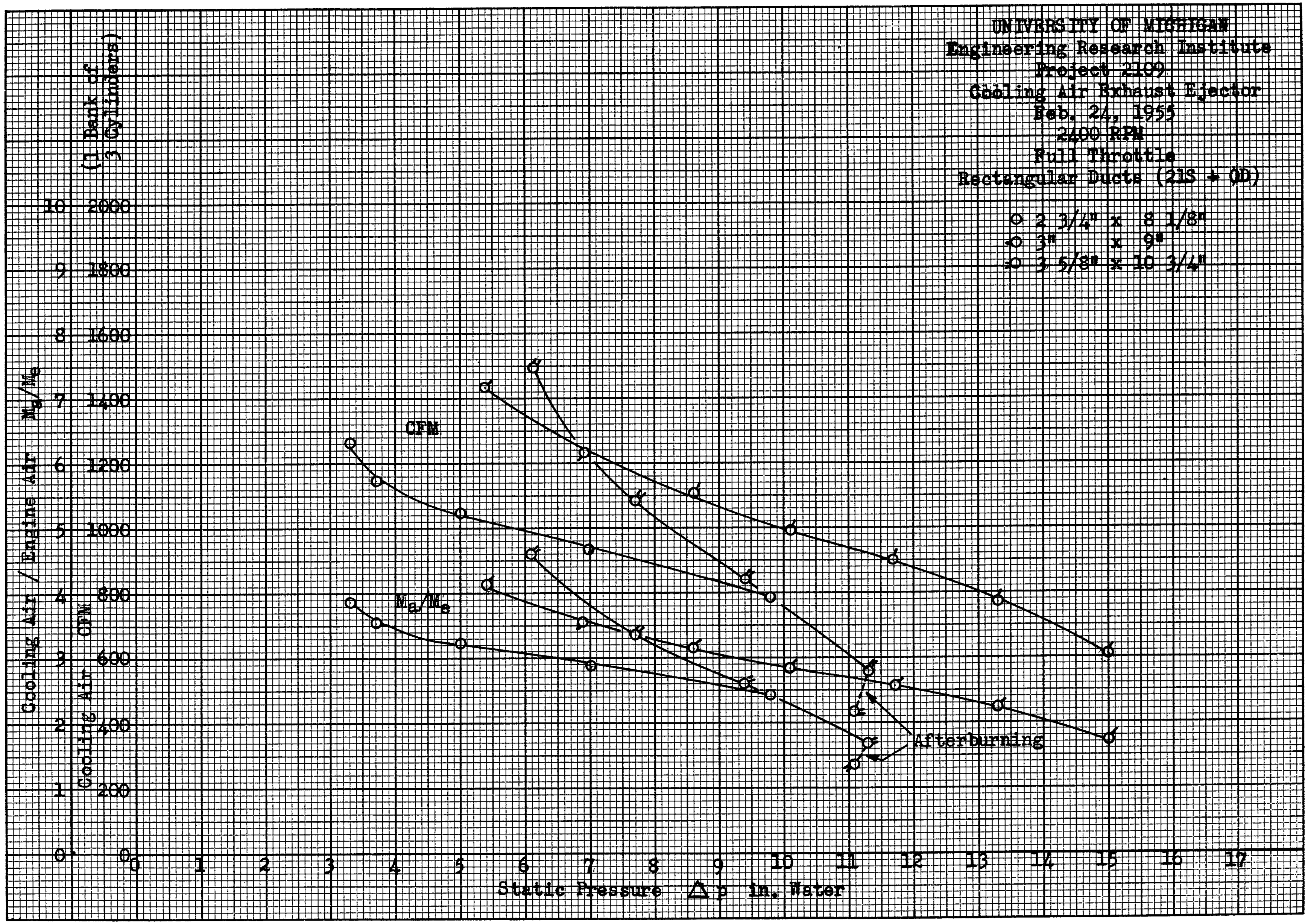
UNIVERSITY OF MICHIGAN
Engineering Research Institute
Project 2109
Cooling Air Exhaust Ejector
Feb. 24, 1955
2400 RPM
Full Throttle
Rectangular Ducts (21S + 0D)
2 3/4" x 8 1/8"
3" x 9"
3 5/8" x 10 3/4"
CFM
M_a/M_e
Afterburning
Cooling Air / Engine Air M_a/M_e
Cooling Air CFM
(1 Bank of 3 Cylinders)
Static Pressure Δp in. Water
0 1 2 3 4 5 6 7 8 9 10 11 12 13 14 15 16 17
0 200 400 600 800 1000 1200 1400 1600 1800 2000
0 1 2 3 4 5 6 7 8 9 10

Fig. 21

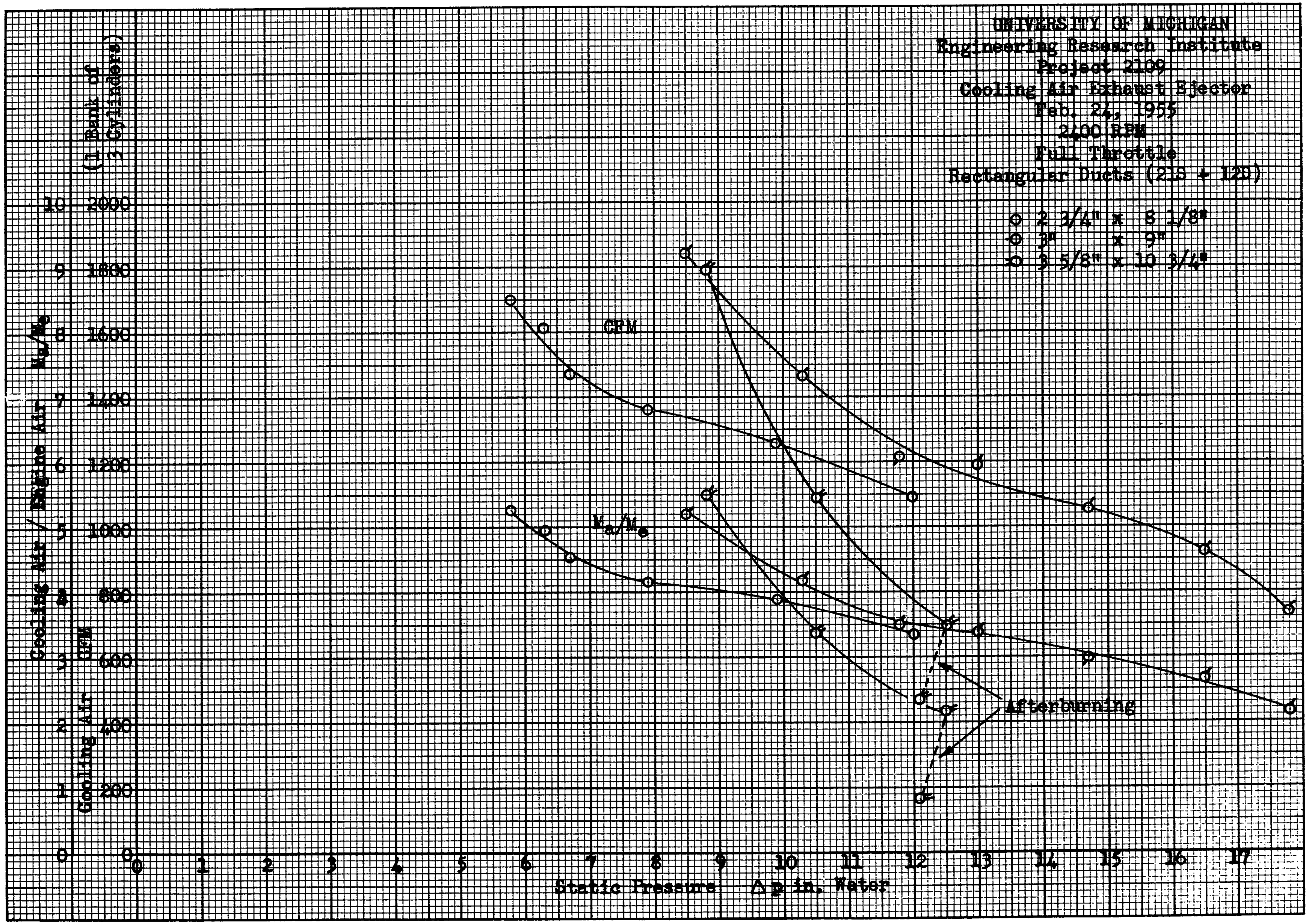
UNIVERSITY OF MICHIGAN
Engineering Research Institute
Project 2109
Cooling Air Exhaust Ejector
Feb. 24, 1955
2400 RPM
Full Throttle
Rectangular Ducts (21S + 12D)
2 3/4" x 8 1/8"
3" x 9"
3 5/8" x 10 3/4"
CFM
M_a/M_e
Afterburning
Cooling Air / Engine Air M_a/M_e
Cooling Air CFM
(1 Bank of 3 Cylinders)
Static Pressure Δp in. Water
0
1
2
3
4
5
6
7
8
9
10
11
12
13
14
15
16
17
200
400
600
800
1000
1200
1400
1600
1800
2000

Fig. 22

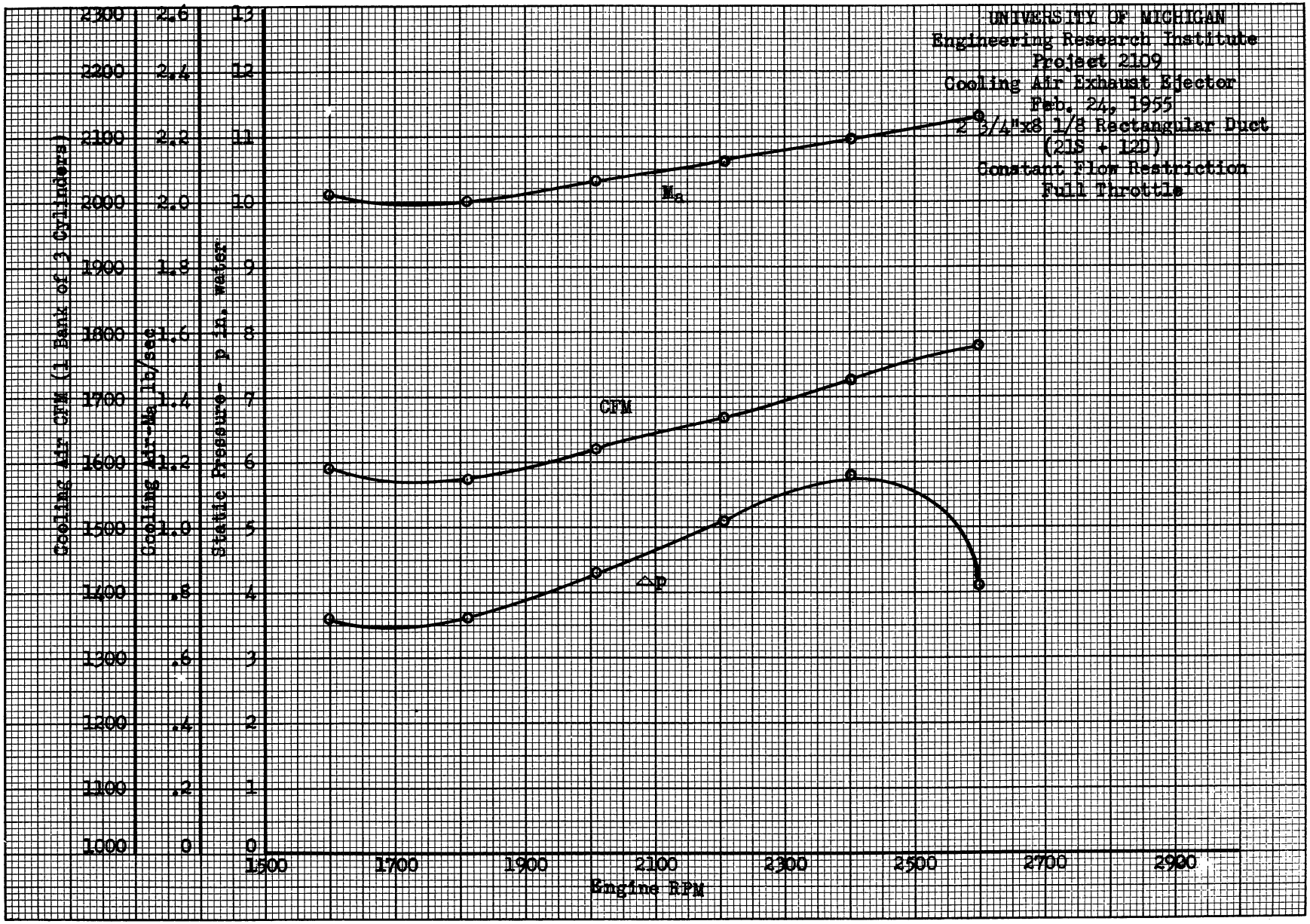
UNIVERSITY OF MICHIGAN
Engineering Research Institute
Project 2109
Cooling Air Exhaust Ejector
Feb. 24, 1955
2 3/4"x8 1/8 Rectangular Duct
(21S + 12D)
Constant Flow Restriction
Full Throttle
Cooling Air CFM (1 Bank of 3 Cylinders)
Cooling Air Wt. lb/sec
Static Pressure - p.s.i. Water
Engine RPM
CFM
ΔP
M_a
2300
2200
2100
2000
1900
1800
1700
1600
1500
1400
1300
1200
1100
1000
2.6
2.4
2.2
2.0
1.8
1.6
1.4
1.2
1.0
.8
.6
.4
.2
0
13
12
11
10
9
8
7
6
5
4
3
2
1
0
1500
1700
1900
2100
2300
2500
2700
2900

Fig. 23

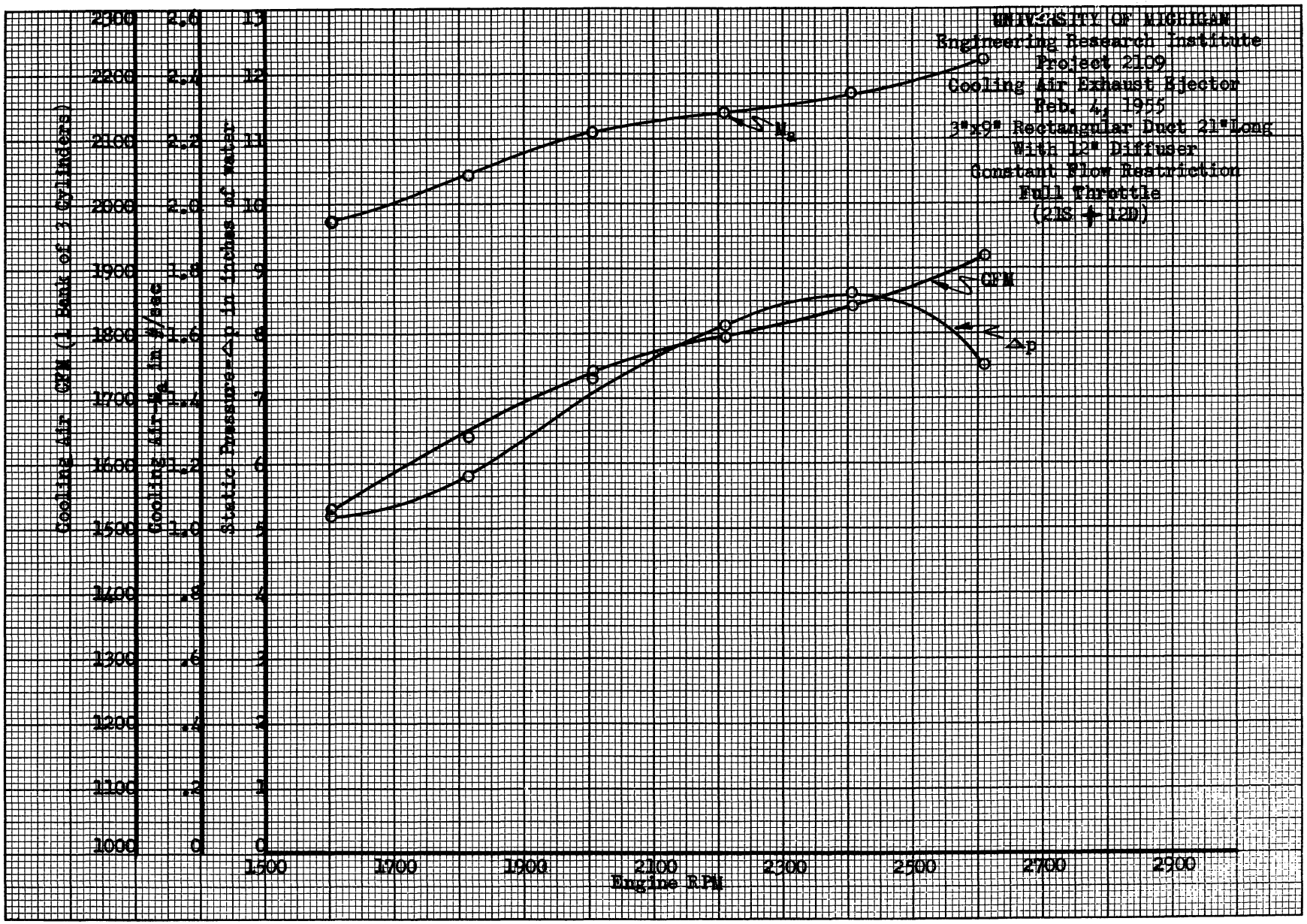
UNIVERSITY OF MICHIGAN
Engineering Research Institute
Project 2109
Cooling Air Exhaust Ejector
Feb. 4, 1955
3"x9" Rectangular Duct 21"Long
With 12° Diffuser
Constant Flow Restriction
Full Throttle
(2IS + 12D)
Ma
CFM
Δp
Cooling air, CFM (1 Bank of 3 Cylinders)
Duct Mach No.
Static Pressure, Δp, Inches Water
Engine RPM
2300
2200
2100
2000
1900
1800
1700
1600
1500
1400
1300
1200
1100
1000
2.6
2.4
2.2
2.0
1.8
1.6
1.4
1.2
1.0
.8
.6
.4
.2
0
13
12
11
10
9
8
7
6
5
4
3
2
1
0
1500
1700
1900
2100
2300
2500
2700
2900

Fig. 24

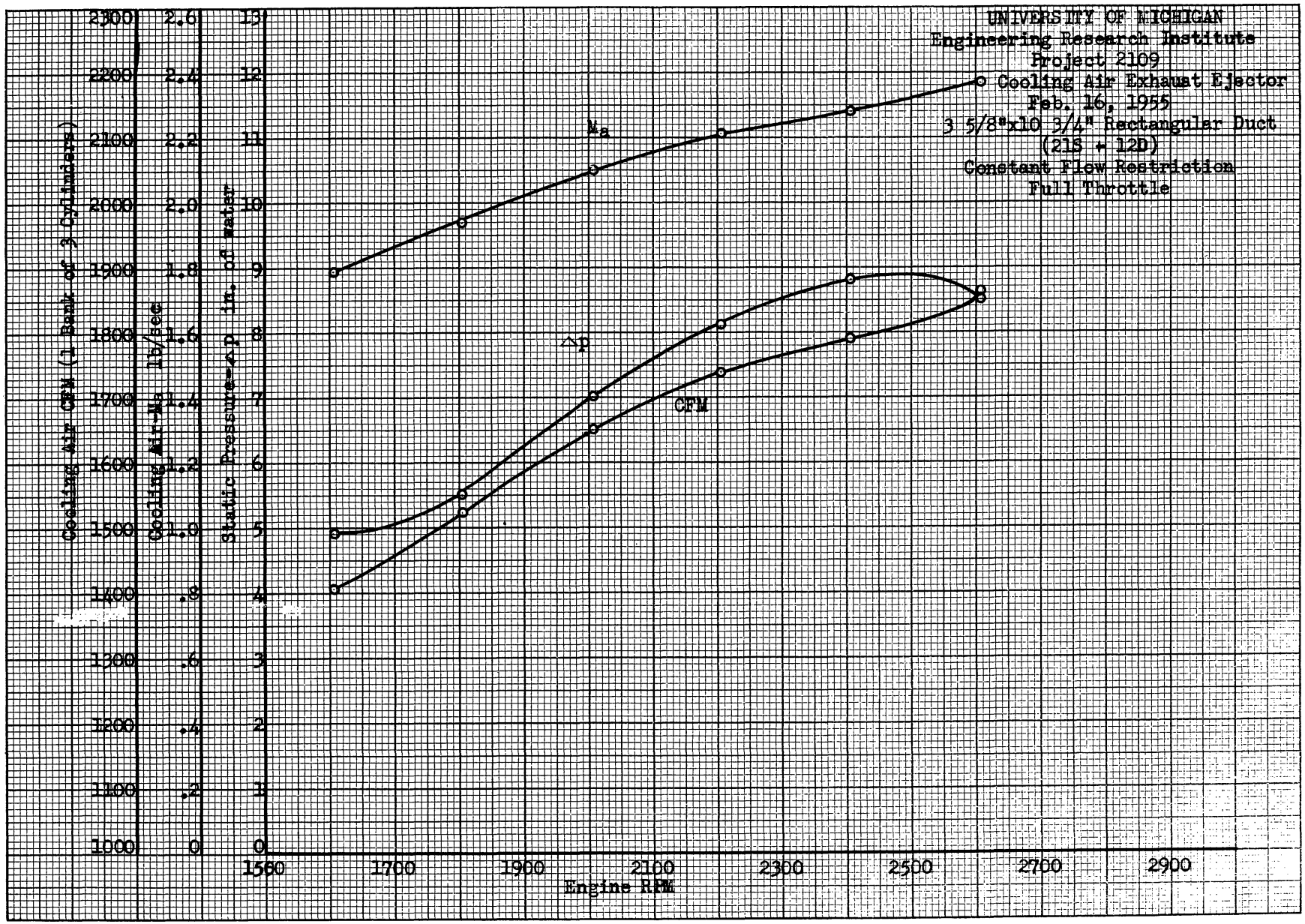
UNIVERSITY OF MICHIGAN
Engineering Research Institute
Project 2109
Cooling Air Exhaust Ejector
Feb. 16, 1955
3 5/8"x10 3/4" Rectangular Duct
(21S + 12D)
Constant Flow Restriction
Full Throttle
Cooling Air CFM (1 Bank of 3 Cylinders)
Cooling Air-Ma lb/sec
Static Pressure-s.p. in. of water
Engine RPM
Ma
ΔP
CFM
2300
2200
2100
2000
1900
1800
1700
1600
1500
1400
1300
1200
1100
1000
2.6
2.4
2.2
2.0
1.8
1.6
1.4
1.2
1.0
.8
.6
.4
.2
0
15
12
11
10
9
8
7
6
5
4
3
2
1
0
1500
1700
1900
2100
2300
2500
2700
2900

Fig. 25

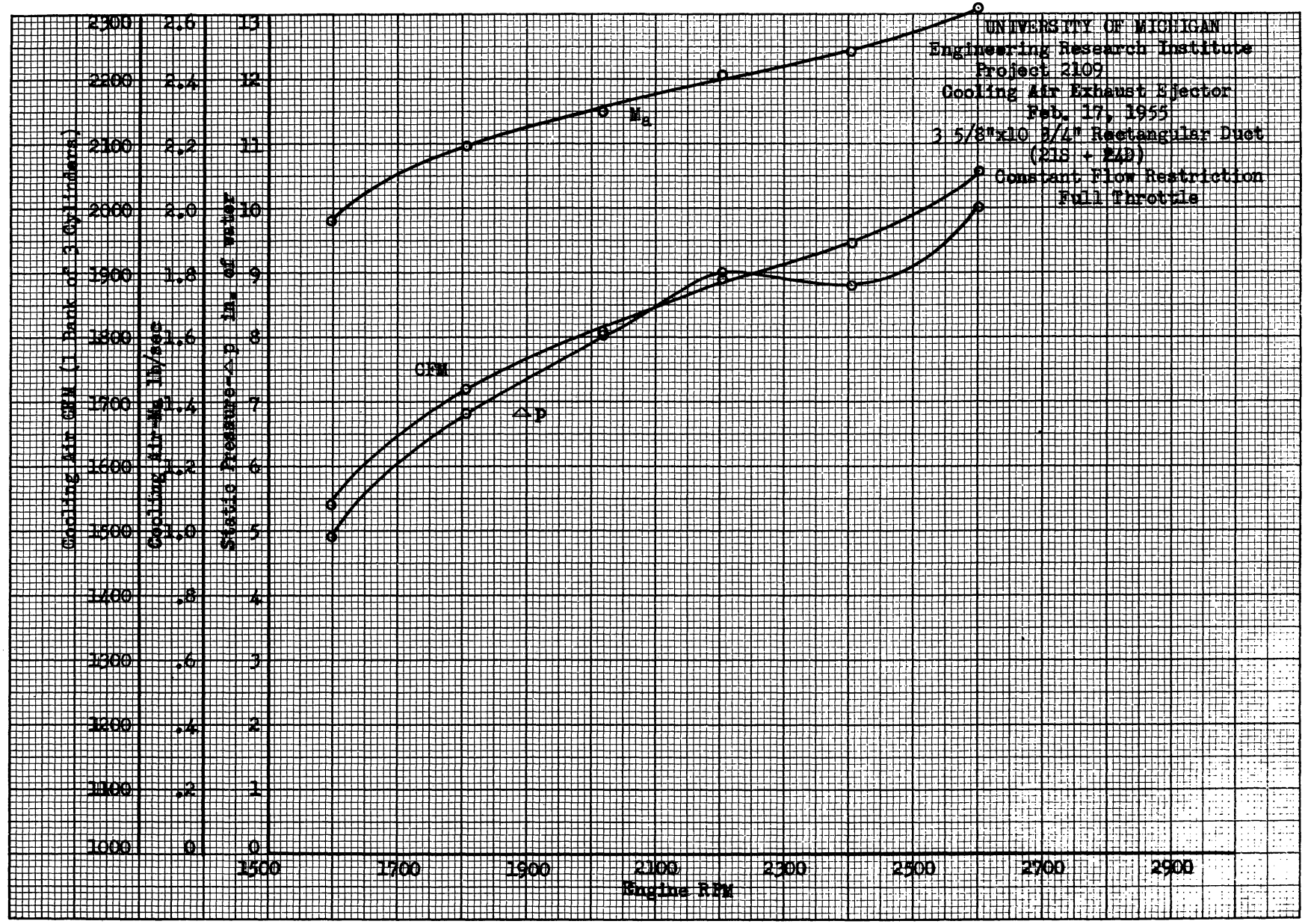
UNIVERSITY OF MICHIGAN
Engineering Research Institute
Project 2109
Cooling Air Exhaust Ejector
Feb. 17, 1955
3 5/8"x10 3/4" Rectangular Duct
(218 + 240)
Constant Flow Restriction
Full Throttle
Cooling Air CFM (1 bank of 3 cylinders)
Cooling Air Velocity ft/sec
Static Pressure-Δp in. of water
Engine RPM
CFM
Δp
M_a
2300
2200
2100
2000
1900
1800
1700
1600
1500
1400
1300
1200
1100
1000
2.6
2.4
2.2
2.0
1.8
1.6
1.4
1.2
1.0
.8
.6
.4
.2
0
13
12
11
10
9
8
7
6
5
4
3
2
1
0
1500
1700
1900
2100
2300
2500
2700
2900

Fig. 26

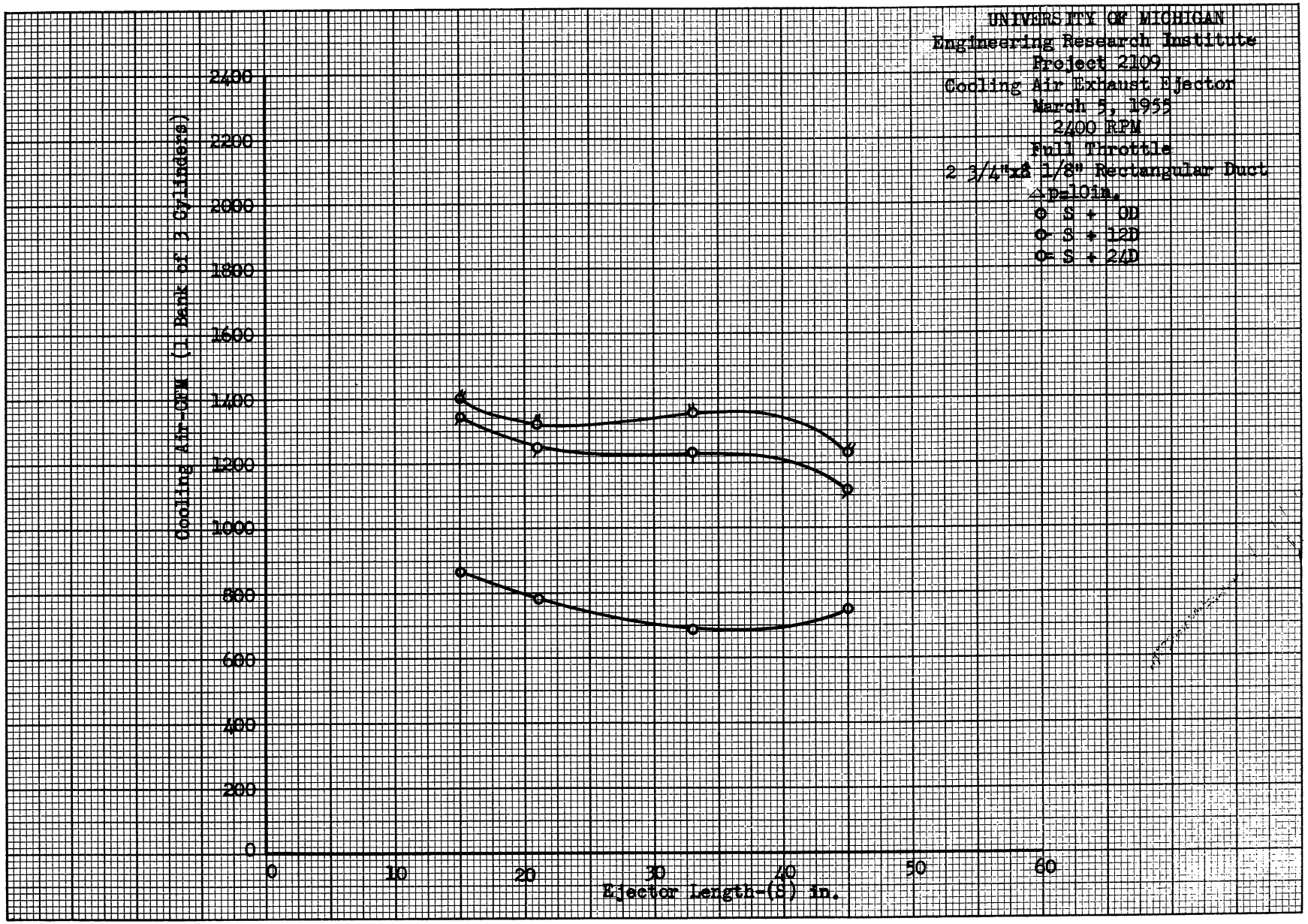
UNIVERSITY OF MICHIGAN
Engineering Research Institute
Project 2109
Cooling Air Exhaust Ejector
March 5, 1955
2400 RPM
Full Throttle
2 3/4"x 1/8" Rectangular Duct
△p=10in.
S + OD
S + 12D
S + 24D
Cooling Air-CFM (1 Bank of 3 Cylinders)
2400
2200
2000
1800
1600
1400
1200
1000
800
600
400
200
0
0
10
20
30
40
50
60
Ejector Length-(S) in.

Fig. 27

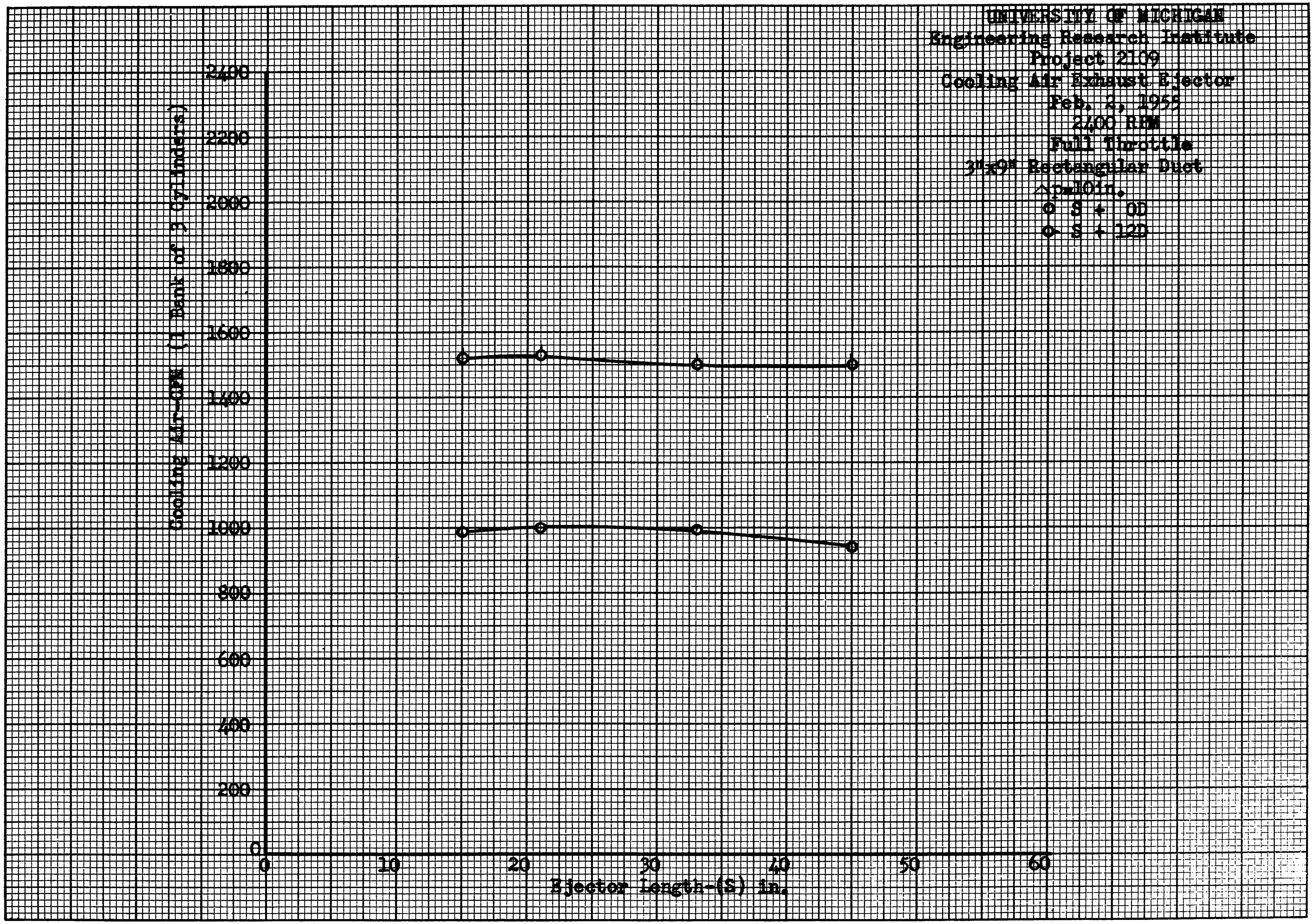
UNIVERSITY OF MICHIGAN
Engineering Research Institute
Project 2109
Cooling Air Exhaust Ejector
Feb. 2, 1955
2400 RPM
Full Throttle
3"x9" Rectangular Duct
Δp=10in.
S + 0D
S + 12D
Cooling Air-CFM (1 Bank of 3 Cylinders)
0
200
400
600
800
1000
1200
1400
1600
1800
2000
2200
2400
0
10
20
30
40
50
60
Ejector Length-(S) in.

Fig. 28

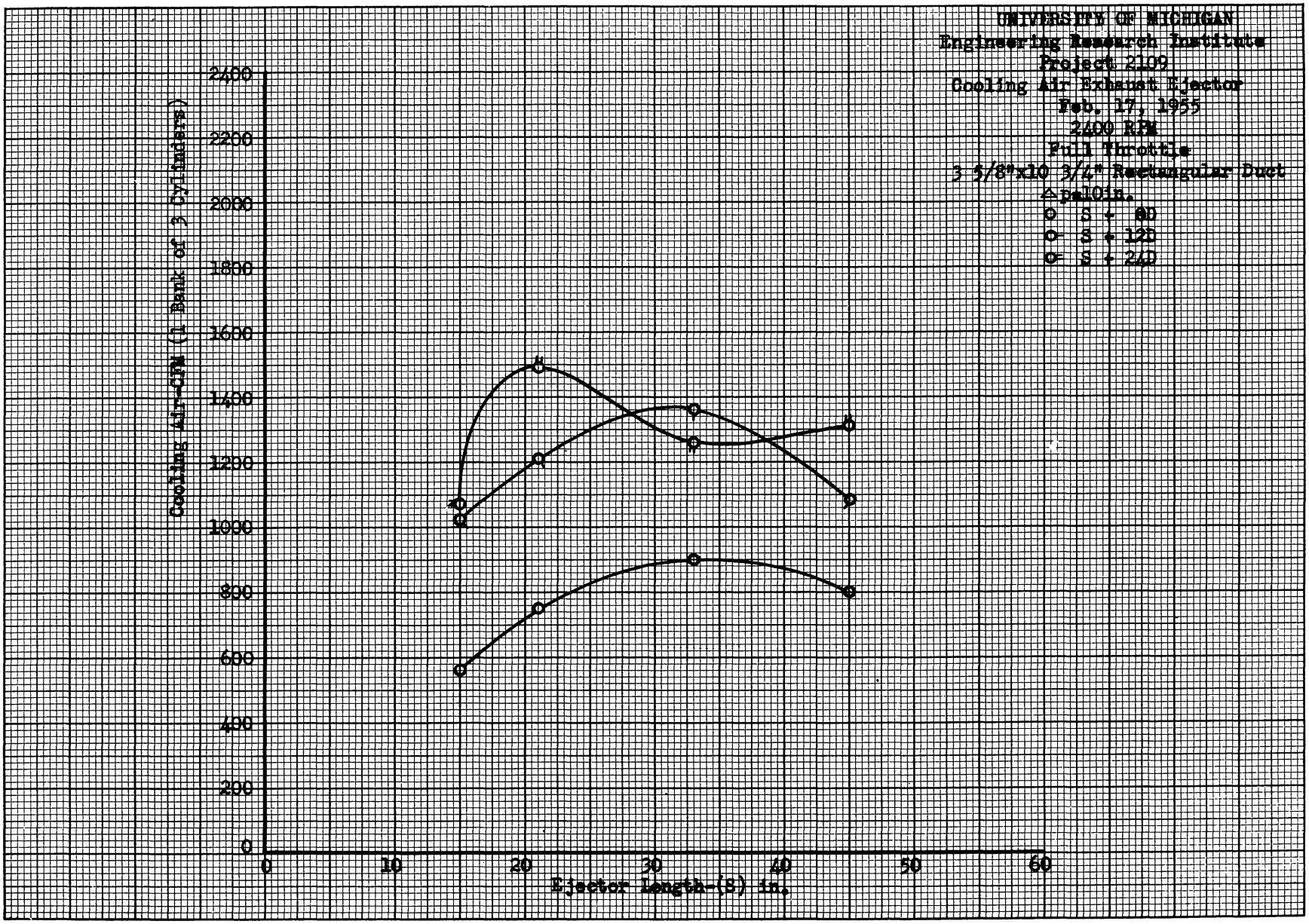
UNIVERSITY OF MICHIGAN
Engineering Research Institute
Project 2109
Cooling Air Exhaust Ejector
Feb. 17, 1955
2400 RPM
Full Throttle
3 5/8"x10 3/4" Rectangular Duct
Δpe10 in.
S + 00
S + 120
S + 240
Cooling Air-CFM (1 Bank of 3 Cylinders)
2400
2200
2000
1800
1600
1400
1200
1000
800
600
400
200
0
0
10
20
30
40
50
60
Ejector Length-(S) in.

Fig. 29

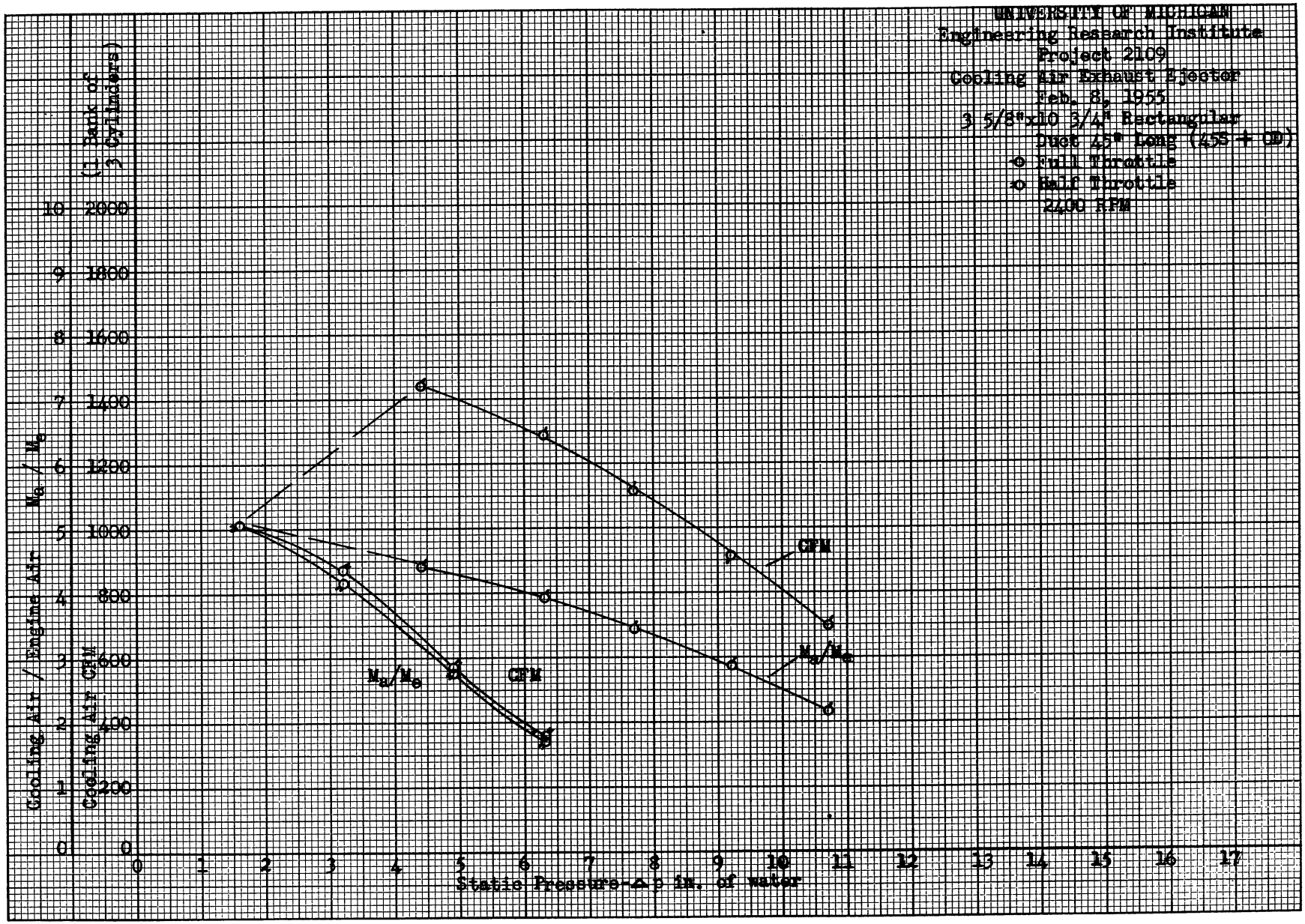
UNIVERSITY OF MICHIGAN
Engineering Research Institute
Project 2109
Cooling Air Exhaust Ejector
Feb. 8, 1955
3 5/8"x10 3/4" Rectangular
Duct 45° Long (45S + OD)
Full Throttle
Half Throttle
2400 RPM
(1 Bank of 3 Cylinders)
Cooling Air / Engine Air
Ma / Me
Cooling Air CFM
Ma/Me
CFM
Ma/Me
CFM
Static Pressure-Δp in. of water
0
1
2
3
4
5
6
7
8
9
10
11
12
13
14
15
16
17
200
400
600
800
1000
1200
1400
1600
1800
2000

Fig. 30

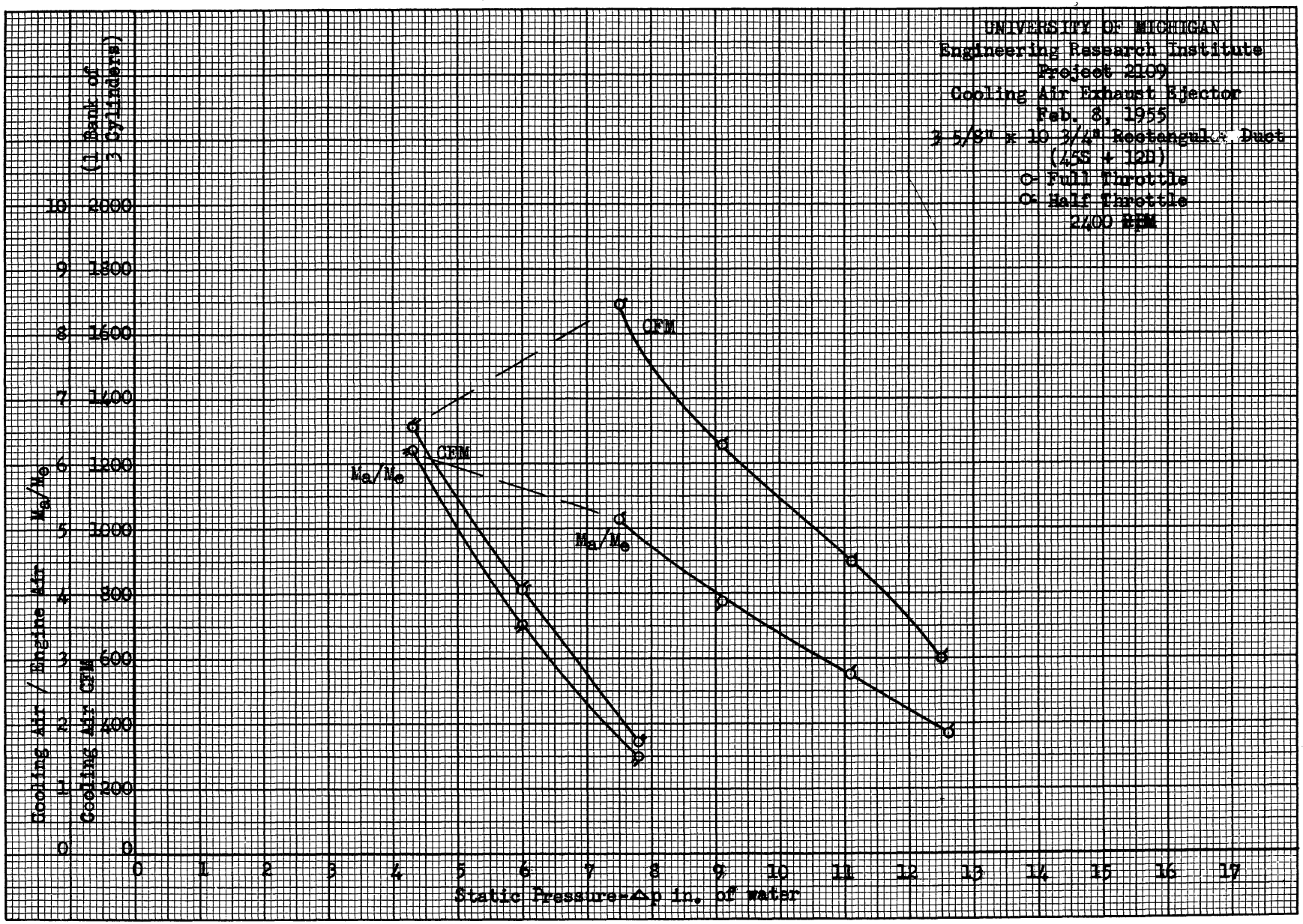
UNIVERSITY OF MICHIGAN
Engineering Research Institute
Project 2109
Cooling Air Exhaust Ejector
Feb. 8, 1955
2 5/8" x 10 3/4" Rectangular Duct
(4.5S + 12D)
C- Full Throttle
C½ Half Throttle
2400 RPM
CFM
M_a/M_e
Cooling Air CFM (1 Bank 3 Cylinders)
Cooling air / Engine air M_a/M_e
Static Pressure-Δp in. of water
0
200
400
600
800
1000
1200
1400
1600
1800
2000
1
2
3
4
5
6
7
8
9
10
11
12
13
14
15
16
17

Fig. 31

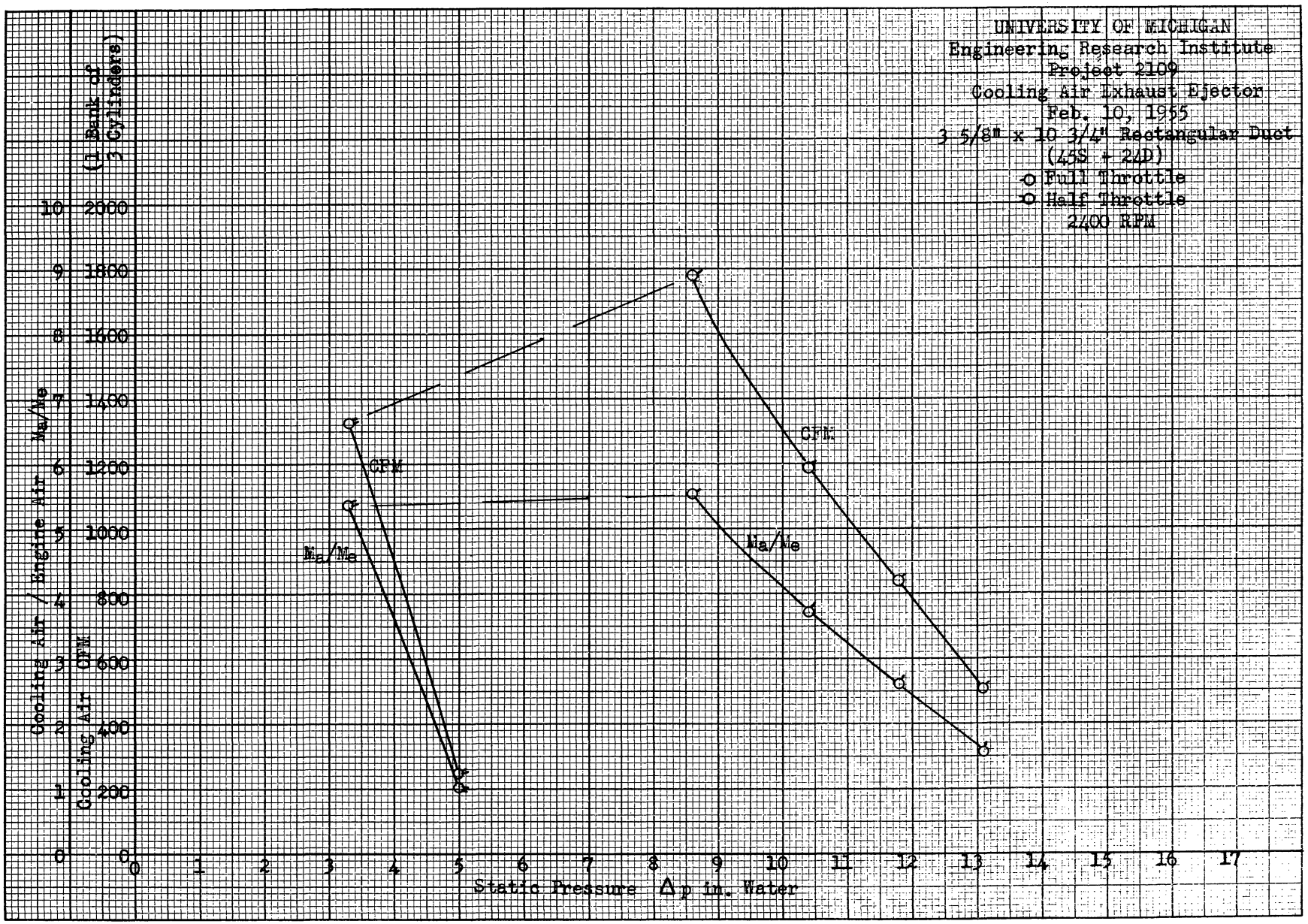
UNIVERSITY OF MICHIGAN
Engineering Research Institute
Project 2109
Cooling Air Exhaust Ejector
Feb. 10, 1955
3 5/8" x 10 3/4" Rectangular Duct
(4S + 2D)
Full Throttle
Half Throttle
2400 RPM
Cooling Air / Engine Air Wa/We
(1 Bank of 3 Cylinders)
Cooling Air CFM
CFM
Wa/We
Wa/We
Static Pressure Δp in. Water
0
1
2
3
4
5
6
7
8
9
10
11
12
13
14
15
16
17
200
400
600
800
1000
1200
1400
1600
1800
2000

Fig. 32

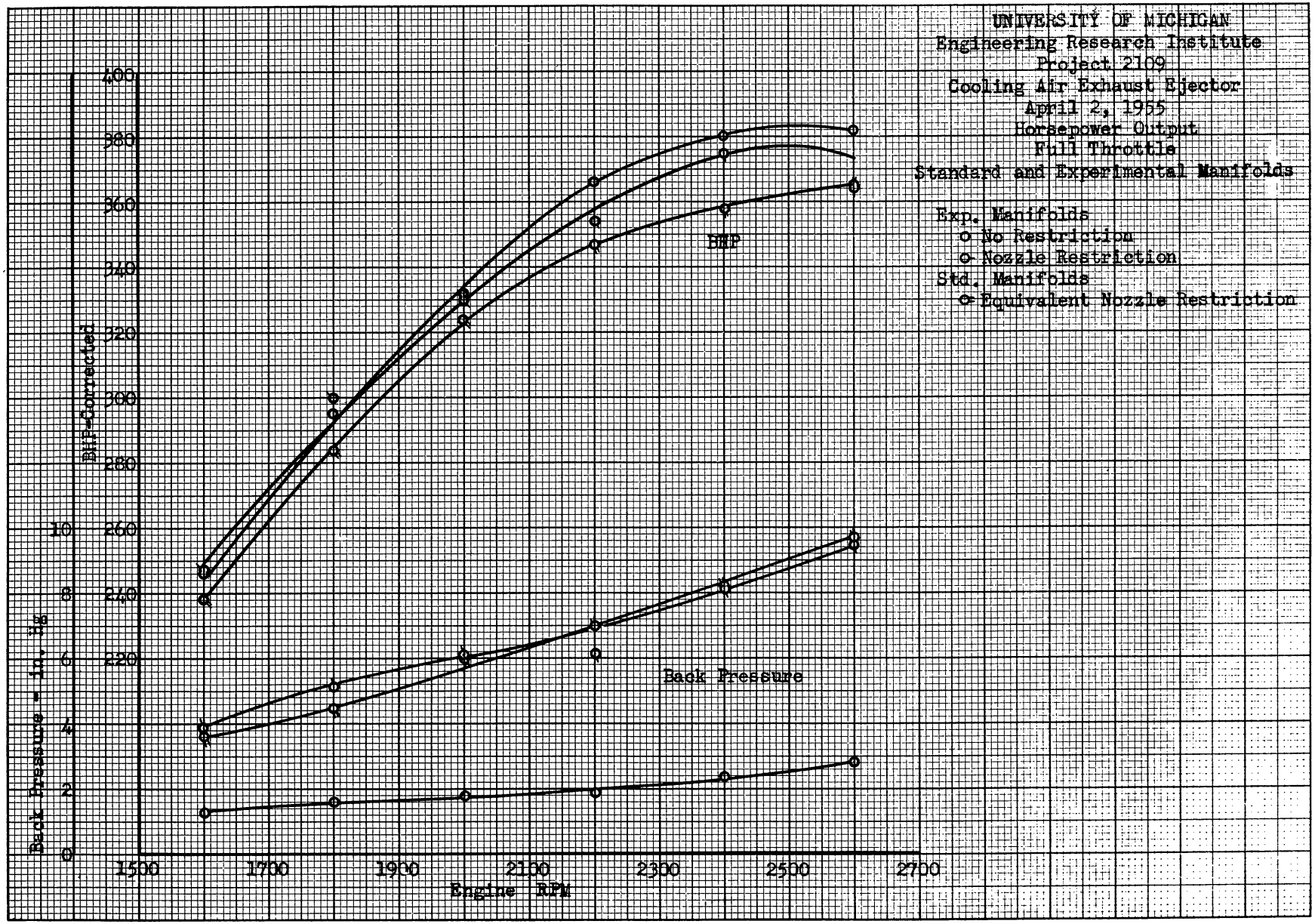
UNIVERSITY OF MICHIGAN
Engineering Research Institute
Project 2109
Cooling Air Exhaust Ejector
April 2, 1955
Horsepower Output
Full Throttle
Standard and Experimental Manifolds
Exp. Manifolds
No Restriction
Nozzle Restriction
Std. Manifolds
Equivalent Nozzle Restriction
BHP
Back Pressure
BHP-Corrected
Back Pressure - in. Hg
Engine RPM
400
380
360
340
320
300
280
260
240
220
10
8
6
4
2
0
1500
1700
1900
2100
2300
2500
2700

Fig. 33

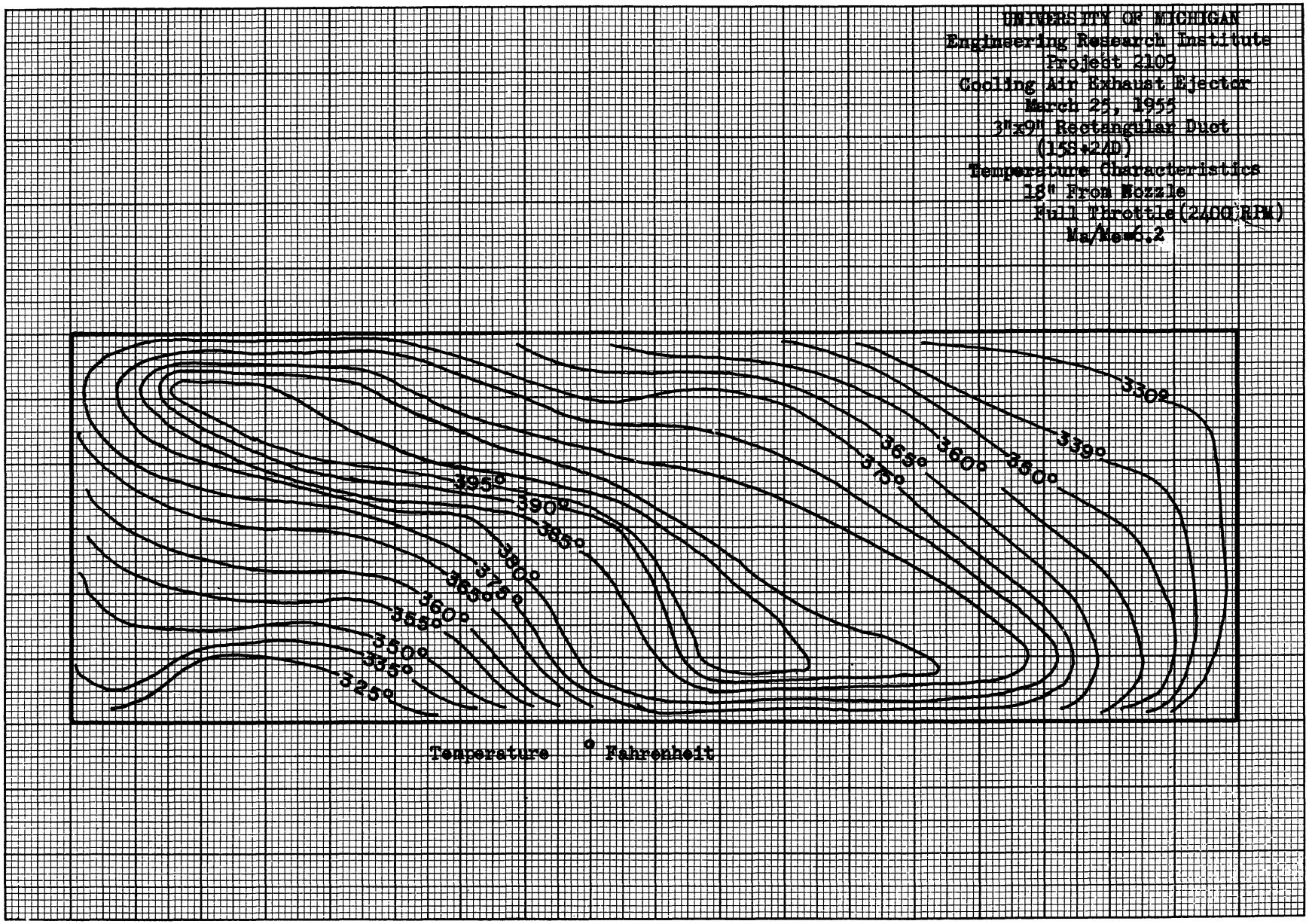
UNIVERSITY OF MICHIGAN
Engineering Research Institute
Project 2109
Cooling Air Exhaust Ejector
March 25, 1955
3"x9" Rectangular Duct
(158.2D)
Temperature Characteristics
18" From Nozzle
Full Throttle (2400 RPM)
Ma/Mo=6.2
395°
390°
385°
380°
375°
370°
365°
360°
355°
350°
345°
325°
330°
335°
340°
345°
350°
355°
360°
365°
370°
375°
Temperature ° Fahrenheit

Fig. 34

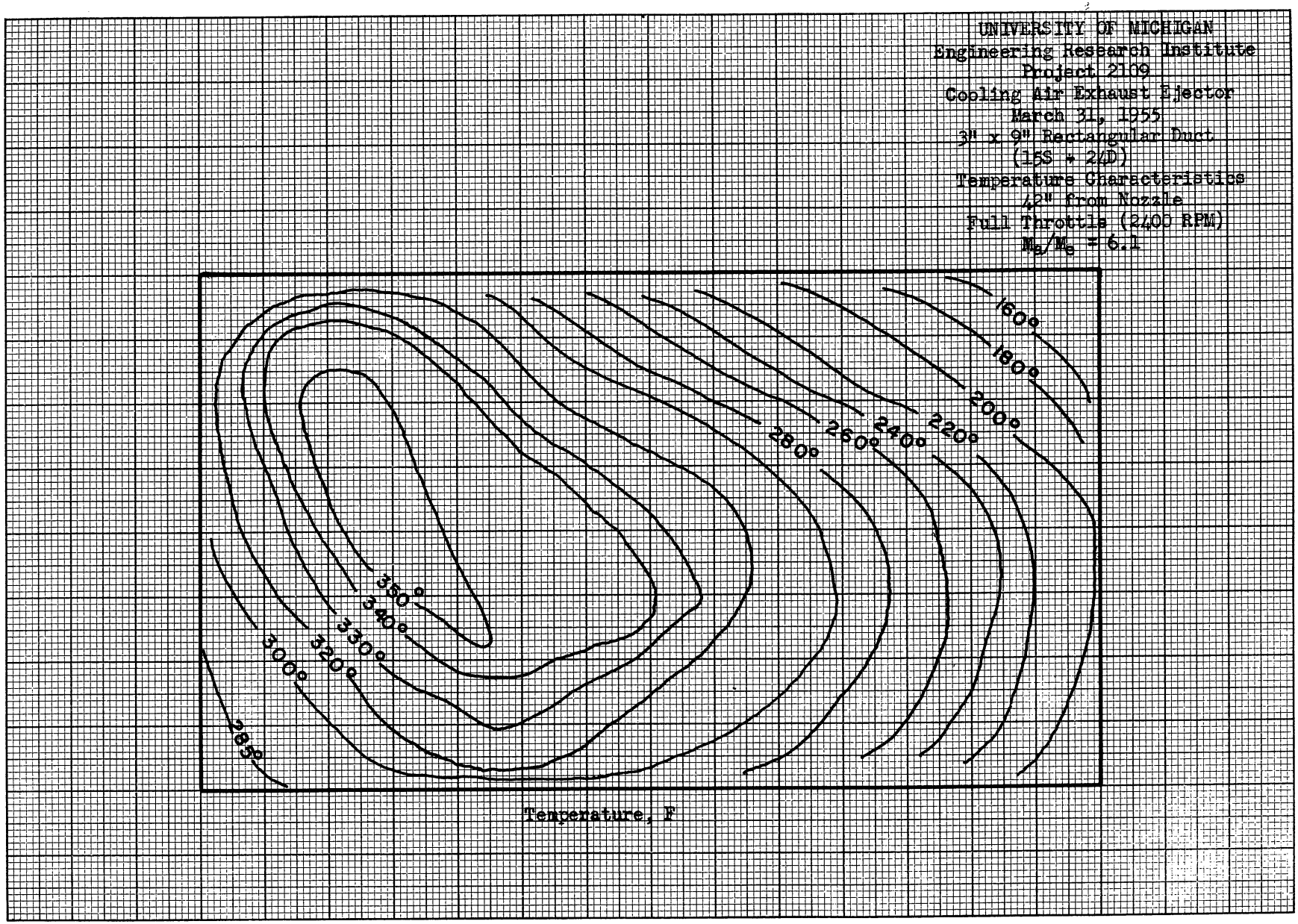
UNIVERSITY OF MICHIGAN
Engineering Research Institute
Project 2109
Cooling Air Exhaust Ejector
March 31, 1955
3" x 9" Rectangular Duct
(1S + 2D)
Temperature Characteristics
42" from Nozzle
Full Throttle (2400 RPM)
M_s/M_e = 6.1
1600
1800
2000
2200
2400
2600
2800
3000
3200
3300
3400
3600
Temperature, F

Fig. 35

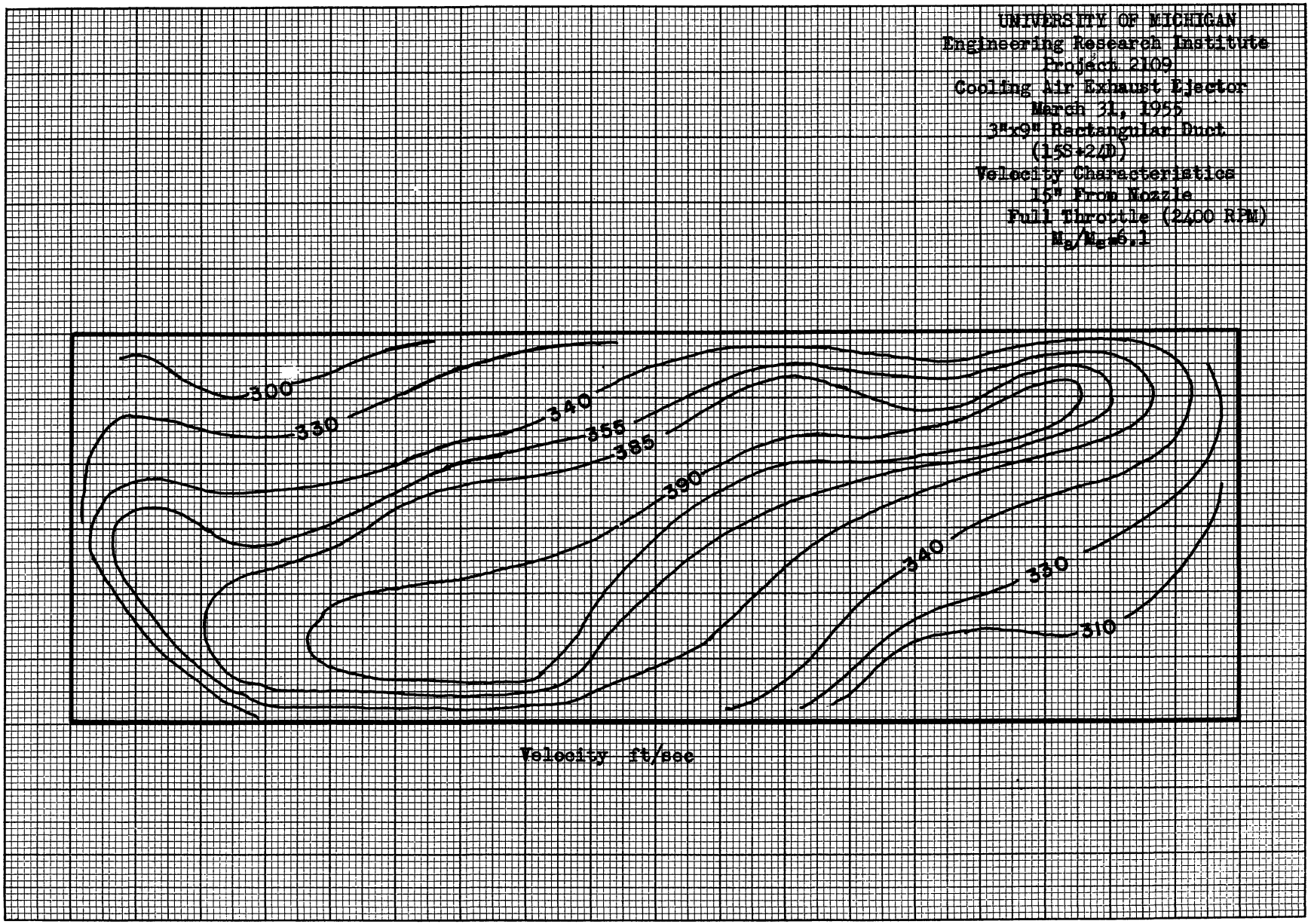
UNIVERSITY OF MICHIGAN
Engineering Research Institute
Project 2109
Cooling Air Exhaust Ejector
March 31, 1955
3"x9" Rectangular Duct
(158+24D)
Velocity Characteristics
15" From Nozzle
Full Throttle (2400 R.P.M)
M_s/M_e=6.1
300
330
340
355
365
390
340
330
310
Velocity ft/sec

Fig. 36

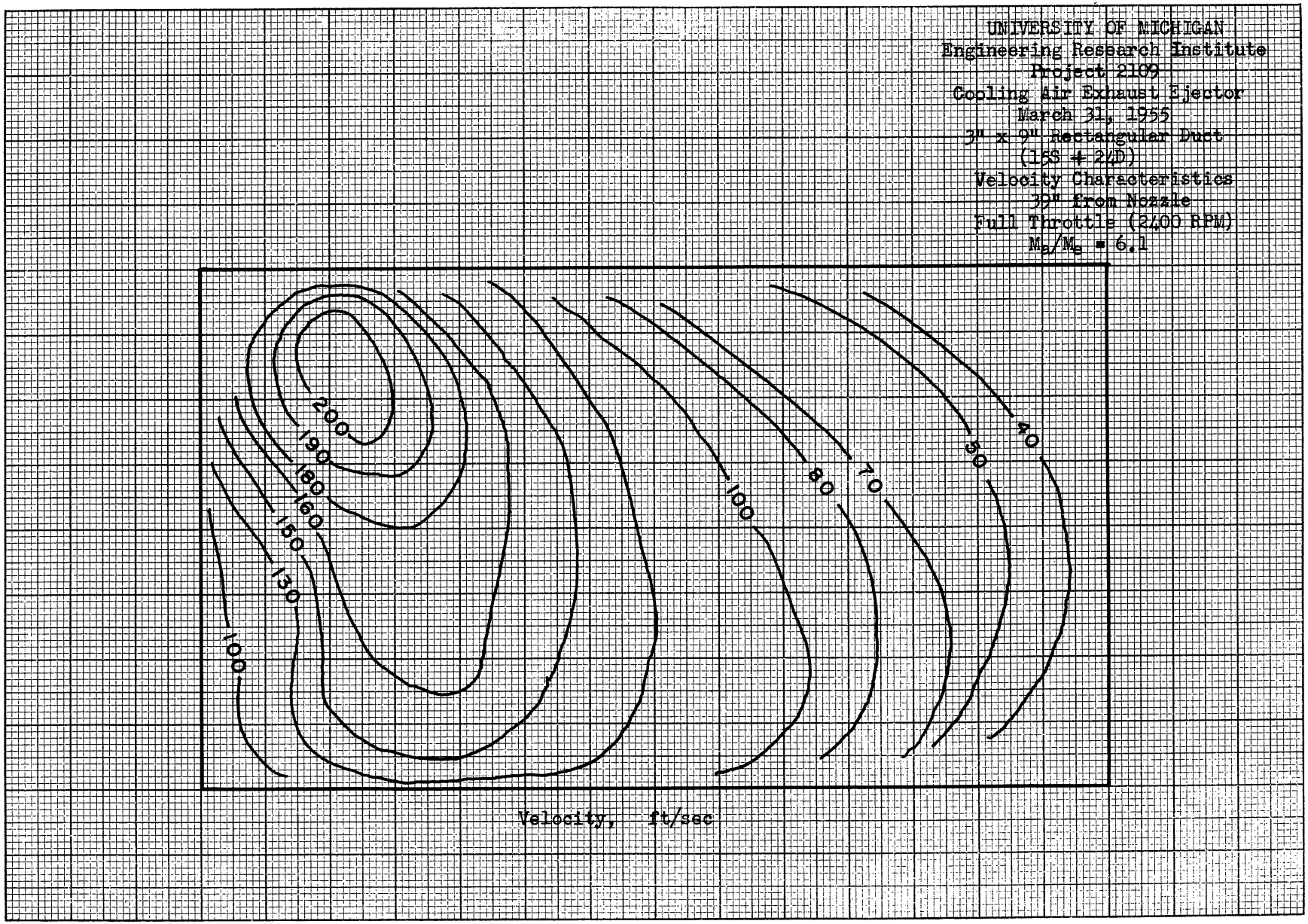
UNIVERSITY OF MICHIGAN
Engineering Research Institute
Project 2109
Cooling Air Exhaust Ejector
March 31, 1955
3" x 9" Rectangular Duct
(1S + 2D)
Velocity Characteristics
39" from Nozzle
Full Throttle (2400 RPM)
M_a/M_s = 6.1
200
190
180
170
160
150
140
130
120
110
100
90
80
70
60
50
40
Velocity, ft/sec

Fig. 37

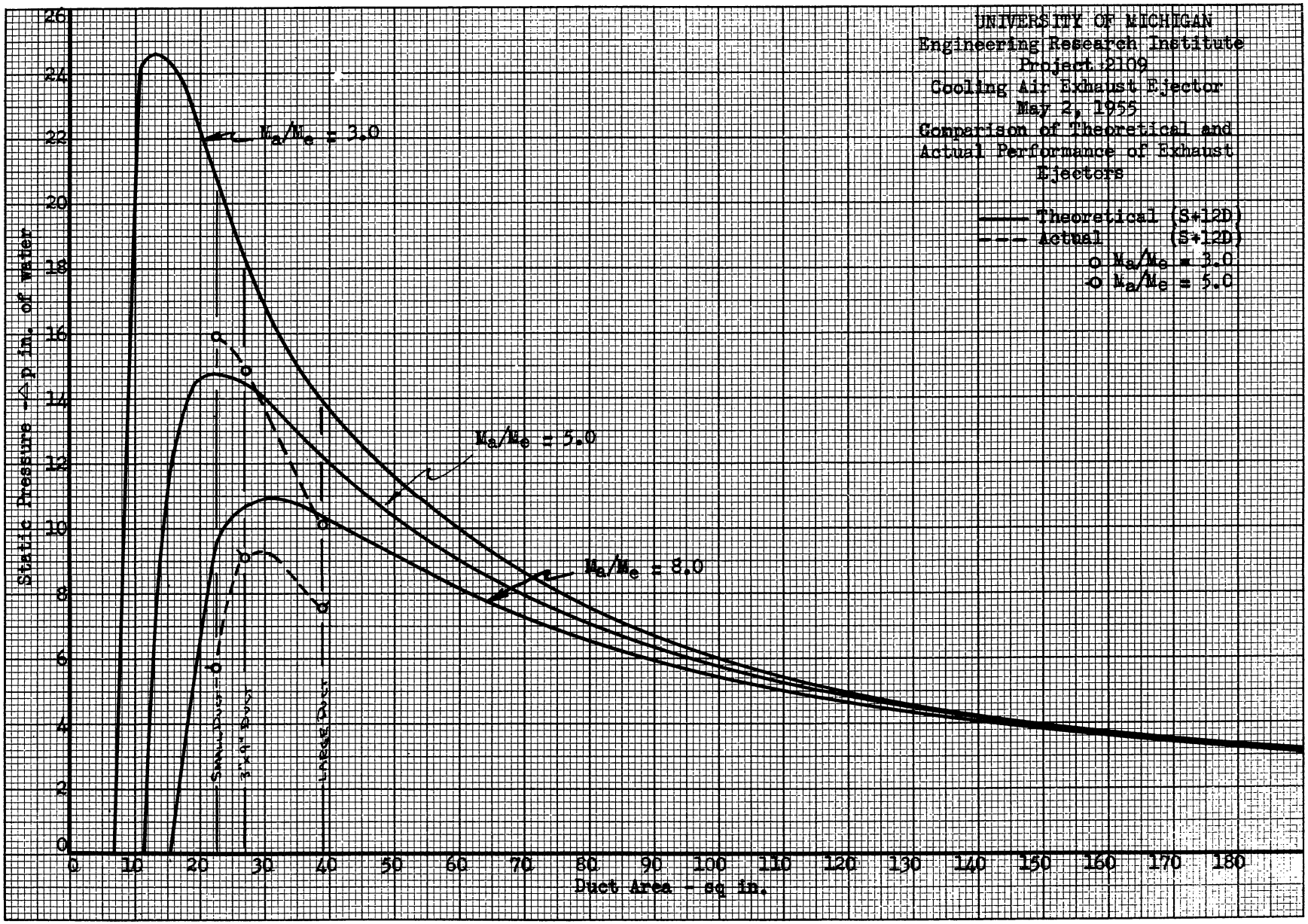
UNIVERSITY OF MICHIGAN
Engineering Research Institute
Project 2109
Cooling Air Exhaust Ejector
May 2, 1955
Comparison of Theoretical and Actual Performance of Exhaust Ejectors
Theoretical (S+12D)
Actual (S+12D)
M_a/M_e = 3.0
M_a/M_e = 5.0
M_a/M_e = 3.0
M_a/M_e = 5.0
M_a/M_e = 8.0
Static Pressure - ΔP in. of Water
Duct Area - sq in.
0
2
4
6
8
10
12
14
16
18
20
22
24
26
0
10
20
30
40
50
60
70
80
90
100
110
120
130
140
150
160
170
180

Fig. 38

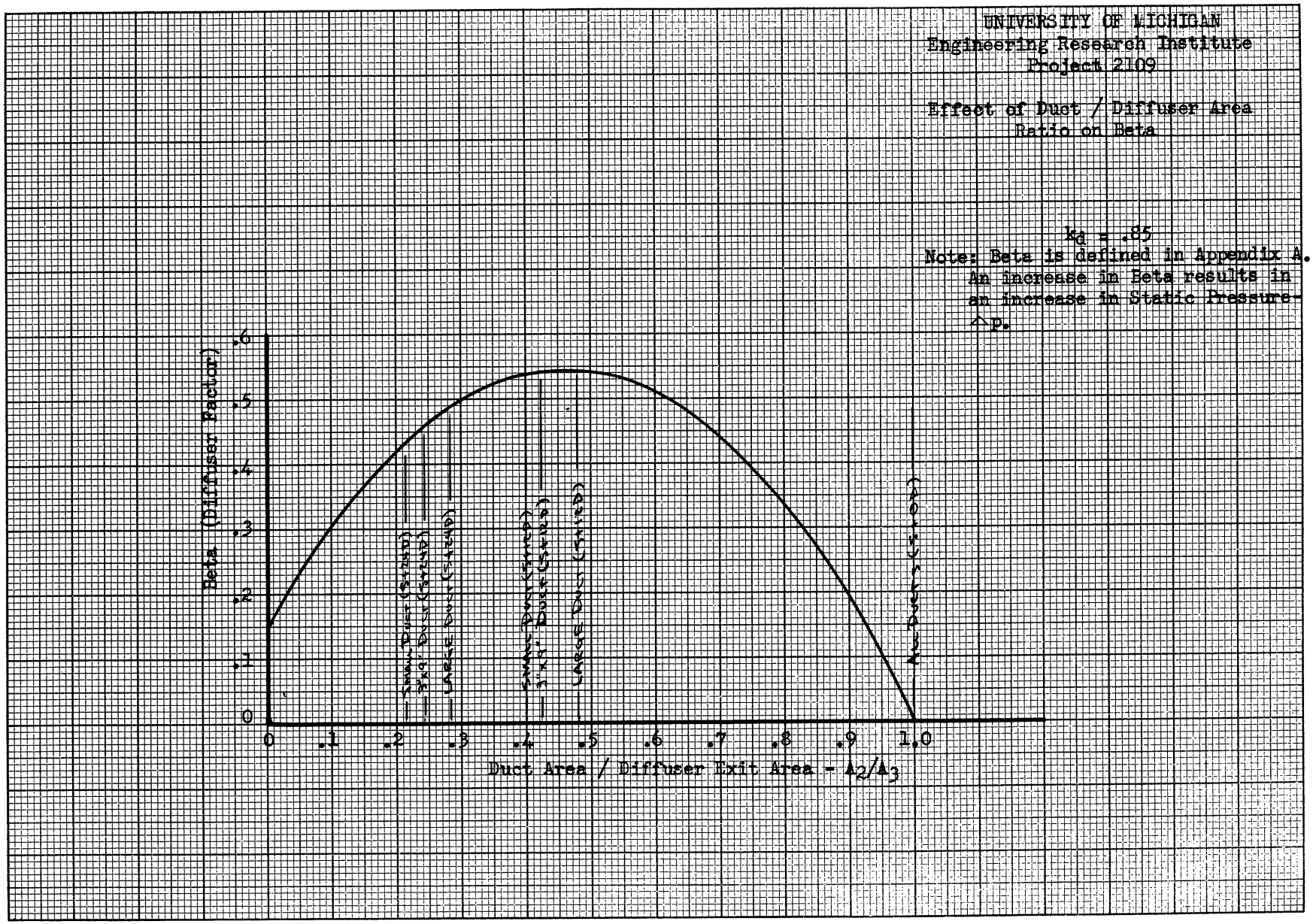
UNIVERSITY OF MICHIGAN
Engineering Research Institute
Project 2109
Effect of Duct / Diffuser Area Ratio on Beta
K_d = .85
Note: Beta is defined in Appendix A. An increase in Beta results in an increase in Static Pressure-Δp.
Beta (Diffuser Factor)
0
.1
.2
.3
.4
.5
.6
0
.1
.2
.3
.4
.5
.6
.7
.8
.9
1.0
Duct Area / Diffuser Exit Area - A_2/A_3
Constant Area Duct
Constant Area Duct
Constant Area Duct
Constant Area Duct
Constant Area Duct

Fig. 38a

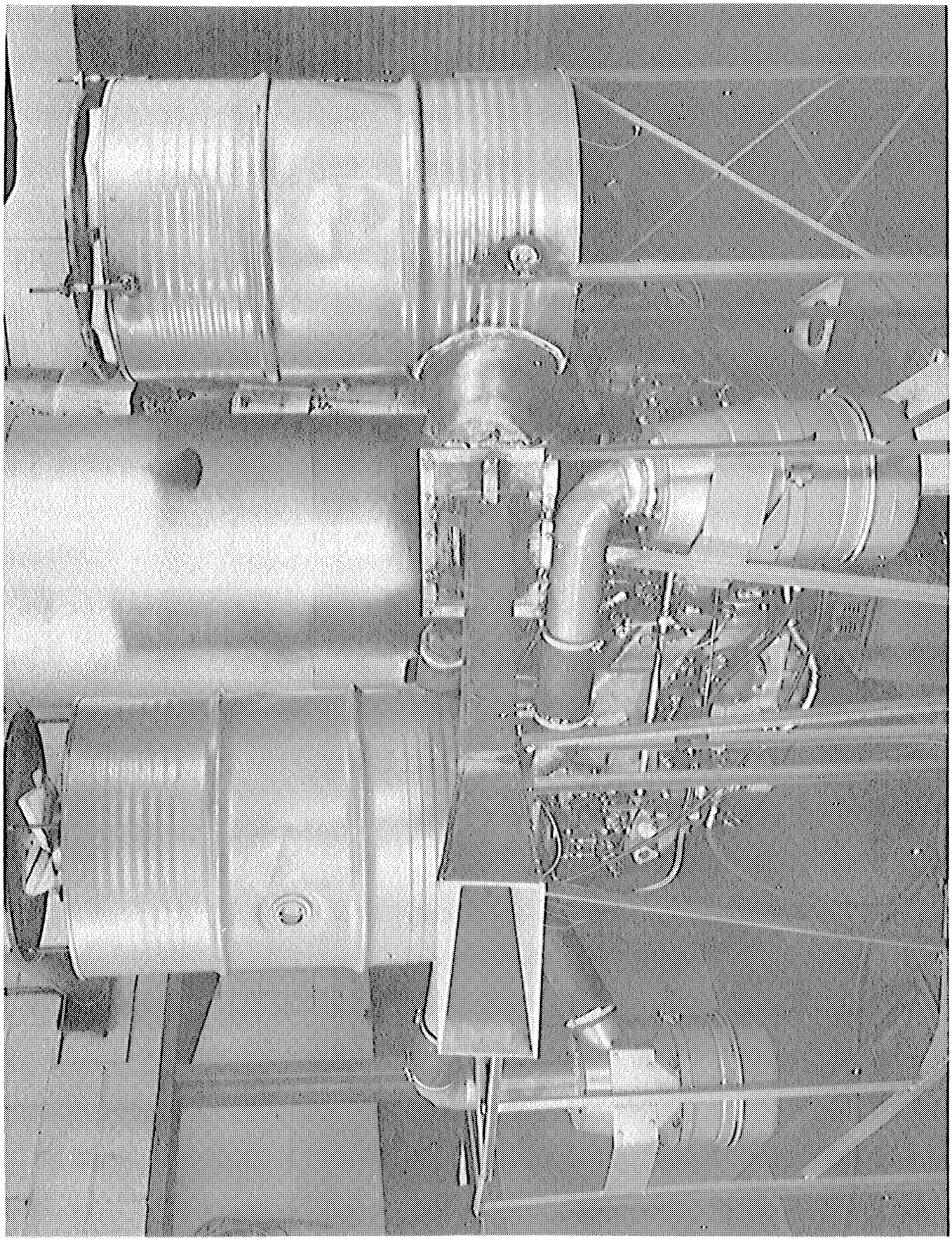

Fig. 39

Fig. 40

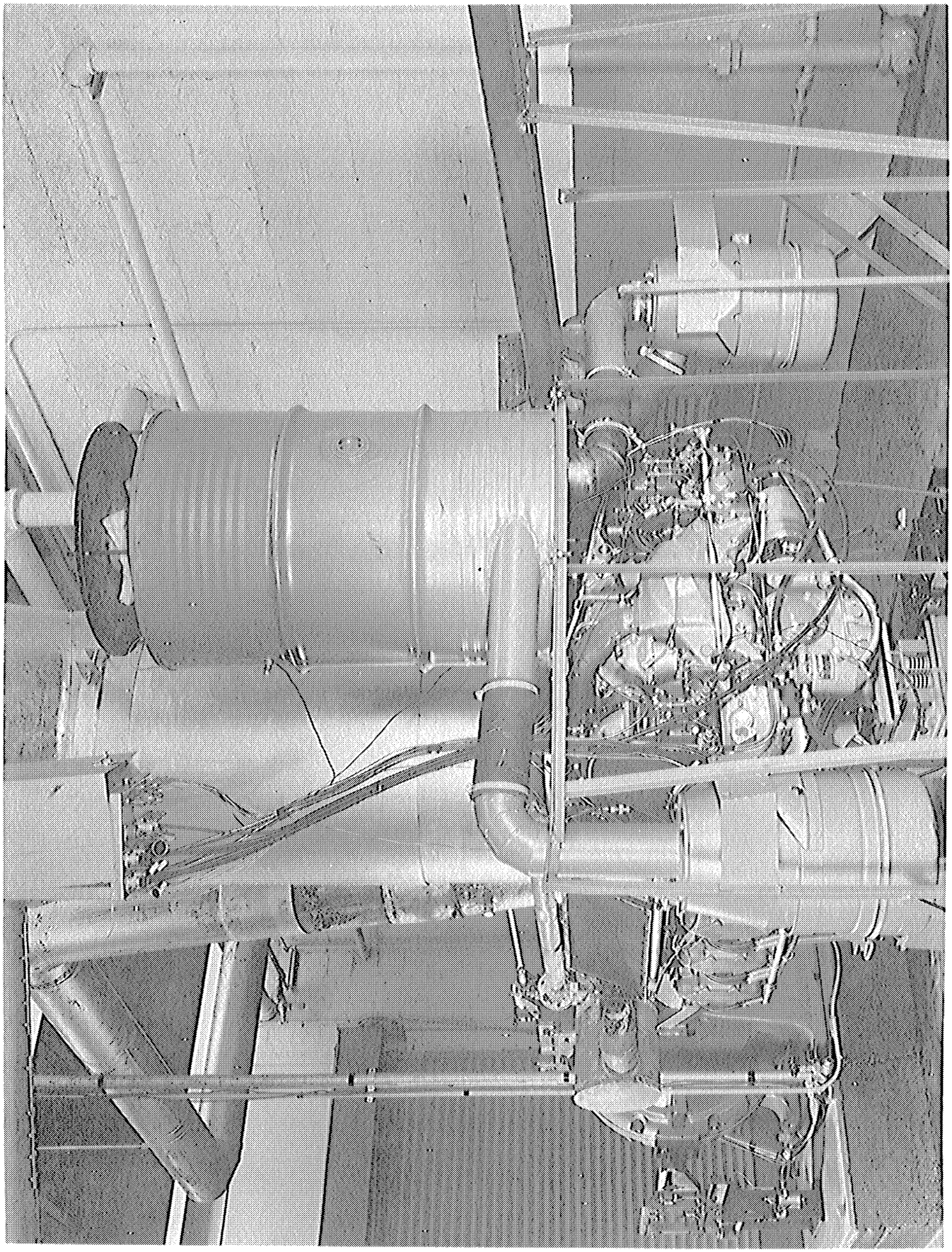

Fig. 41

APPENDIX

The derivation which follows was developed by Manganiello and Bogatsky, NACA report ARR No. E 4E 31.

DERIVATION OF EQUATIONS

SYMBOLS

M average mass rate of gas flow, (slugs) / (sec)
V average gas velocity, (ft) / (sec)
$\overline{V}$ mean effective gas velocity, (ft) / (sec)
p static pressure, (lb) / (sq ft)
A ejector cross-sectional area, (sq ft)
A_e cross-sectional area of exhaust-gas jet at section 1, (sq ft)
ρ density of gas, (slugs) / (cu ft)
R gas constant, (ft-lb) / (slug)(°F)
T gas temperature, (°F absolute)
c_p specific heat at constant pressure, (Btu) / (slug)(°F)
k_d loss coefficient in diffuser
L straight-mixing-section length of ejector, (in.)
D_h hydraulic diameter of ejector cross section $\left(\frac{4A}{\text{perimeter}}\right)$, (in.)
α factor accounting for reduction of ejector-entrance area due to presence of exhaust-gas jet $\left[\frac{A_2(A_2 - 2A_e)}{(A_2 - A_e)^2}\right]$
β diffuser factor $\left[1 - \left(\frac{A_2}{A_3}\right)^2 - k_d\left(1 - \frac{A_2}{A_3}\right)^2\right]$

SUBSCRIPTS

a with reference to cooling air
e with reference to exhaust gas
m with reference to mixture
0 entrance to convergent section of ejector
1 entrance to straight mixing section
2 exit of straight mixing section or entrance to diffuser
3 exit of diffusing section

SIMPLIFIED ANALYSIS

The simplified analysis that follows considers the effect of pertinent variables and predicts performance in terms of known engine quantities. The pressure rise across the ejector is obtained as a function of the mass flowrate of air pumped, the ejector cross-sectional area, and the mass flowrate and velocity of exhaust gas available.

The effect of the pulsating exhaust gas is taken into account by the use of an effective exhaust-gas velocity $\overline{V}_e$ introduced in reference 8 as that equivalent velocity which, when multiplied by the steady-flow average mass flowrate of exhaust gas, would produce the average momentum obtained by thrust measurements. In view of the complicated nature of the pulsating air and the mixture flow and their dependence on M_a/M_e, ejector dimensions, and engine operating conditions, steady-flow values are assumed.

Straight Ejectors.—A uniform velocity distribution and complete mixing are assumed at station 2 (see Fig. 3). If the laws of conservation of momentum and conservation of mass are applied between stations 1 and 2 and if friction is neglected, the following equation may be written

$$M_e\overline{V}_e + M_aV_{a_1} + p_1A_1 = (M_a + M_e)\,V_{m_2} + p_2A_2 \quad . \tag{1}$$

If the equation is rearranged and the pressure rise across the mixing section wherein $A_1 = A_2$ is solved,

$$p_2 - p_1 = \frac{M_e\overline{V}_e}{A_2} + \frac{M_aV_{a_1}}{A_2} - \frac{(M_a + M_e)\,V_{m_2}}{A_2} \quad . \tag{2}$$

The air and mixture velocities may be expressed as

$$V_{m_2} = \frac{(M_a + M_e)}{\rho_{m_2}\,A_2} \tag{3}$$

and

$$V_{a_1} = \frac{M_a}{\rho_{a_1}\,(A_2 - A_e)}$$

where A_e is the cross-sectional area of the exhaust-gas jet in section 1. The pressure differences existing throughout the ejector in the present application have negligible effect upon density; hence ρ_{a_1} may be taken as

equal to ρ_{a_o}, or simply as ρ_a, and in conjunction with the perfect gas equation

$$\rho_{m_2} = \rho_m = \frac{\rho_a R_a T_a}{R_m T_m} . \tag{4}$$

When Equations (3) and (4) are substituted in Equation (2), there is obtained

$$p_2 - p_1 = \frac{M_e \bar{V}_e}{A_2} + \frac{M_a^2}{\rho_a A_2 (A_2 - A_e)} - \frac{(M_a + M_e)^2}{A_2^2 \rho_a} \frac{R_m T_m}{R_a T_a} . \tag{5}$$

If Bernoulli's equation is applied between sections 0 and 1 and the air velocity at section 0 is assumed to be equal to zero,

$$p_1 = p_o - \frac{1}{2} \rho_a V_{a_1}^2$$

or

$$p_1 - p_o = - \frac{1}{2} \frac{M_a^2}{\rho_a (A_2 - A_e)^2} . \tag{6}$$

The pressure rise from 0 to 2 is obtained from Equations (5) and (6):

$$p_2 - p_o = \frac{M_e \bar{V}_e}{A_2} + \frac{M_a^2}{\rho_a A_2 (A_2 - A_e)} - \frac{1}{2} \frac{M_a^2}{\rho_a (A_2 - A_e)^2} - \frac{(M_a + M_e)^2}{A_2^2 \rho_a} \frac{R_m T_m}{R_a T_a} \tag{7}$$

which may be written

$$p_2 - p_o = \frac{M_e \bar{V}_e}{A_2} + \left(\frac{M_e}{A_2}\right)^2 \frac{1}{\rho_a} \frac{M_a}{M_e} \left[\frac{\alpha}{2} \frac{M_a}{M_e} - \left(\frac{M_a}{M_e} + 1\right)\left(\frac{M_e}{M_a} + 1\right) \frac{R_m T_m}{R_a T_a}\right] \tag{8}$$

where

$$\alpha = \frac{A_2 (A_2 - 2A_e)}{(A_2 - A_e)^2}$$

is the factor accounting for the reduction in available area for air flow

in section 1 due to the presence of the exhaust-gas jet. For practical cases A_e is small relative to A_2 and α may be taken as unity.

R_m and T_m may be expressed in terms of the properties and temperatures of the air and the exhaust gas.

From the general energy equation, neglecting the kinetic-energy terms, there is obtained

$$(M_a + M_e)\, c_{p_m} T_m = M_a\, c_{p_a}\, T_a + M_e\, c_{p_e}\, T_e \,. \tag{9}$$

The specific heat of the gas mixture is given by

$$c_{p_m} = \frac{(M_a/M_e)\, c_{p_a} + c_{p_e}}{(M_a/M_e) + 1} \,. \tag{10}$$

Similarly, the gas constant of the gas mixture is given by

$$R_m = \frac{(M_a/M_e)\, R_a + R_e}{(M_a/M_e) + 1} \,. \tag{11}$$

Equations (9), (10), and (11) are combined to obtain

$$\frac{R_m T_m}{R_a T_a} = \frac{\left(\frac{M_a}{M_e} + \frac{R_e}{R_a}\right)\left(\frac{M_a}{M_e} + \frac{c_{p_e}}{c_{p_a}}\frac{T_e}{T_a}\right)}{\left(\frac{M_a}{M_e} + 1\right)\left(\frac{M_a}{M_e} + \frac{c_{p_e}}{c_{p_a}}\right)} \,. \tag{12}$$

By substitution of Equation (12) in Equation (8)

$$p_2 - p_o = \frac{M_e \bar{V}_e}{A_2} + \left(\frac{M_e}{A_2}\right)^2 \frac{1}{\rho_a}\frac{M_a}{M_e}\left[\frac{\alpha}{2}\frac{M_a}{M_e} - \left(\frac{M_e}{M_a} + 1\right)\left(\frac{M_a}{M_e} + \frac{R_e}{R_a}\right)\frac{\left(\frac{M_a}{M_e} + \frac{c_{p_e}}{c_{p_a}}\frac{T_e}{T_a}\right)}{\left(\frac{M_a}{M_e} + \frac{c_{p_e}}{c_{p_a}}\right)}\right] \,. \tag{13}$$

If the difference in specific heats and gas constants between air and exhaust gas is neglected and if the area of the exhaust-gas jet is small compared with the area of the ejector, Equation (13) may be simplified to

$$p_2 - p_o = \frac{M_e \bar{V}_e}{A_2} + \left(\frac{M_e}{A_2}\right)^2 \frac{1}{\rho_a} \frac{M_a}{M_e} \left[\frac{1}{2} \frac{M_a}{M_e} - \left(\frac{M_a}{M_e} + 1\right) \left(1 + \frac{M_e}{M_a} \frac{T_e}{T_a}\right)\right] \qquad (14)$$

which may be written

$$p_2 - p_o = \frac{M_e \bar{V}_e}{A_2} + \frac{1}{\rho_a} \left(\frac{M_e}{A_2}\right)^2 f\left(\frac{M_a}{M_e}, \frac{T_e}{T_a}\right) . \qquad (15)$$

Thus the pressure rise of the exhaust-gas ejector pump is given as the sum of two terms: (1) the exhaust-gas thrust per unit ejector area and (2) the product of the square of the mass flowrate of exhaust gas per unit ejector area, the specific volume of air, and a function of the mass flow ratio and of the ratio of exhaust-gas temperature to air temperature. The second term is negative for all values of M_a/M_e.

With the range of variables encountered, the second term of the right side of Equation (14) is negative indicating the existence of an optimum ejector area.

Diffuser Exit.—Addition of a diffusing exit to the straight ejector permits conversion of part of the kinetic head into pressure head. The pressure rise attributable to the diffuser may be readily evaluated in terms of the pertinent factors already used. Application of Bernoulli's equation and the continuity equation between sections 2 and 3 and assumption of constant density gives the familiar diffuser equation

$$p_3 - p_2 = \frac{1}{2} \rho_m {V_m}_2^2 \left[1 - \left(\frac{A_2}{A_3}\right)^2\right] . \qquad (16)$$

The efficiency of pressure recovery of a diffuser is dependent on both the expansion angle and the expansion ratio. Equation (16) is thus modified to

$$p_3 - p_2 = \frac{1}{2} \rho_m {V_m}_2^2 \left[1 - \left(\frac{A_2}{A_3}\right)^2 - k_d \left(1 - \frac{A_2}{A_3}\right)^2\right] \qquad (17)$$

where k_d, the loss coefficient in the diffuser, is a function of diffuser angle.

Substitution of the expressions for V_{m_2}, ρ_m, and $\frac{R_m T_m}{R_a T_a}$ from Equations (3), (4), and (12) in Equation (17) gives

$$p_3 - p_2 = \frac{1}{2\rho_a}\left(\frac{M_a+M_e}{A_2}\right)^2\left[1-\left(\frac{A_2}{A_3}\right)^2-k_d\left(1-\frac{A_2}{A_3}\right)^2\right]\left[\frac{\left(\frac{M_a}{M_e}+\frac{R_e}{R_a}\right)\left(\frac{M_a}{M_e}+\frac{c_{p_e}}{c_{p_a}}\frac{T_e}{T_a}\right)}{\left(\frac{M_a}{M_e}+1\right)\left(\frac{M_a}{M_e}+\frac{c_{p_e}}{c_{p_a}}\right)}\right] . \quad (18)$$

With addition of Equation (18) to Equation (13), the total pressure rise in an ejector ($p_3 - p_o = \Delta p$) with a diffuser exit becomes

$$\Delta p = \frac{M_e\bar{V}_e}{A_2}+\left(\frac{M_e}{A_2}\right)^2\frac{1}{\rho_a}\frac{M_a}{M_e}\left[\frac{\alpha}{2}\frac{M_a}{M_e}+\left(\frac{M_e}{M_a}+1\right)\left(\frac{M_a}{M_e}+\frac{R_e}{R_a}\right)\frac{\left(\frac{M_a}{M_e}+\frac{c_{p_e}}{c_{p_a}}\frac{T_e}{T_a}\right)}{\left(\frac{M_a}{M_e}+\frac{c_{p_e}}{c_{p_a}}\right)}\left(\frac{\beta}{2}-1\right)\right] . \quad (19)$$

where

$$\beta = \left[1-\left(\frac{A_2}{A_3}\right)^2-k_d\left(1-\frac{A_2}{A_3}\right)^2\right] .$$

If the simplifying assumption made in going from Equation (13) to Equation (14) is again applied, Equation (19) reduces to

$$\Delta p = \frac{M_e\bar{V}_e}{A_2}+\left(\frac{M_e}{A_2}\right)^2\frac{1}{\rho_a}\frac{M_a}{M_e}\left[\frac{1}{2}\frac{M_a}{M_e}+\left(\frac{M_a}{M_e}+1\right)\left(1+\frac{M_e}{M_a}\frac{T_e}{T_a}\right)\left(\frac{\beta}{2}-1\right)\right] . \quad (20)$$

Equation (19) or (20) may be considered the general equation for straight as well as diffuser ejectors. For straight ejectors $\beta = 0$, Equation (19) reduces to Equation (13), and Equation (20) reduces to Equation (14). The theoretical curves used in this report were calculated by means of Equation (19); over the range of ejector operation of practical interest in the present application, use of the approximate Equation (20) introduces negligible deviation from Equation (19).